AD 265 071

REPORT NO. ARD-286

ADVANCED RESEARCH

DIVISION OF
HILLER AIRCRAFT CORP

ARD-286

INTERIM SUMMARY REPORT OF INVESTIGATION OF THE PROCESS OF ENERGY TRANSFER FROM AN INTERMITTENT JET TO SECONDARY FLUID IN AN EJECTOR-TYPE THRUST AUGMENTER

PALO ALTO CALIFORNIA • CABLE ADDRESS HILLER • TELEPHONE DAVENPORT 5-3241

HILLER
AIRCRAFT CORP

In Reply Please Refer to:
ARD-61-M41 ERS:hg

October 16, 1961

To: Distribution List

Via: Bureau of Naval Weapons Representative,
Palo Alto, California

Subject: Distribution of Final Report Contract
Nonr 3082(00), Hiller Report No. ARD-286

Encl.: (1) Subject Report

1. Subject report is hereby, transmitted to the addressees listed in the Distribution List per instructions of the Office of Naval Research, Code 461.

2. We would like to hear from you, if this report raises any questions or comments.

HILLER AIRCRAFT CORP.

E R Sargent

E. R. Sargent,
Manager, Propulsion Dept.
Advanced Research

4331/Nonr 3082(00)
RHV:mmg
Ser 1276
18 Oct 1961

FIRST ENDORSEMENT on HILLER AIRCRAFT CORP. ltr ARD-61-M41 ERS:hg of 16 Oct 1961

From: Bureau of Naval Weapons Representative, Palo Alto, California
To: Distribution List

Subj: Distribution of Final Report Contract Nonr 3082(00), Hiller Report No. ARD-286

1. Forwarded for information and comment, if appropriate.

G Robinson
G. ROBINSON

Copy to:
Hiller Aircraft Corp

Report No. ARD-286

31 March 1961

INTERIM SUMMARY REPORT ON INVESTIGATION OF THE PROCESS OF ENERGY TRANSFER FROM AN INTERMITTENT JET TO SECONDARY FLUID IN AN EJECTOR-TYPE THRUST AUGMENTER

An Experimental Research Program for the
Office of Naval Research
Department of the Navy
Contract Nonr 3082(00)

Raymond M. Lockwood
Principal Investigator

ADVANCED RESEARCH
DIVISION OF HILLER AIRCRAFT CORP.

TABLE OF CONTENTS

LIST OF FIGURES

ACKNOWLEDGEMENTS

This contract was sponsored by the Air Branch of the Office of Naval Research. The principal investigator is pleased to acknowledge valuable assistance from the following individuals, either directly or as benefit from conferences and conversations; but the responsibility for direction of the program and conclusions is the author's.

Joseph Beckett for continuing assistance with details of the test stand, its associated equipment, and operation;

David A. Graber for construction and operation of the test equipment and assistance in conducting the experiments;

Elbert R. Sargent, Manager of the Propulsion Department for overall supervision and valuable counsel;

Henry Wichers for assistance in developing the photographic equipment and techniques;

Robert W. Drury, consultant, for his continuing interest in the portable schlieren photographic equipment, as designer of the original equipment and for assistance in converting the schlieren equipment for high-speed color photography;

Mr. William G. Patterson for project assistance since January 1961 particularly in connection with the high speed motion picture color schlieren system and preparation and analysis of the color streak photographs and assistance in editing and publishing this report.

The Principal Investigator has benefited from conversations with the following: Personnel at the Detonation Laboratory, Richmond Field Station of

ACKNOWLEDGEMENTS (Continued)

the University of California, particularly Dr. A. K. Oppenheim and Dr. Raul A. Stern. A result of these contacts has been to point the immediate major effort for analysis in the direction of the use of wave diagrams. Dr. Robin Gray, School of Aeronautical Engineering, Georgia Institute of Technology, for his interest in the problems of analysis of the phenomenon; Dr. George Matthews, formerly ONR Project Engineer, now in the Department of Aeronautical Engineering, University of Virginia, for keen interest, encouragement, technical perspective and stimulating discussions.

I. SUMMARY

The program approach in Phase II has been one of concurrent observation and measurement on one hand and the search for methods of analysis on the other. Experimental evidence supports the idea that techniques of analysis developed in the study of one-dimensional unsteady gas dynamics are applicable to the problem at hand. Support is given to the postulation made prior to Phase I that the transfer of energy from the primary jet to secondary air is explained by considering that the intermittent primary jet acts as an air or jet piston as it leaves the tail pipe and enters the thrust augmenter. This inferred that the main exchange of energy took place across the face of the jet as a direct exchange of pressure with the fluid in front of the interface and behind, so that inflow is induced by a rarefaction wave that is created behind the jet interface, and a positive pressure is built up along the walls of the augmenter ahead of the interface by a compression wave.

Greatly improved visualization of the motion of the jet interface and measurement of its velocity through the augmenter have been made using high-speed motion picture "color schlieren" photography; and limited "instantaneous" pressure measurements have been made in the augmenter throat concurrently with the motion picture sequences. Measurements of the average flow rate through the intermittent jet augmenter combination have been accomplished for the first time.

A technique for measurement of unsteady gas flow, which uses an ultrasonic thermometer in conjunction with the schlieren photographic system is being evaluated. The original intention was to provide a means of calibrating the color schlieren system so that bands of color in the photographs would produce a continuous map of temperature distribution in the intermittent jet and thrust augmenter gases. However, as the schlieren photograph portrays the temperature gradient rather than the temperature itself, the results have been difficult to analyze.

Important and immediate practical results have stemmed from this research project because of the support information fed into the Pulse Reactor development contract NOa(s) 59-6055c. Trends revealed in the small-scale research investigation made it possible to increase the thrust augmentation of full-size tailpipe augmenters from 77 percent to 140 percent in only one step.

Preliminary research equipment has been completed and initial checkout tests are encouraging with a device to convert steady flow to intermittent flow without causing upstream disturbance. This reveals the possibility of developing a simple mechanical device compatible with steady flow jets such as are produced by air turbines and water impellers which may double the thrust of the steady flow device by the use of simple intermittent jet thrust augmenters.

2. INTRODUCTION

The major effort in the second phase program has been to verify or modify the postulated description of the mechanism of energy transfer that was described in section 4.5 of Reference 3 (Report ARD-238, Final Report for Contract Nonr 2761(00). The program approach has been one of concurrent observation and measurement on one hand and the search for methods of analysis on the other hand. Great difficulty has been encountered in observing and measuring the phenomenon because of the problem of visualizing flow in the engine cycle operating between 200 and 300 cycles per second. It was necessary to place initial emphasis on observing and measuring so that "instantaneous" values could be obtained to check against any ideas for mathematical models. The tailoring of experimental techniques to apply to this particular situation is continuing.

In the final report of the first phase work (ARD-238), a mechanism of thrust augmentation of intermittent jets was postulated on the idea that the intermittent jet acts as an air or jet piston as it leaves the tail pipe and enters the thrust augmenter. This inferred that the main exchange of energy took place across the face of the jet as a direct exchange of pressure with the fluid in front of it.* In the second phase, closer attention has been given to the details of this energy exchange. Actual pressure measurements in the augmenter have been taken and initial calculations have been made. At this stage of the program it appears that techniques developed in the study of one-dimensional unsteady gas dynamics are applicable to the problem at hand.

The most important practical result of the first phase program was the development of full scale augmenters of a divergent type which are shown to be quite superior to cylindrical augmenters (Ref. 4). The performance of these augmenters is shown in Figure 2. With the models of the augmenters a basic U-shaped valveless combustor is shown in Figures 3 and 4. The cutaway of Figure 4 emphasizes the great simplicity of the valveless engine system which has been named the Pulse Reactor. As a result of this development, the Pulse Reactor has achieved performance which is competitive with that of turbojet engines as far as static performance is concerned. In other

*and behind it.

words, a thrust specific fuel consumption of better than one pound of fuel per pound of thrust per hour has been achieved (Fig. 7) with the immediate promise of a thrust-to-weight ratio of 10 to 1, and a likelihood of considerable improvement beyond that value.

It has also been demonstrated that the Pulse Reactor lift-propulsion system has uniquely favorable characteristics due to its novel cycle when operated near the surface over unprepared terrain. The effect of the thrust augmenters is to reduce the downwash temperature to only about 200°F and downwash velocity to less than 200 ft/sec at a distance of seven tailpipe exit diameters, as compared to 750°F and 1000 ft/sec for a typical turbojet engine.

Whereas the gas turbine engine is quite susceptible to damage from ingestion of the foreign particles that are stirred up by the jet downwash, the Pulse Reactor is not. First, there are no moving parts in the Pulse Reactor to be damaged by the foreign particles. Second, it has been demonstrated, as indicated in Figure 8, that the Pulse Reactor engine rejects particles that are significantly heavier than air. Instead of being sucked into the engine, the particles are swept away by the jet efflux before they can be sucked into the engine inlet.

3. EXPERIMENTAL RESEARCH

3.1 Flow Visualization

The basic high speed schlieren photographic system is shown in Figure 5a This system has been modified with the addition of a color schlieren system (Fig.5b) which greatly improves the visualization of the hot jet efflux. The main problem so far with the system has been concerned with the reduction in transmitted light due to the color filters. The light intensity is somewhat marginal at the highest speed of 7500 frames per second. An improved light source has been installed, although it is basically a tungsten filament as was the previous light source. Consideration has been given to the use of a zirconium filament lamp. The use of flat walls of high quality glass has permitted detailed study of the flow inside of the augmenters. Some of the results are shown in Figure 9, which is made up a series of random shots using the flash photographic setup. High speed movies of the intermittent jet cycle, showing the jet passing from the tailpipe into the open air, are sketched in Figure 13. These sketches reveal the typical club shape of the jet and reveal the fact that it tends to expand to about 2-1/2 times the size of the tail pipe, then remains fairly constant as it sweeps across the schlieren mirror.

In Figure 14a an intermittent jet thrust augmenter test setup is shown in which the forward and rear walls of the augmenter are made up of glass plates. High speed motion pictures of this test setup are shown in Figure 14b. The 16 mm movies have been enlarged and traced for clarity. Here it can be seen how ambient air is caught between the slugs of the primary jet within the augmenter, and that it appears to be compressed between the face of the current jet and the rear of the preceding slug of primary jet fluid.

On picture 21 of the jet cycle is shown a flash mark. This mark represents the start of a pressure trace which was displayed on an oscilloscope and redrawn on Figure 14c. The display of a pressure trace taken simultaneously with the high speed movies which reveal motion of the intermittent jet was made possible by the test setup shown in Figures 6a and 6b. If the high speed motion picture camera had been of a type which permits display of pressure signals on the edge of the high speed motion picture frame, the problem would have been simplified. Lacking this type of equipment, the following setup

was used: A time delay unit was used to allow sufficient time for the high speed camera to get up to its maximum speed. After about 0.4 of a second, the time delay unit triggered the switch to discharge the flash light which showed up on movie frame 21 of the cycle, and at the same instant closed a switch between the high speed pressure gage mounted in the augmenter throat and the external sweep trigger of the oscilloscope. The oscilloscope was provided with an "end of sweep lock-out", which means that only one sweep of the oscilloscope beam was made across the face of the 'scope to expose the film in the Polaroid oscilloscope camera.

3.2 Jet Interface Velocity Measurements

The addition of a timing light generator to the high speed motion picture camera has permitted frame-to-frame analysis of the velocity of the interface between the hot jet and the cold air in the augmenter, and has resulted in the information shown in Figures 13, 14, 15, 16 and 17. The interface velocities were first calculated from a study of Figures 13 and 14. Rather sharp differences in velocity from frame to frame proved the inaccuracy of determining interface velocity by this method. The camera was then modified for streak photography by removing the gearing mechanism for the revolving prism. The schlieren mirror was masked down to a 1" wide strip running axially from the tailpipe through the augmenter. Figure 16b is a sketch of a typical streak photograph of the augmented dynajet.

Jet interface velocity calculations were made by determining the film speed from the timing light marks and measuring the slope of the streak.

Interface velocities for the Tigerjet and Dynajet, augmented and unaugmented are shown in Figures 15 and 16.

When the color system was used for streak photography, improved visualization was achieved. Also, steep streaks were observed which preceded the jet interface. These streaks are at angles which indicate

acoustic velocities and are presumedly caused by pressure waves. The sensitivity required of the color schlieren system to photographically record pressure waves is attributed to three factors: first, the filament light source is reflected onto the center color band of the filter and is transmitted through to the film plane rather than being blocked by the edge of the prism (as in the black and white schlieren system). Therefore, very small temperature gradients will show up in the film plane as variations in intensity of the center color or background color. Second, the center or background color band may be made as narrow as is just required to hold the width of the filament image when focused upon it. The neighboring color bands will then transmit light refracted only a minute amount by the jet gases. Third, the multicolored photograph offered by the various color bands in the filter presents a greater contrast than the variation in grays and light intensity offered by the black and white system.

Four 35mm. duplicate slides are presented in Figure 27 with their descriptions. These slides were constructed from strips of 16mm. high-speed color schlieren motion pictures.

3.3 <u>"Instantaneous" Pressure Measurements</u> (Fig. 14b, picture 21 and Fig. 14c)

The problem of taking instantaneous pressure measurements simultaneously with motion pictures which show the motion of the jet interface was discussed in Section 3.1. Motion pictures were taken in which the high speed movie camera was used with black and white schlieren, that is, with knife-edge focus, and these motion pictures were keyed to simultaneous high-speed pressure measurements in the augmenter throat as indicated in Figure 6 and Table No. 1. Much effort has been required to get this type of data. It is evident that there is a serious need for simultaneous pressure measurements in at least two positions in the thrust augmenter. Some effort will also be made to correlate the unsteady pressure measurements with average readings taken with U-tube manometers. The initial high speed pressure data has, however, served to support the idea that the energy transfer from

Table No. 1

PRESSURE VARIATIONS IN AUGMENTER THROAT

Picture Sequence Number		Time - Seconds	Instantaneous Pressure - Psig	
21		0	-2.3	
22		.0001333	-1.1	
23		.0002666	+ .2	
24		.0003999	+1.5	
25		.0005332	+2.5	
26		.0006665	+ .6	
27		.0007998	-1.1	
28		.0009331	- .3	
29		.0010664	+ .6	
30		.0011997	+1.5	
31		.0013330	+ .5	
32		.0014663	-1.2	
33		.0015996	- .4	
34		.0017329	+ .5	
35		.0018662	-2.3	
36		.0019995	-2.1	
37		.0021328	-1.0	
38	(1)*	.0022661	+ .8	(+ .8)
39	(2)	.0023994	+2.0	(+2.0)
40	(3)	.0025327	+2.6	(+2.6)
	(4)	.0026660		(+2.0)
	(5)	.0027993		(-1.0)
	(6)	.0029326		(- .5)
	(7)	.0030659		(+1.0)
	(8)	.0031992		(+ .8)
	(9)	.0033325		(- .9)
	(10)	.0034658		(- .1)
	(11)	.0035991		(+ .5)
	(12)	.0037324		(- .5)
	(13)	.0038657		(-3.3)
	(14)	.0039990		(-1.8)
	(15)	.0041323		(- .2)
	(16)	.0042656		(+3.0)
	(17)	.0043989		(+2.0)
	(18)	.0045322		(+1.0)

*Numbers in brackets refer to earlier picture sequences believed to be typical, so are used to compare with the continuing pressure data from Figure 14c.

the primary jet to the secondary fluid does occur by means of compression and expansion waves that pass back and forth through the thrust augmenter, as discussed in Section 5.

3.4 Average Flow Rate Measurement

The flow box test set-up, shown in Figures 11a, b, c and d, provides measurement of rate of flow through intermittent jet thrust augmenters for the first time. As a matter of fact, the writer is aware of only two references in the literature that report the measurement of flow through the basic pulse jet engines (References 13 and 14).

Measurement is difficult because of the intermittent nature of the flow. Ordinary flow measurement devices such as sharp-edged orifices and flow nozzles are inaccurate when the flow is not steady. A satisfactory technique is to measure the highly unsteady flow as follows: An air-tight flow-box is used and the inflow to this box is measured with a Meriam laminar flow element. This flow measuring device depends on the fact that when flow is laminar (Reynolds No. less than 2000), the relationship between pressure drop and flow rate is linear; therefore, the average measurements of the unsteady flow are accurate values.

A comparison of the pumping capacity of cylindrical and divergent thrust augmenters is given in Figure 24a. Here the weight flow rate is plotted versus the length-to-diameter ratio of the augmenter. It is shown that the 8^{o} divergent augmenter is superior to the cylindrical augmenter as a jet pump, as well as a thrust augmenter.

To eliminate the slight vacuum created in the flow box by the pressure drop through the flow meter, a blower was installed. Figure 24b compares the pumping rates with an 8^{o} divergent augmenter for flow box pressures of atmospheric and below atmospheric (pumping against a head). Figure 24c shows the flow rate augmentation ratio of the 8^{o} divergent augmenter.

3.5 Temperature Measurement of Unsteady Gas Flow

Techniques using an ultrasonic thermometer are being evaluated in connection with the schlieren system. The system works as follows: A piezo-electric crystal (quartz, X-cut) is placed in the side wall of the thrust augmenter. An ultrasonic disturbance is supposed to be made visible with the schlieren photographic setup, and therefore the wave length should be measurable from photographs. This technique has been demonstrated in connection with shock tube work and is described in Reference 9. Knowing the crystal frequency and measuring the wave length then permits the direct calculation of the velocity of the disturbance; that is, the speed of sound from which can be calculated the instantaneous gas temperature as follows:

Speed of sound, $a = 49.1\sqrt{T}$ where T is absolute temperature in degrees Rankine.

The ultrasonic thermometer provides the instantaneous gas temperature at one station. This information is, of course, important; but the combination of the ultrasonic thermometer with the color schlieren system is even more important because it may permit the calibrating of the color schlieren system at the station where the piezo-electric crystal is located. Then the color schlieren system will provide a continuous map of temperature distribution for the entire region throughout the interior of the augmenter. Thus far in our program we have not yet been able to observe the ultrasonic disturbance. The oscillator which drove the piezo-electric crystal was damaged in the fire previously mentioned, which has delayed further tests.

3.6 Devices for Creating Intermittent Jets

3.6.1 Valved Pulsejets

Most testing has been conducted with small valved pulsejets in order to tie in with the considerable amount of previous data from Phase I and with data reported by other investigators using the same engines (e.g., Ref. 15). Dynajet engines and a small Japanese copy, called the Tiger-Jet, are being used.

3.6.2 Valveless Pulsejets

Use of the valveless pulsejets has been postponed in order to take advantage of the development and construction of very small engines underway on other projects, thus saving this project money. The jets must be very small because of the limited size of the schlieren photographic equipment.

3.6.3 Piston-in-Tube Mechanically Driven

As described in ARD-238, the piston-in-tube device was not very successful because it provided only very small thrusts at frequencies of less than 5 cycles per second. Above this frequency the thrust was too small to measure accurately. The limitation seems to be concerned with the problem of refilling the tube from the tail end. When used in water, too rapid piston motion during refill causes cavitation.

The piston-in-tube device has since been improved over that previously described by using a cam shape (Figure 10) which permits refill time in the tube 5 times greater than the efflux time. That is, the piston in motion for inflow has only 1/5 of the maximum velocity of the piston in motion during efflux. The piston-in-tube device, however, still seems limited to about 10 cycles per second for production of moderate jet thrust, and it does not seem to be nearly as good a method for creating intermittent jets as that described in the following section.

3.6.4 Converter from Steady Flow to Intermittent Without Creating Upstream Disturbances

Preliminary hardware has been completed and initial checkout tests are encouraging with a device to convert steady flow to intermittent flow without causing upstream disturbance. This device is shown in Figures 19, 20 and 21. Upstream disturbance is prevented because the upstream flow always "sees" fully open discharge ports. This is achieved by having one set of ports opening while the other set of ports are closing.

Downstream of the interrupter ports, however, the flow is strongly intermittent. Sudden closure of the inlet ports causes a sudden pressure drop to occur at the upstream end of the discharge tubes creating a rarefaction wave

which travels down the tube to the open end where it is reflected as a compression wave which, in turn, travels back upstream to the port. When the rarefaction wave is reflected from the open end of the tube, it induces flow back into the tube in the same manner as flow reverses back into a pulsejet tailpipe, so it is then possible to take advantage of the high thrust augmentation available with intermittent jet flow. The hope, of course, is that such a device might be able to double the thrust of a steady flow engine such as a turbojet. Flow rate measurements, thrust augmentation and flow visualization tests are planned.

4. EQUIPMENT

The items of equipment used in the Phase I program are listed in Section 3.4 of Report ARD-238 (Ref. 3). Several new items of equipment have been added during the Phase II program. Most of these items are shown in Figures 6 (listed in 6c) 10, 11, 18, 19, 20, 21 and 22.

4.1 Simultaneous Multiple Channel Electronic Switch

Ordinary switch means were inadequate for closing several channels simultaneously. Therefore, a special electronic switch was designed for the purpose. The functional block diagram is shown in Figure 25. The high-speed mercury arc lamp (BH-6) is flashed to appear on the high-speed motion picture film. The light which exposes the film also shines on a silicon solar cell, which, in turn operates a Schmidt trigger, and activates a delay circuit (of approximately 150 μsec.) in the electronic switch. At the same time that the delay circuit is activated, a negative pulse is directed to the oscilloscope and the horizontal sweep is triggered. This establishes four short horizontal lines that represent the neutral or reference lines for the high-speed pressure traces. Following the time delay, the four circuits from the high-speed pressure transducers are closed and the pressure traces are displayed on the oscilloscope. The traces are prevented from repeating by use of an "end of sweep lockout" feature on the oscilloscope. The circuit diagram for the simultaneous closing multiple channel electronic switch is shown in Figure 26.

In the next phase of this program it is planned to procure the following equipment to satisfactorily record as many as four high-speed pressure traces and to synchronize these traces with high-speed motion pictures of the jet interface:

Tektronix Dual-beam oscilloscope type 502 (200 μvolt/cm)
Tektronix Dual-Trace plug-in units, type C-A (electronic switches)
Tektronix Power Supply, type 127
Kistler Miniature pressure pickups, Model No. 601 (piezo-electric type)
Kistler Electrostatic Charge Amplifiers, Model 565.

5. ANALYSIS OF MECHANISM OF ENERGY TRANSFER FROM INTERMITTENT PRIMARY JET TO SECONDARY FLUID IN EJECTOR TYPE THRUST AUGMENTER

An attempt to explain the action of the intermittent jet device will be made by postulating that when the intermittent jet with the ring vortex that develops at its head (Figures 1 and 9) enters the thrust augmenter throat, the interface between the head of the jet and the ambient air in the augmener acts as a contact discontinuity which is immediately followed by an expansion wave (Q-wave) which causes an immediate pressure drop in the throat of the augmenter in the cool gases surrounding the hot jet core, and, accordingly, inflow (with its associated pressure drop) begins around the lip of the augmenter.

It was previously postulated that in the case of the divergent augmenter, the thrust due to pressure drop on the augmenter lip flare was reinforced by the effect of the compression wave (P-wave) which precedes the interface and thereby causes a pressure build-up on the divergent augmenter walls downstream of the throat. This would then explain the superior thrust augmentation of the divergent augmenter compared to the cylindrical augmenter. However, average static pressure readings taken along the walls of the divergent augmenter are below atmospheric pressure. This suggests that superior thrust in the case of the divergent augmenter must then be attributed to increased pressure drop on the lip flare.

It is further known that both expansion and compression waves tend to reflect from the open ends of tubes as waves of the opposite kind (i.e., a compression wave reflects as a rarefaction wave and vice-versa). Finally, it may be shown that waves are partially transmitted and partially reflected from a contact (temperature) discontinuity, depending on factors such as the strength of the waves before contact, etc.

It is proposed that the mechanism of thrust augmentation in question may be explained and described by the initial passage of the pressure and rarefaction waves associated with the travel of an interface between the head of the intermittent jet and the secondary fluid in the thrust augmenter, and the reflection of these waves from open ends of the augmenter and the reflection from and transmission of the waves through the interface (or contact discontinuity). Details of these actions are described in the following sections.

5.1 Comparison of Isentropic Wave and Steady Flow Processes

It is important, and it may be surprising to some, to note in Figure 23 how much greater is the pressure rise and how much lower is the pressure drop caused by the passage of isentropic compression and expansion waves, respectively, than can be achieved by steady flow isentropic processes for the same fluid particle velocities. This may well explain the high performance of properly designed intermittent jet thrust augmenters of the ejector type.

Table I, page 6, is a compilation of time and pressure data from Figure 14c keyed to the picture sequences of Figure 14b. The general pattern of pressure changes appears to fit a pattern of the passage of a compression wave that is reflected once as a rarefaction wave from the downstream end of the augmenter with three reflections of the initial rarefaction wave passing the pressure gage in the augmenter throat during the same period. It is assumed that the rarefaction wave that follows the interface between the intermittent jet and ambient air is reflected from the inlet as a compression wave and partly reflected and partly transmitted from the traveling interface. The second strong compression wave shown during the cycle may well represent the passage of the leading compression wave reflected from the outlet as a rarefaction wave and later from the inlet as a compression wave reinforced by the simultaneous passage of a reflection of the trailing rarefaction wave also as a compression wave. However, there is as yet far too little instantaneous pressure data on which to base any positive conclusions. It will be necessary to take repeated pressure readings simultaneously at a minimum of two stations near the ends of the augmenter before the motion and magnitude of the waves can be determined more precisely.

At this stage of the investigation the action of the intermittent jet seems to create pressure rises and pressure reductions in the augmenter that lie between what might be expected from the motion of a solid piston, as illustrated in Figure 23, and the motion of a temperature discontinuity as discussed by Rudinger (Ref. 5, pg. 87) and Shapiro (Ref. 11, pg. 969). The fact that a ring vortex tends to be formed by the intermittent jet prior to its entry into the augmenter seems to change the situation from that of a simple temperature

discontinuity, and it is suspected that it may be the source of a greater pressure drop in the throat of the augmenter than would be caused by a planar temperature discontinuity.

5.2 Mathematical Expressions

The mathematical derivations of equations that describe such unsteady gas flow will not, in general, be repeated here since they are to be found in several textbooks, such as References 5, 6 and 11, which have extensive sections devoted to the theory of unsteady gas dynamics based on quasi-one-dimensional theory; but the important results will be stated for the convenience of the reader.

This theory is restricted to those gas flow problems in which the velocity and the thermodynamic state of the gas depend to a sufficient closeness of approximation on only one space coordinate, x, and the time, t. According to Rudinger (Ref. 5), this strictly limits it to situations in which the cross-sectional dimensions of the duct can be considered small compared to the length of the duct and the flow properties must be uniform across the duct. These limiting assumptions obviously do not apply in the case at hand, but it is believed that the analysis is still useful for the case of the short thrust augmenter. The analyses result in the following important equations (Ref. 11):

Euler's equation for unsteady motion: $$-\frac{1}{\rho}\frac{\partial p}{\partial x} = \frac{\partial u}{\partial t} + u\frac{\partial u}{\partial x} \qquad (5.1)$$

Definition of velocity potential, $\phi(x,t)$: $$u = \frac{\partial \phi}{\partial x} = \phi_x \qquad (5.2)$$

Isentropic relations: $$p/\rho^k = \text{constant}; \quad p/\rho T = \text{constant};$$

$$a = \sqrt{kRT} \qquad \text{where } k = \gamma = c_p/c_v \qquad (5.3)$$

or $$\frac{d\rho}{\rho} = \frac{1}{k}\frac{dp}{p} = \frac{1}{k-1}\frac{dT}{T} = \frac{2}{k-1}\frac{da}{a} \qquad (5.4)$$

The dependent state variables, particle velocity (u) and velocity of sound (a), may be expressed as functions of the independent space variables x and t with the following isentropic relations:

$$\frac{a}{a_o} = \sqrt{\frac{T}{T_o}} = \left(\frac{p}{p_o}\right)^{\frac{k-1}{2k}} = \left(\frac{\rho}{\rho_o}\right)^{\frac{k-1}{2}} \tag{5.4a}$$

Next, the basic equations of continuity, motion and state (not repeated here) are expressed in terms of a and entropy, s, in place of p, ρ and T; the assumption is made that c_v and c_p are constant (i.e., independent of temperature), and then by a transformation introduced by Riemann, the following is finally obtained: (Ref. 6)

$$\frac{\partial}{\partial t}(na+u)+(u+a)\frac{\partial}{\partial x}(na+u)+ua\frac{d\,\ln A}{dx}-\frac{a^2}{\gamma R}\frac{\partial s}{\partial x}-\frac{a}{R}\left(\frac{\partial s}{\partial t}+u\frac{\partial s}{\partial x}\right)=0 \tag{5.5a}$$

and $$\frac{\partial}{\partial t}(na-u)+(u-a)\frac{\partial}{\partial x}(na-u)+ua\frac{d\,\ln A}{dx}+\frac{a^2}{\gamma R}\frac{\partial s}{\partial x}-\frac{a}{R}\left(\frac{\partial s}{\partial t}+u\frac{\partial s}{\partial x}\right)=0 \tag{5.5b}$$

A great simplification is then made by restricting consideration to the isentropic case and constant area, in which case the partial differential equations reduce to the first two terms. Then, the following important definitions are given by Kantrowitz (Ref. 6):

$$P = na + u \qquad \text{and} \qquad Q = na - u$$

However, other authors, such as Rudinger, find it desirable to make the substitution $n = 2/\gamma - 1$.

So $$P = \frac{2}{\gamma - 1}\,a + u \qquad \text{and} \qquad Q = \frac{2}{\gamma - 1}\,a - u \tag{5.6}$$

The preceding equations become:

$$\frac{\partial P}{\partial t} + (u+a)\frac{\partial P}{\partial x} = 0 \qquad \text{and} \qquad \frac{\partial Q}{\partial t} + (u-a)\frac{\partial Q}{\partial x} = 0 \tag{5.6a}$$

and $$dP = \frac{\partial P}{\partial x}dx + \frac{\partial P}{\partial t}dt \qquad \text{and} \qquad dQ = \frac{\partial Q}{\partial x}dx + \frac{\partial Q}{\partial t}dt \tag{5.6b}$$

The solutions of these non-linear equations correspond to the propagation of waves in which a continuous change of shape occurs. However, if one considers a point moving with the velocity u + a, then dx/dt is u + a, and the increment in P vanishes, so P is invariant and Q also in like manner.

The utility of the quantities P and Q (which are sometimes called Riemann invariants) lies in the fact (as stated by Kantrowitz) that they represent the disturbances moving in the positive and negative x directions even in an arbitrary non-simple wave case. Thus, quite generally, P and Q are propagated unchanged; but this is not true for flow velocity, u, and speed of sound, a, except for the case of a simple wave of very small amplitude (acoustic wave), where the equations reduce to:

$$\frac{\partial P}{\partial t} + a_o \frac{\partial P}{\partial x} = 0 \qquad \text{and} \qquad \frac{\partial Q}{\partial t} - a_o \frac{\partial Q}{\partial x} = 0 \tag{5.7}$$

The preceding non-linear equations (5.6a and 5.6b) then apply to the case of isentropic waves of large amplitude, but the invariance of P and Q makes for a convenient treatment of the wave propagation problems by plotting x as abscissa and t as ordinate on an x,t diagram, where curves with the slope $dt/dx = 1/(u+a)$ connect points where P = constant. Still following Kantrowitz, these lines are called P-waves, and in a similar fashion Q-waves are represented by lines of constant Q, which have a slope of $1/(u-a)$. Also notice that

$$u + a = \frac{P}{2}\left(1 + \frac{1}{n}\right) - \frac{Q}{2}(1 - n) \tag{5.8a}$$

$$u - a = \frac{P}{2}\left(1 - \frac{1}{n}\right) - \frac{Q}{2}(1 + n) \tag{5.8b}$$

The foregoing relationships permit making graphical solutions of the non-linear partial differential equations, which describe waves of large amplitude.

Of the several references cited, Shapiro seems to present the most complete and versatile analytical-graphical techniques because of his concurrent use of 3 planes: the physical plane (plots of $c_o t/L$ vs. x/L) previously described, the state plane (c/c_o vs. u/c_o), and the hodograph plane (ϕ_t/c_o^2 vs. u/c_o where ϕ is the velocity potential $u = \partial\phi/\partial x = \phi_x$), and the convenient inter-relations that exist between them.

For example, Shapiro takes note that there exist reciprocal orthogonal relationships between the physical and hodograph planes which require that the physical characteristics be normal to the hodograph characteristics of the opposite family.

$$\left(\frac{dt}{dx}\right)_I = \frac{1}{u + c} \quad ; \quad \left(\frac{dt}{dx}\right)_{II} = \frac{1}{u - c} \tag{5.9 a,b}$$

$$\left(\frac{d\phi_t}{du}\right)_I = -(u - c) \quad ; \quad \left(\frac{d\phi_t}{du}\right)_{II} = -(u + c) \tag{5.10 a,b}$$

Furthermore, Shapiro, pg. 938, defines a set of characteristics coordinate I and II for right-running and left-running waves, respectively (analogous to P and Q used by Kantrowitz and Rudinger), so that

$$\frac{c}{c_o} = \frac{I + II}{1000} - 1 \quad ; \quad \frac{u}{c_o} = \frac{2}{k - 1}\,\frac{I - II}{1000} \tag{5.11 a,b}$$

It turns out that the characteristics in the state plane (c/c_o vs. $u/c_o = \phi_x/c_o$) are two families of straight lines with slopes $\pm(k - 1)/2$ where $k = \gamma = 1.4$ for air.

Thus, one set of curves serves for all cases for constant k ; i.e., γ. Shapiro's Fig. 24.1 shows the state characteristics for k = 1.4. Having the state characteristics makes it easier to find the hodograph characteristics and the physical plane characteristics. As in the case of the state characteristics, a single chart of ϕ_t/c_o^2 vs. u/c_o , consisting of a double family of parabolas instead of straight lines, serves to portray all the hodograph characteristics for a given value of k (see Fig. 24.2 of Shapiro for the plot of k = 1.4). Shapiro demonstrates the convenient graphical inter-relationships between the three planes in his Fig. 24.3 and other examples.

Shapiro also presents a purely numerical procedure of stepwise integration of the partial differential equations of the characteristics by the method of finite differences. This approach is necessary where great accuracy is required, but it does not reveal the physical features of a process as do the graphical representations.

5.3 Inflow Through the Flared Open End of a Duct

Properly flaring the open end of a duct permits inflow to occur as an isentropic process. It is interesting to again compare the difference between the pressure drop at the throat, i, (section of minimum area) of the inlet

with a steady flow isentropic process as compared to a simple isentropic wave process. The equations and associated curves are shown on Figure 23. The pressure reduction is shown to be much less for the steady flow process for comparable velocities.

The next problem is to relate the pressure reduction achieved by the isentropic wave process to a distribution of pressure over the inlet. Shapiro (Ref. 11, pp. 963-964) treats inflow through the flared open end of a duct with a workable approximation by assuming that the flow from the atmosphere into the duct can be considered as though it were quasi-steady at each moment of time. That is, he assumes that "when the rate of change of cross-sectional area is very large, the term $\partial u/\partial t$ is negligible compared with the $u\,\partial u/\partial x$ in the Euler equation, and that similar approximations are applicable in the continuity equation." Based on these assumptions, Shapiro writes the energy equation as:

$$T_r = T_i + u_i^2 / 2c_p$$

where subscript r denotes stagnation conditions in the reservoir and subscript i denotes the duct inlet plane. He eliminates T in favor of "a" through the relationship $a = \sqrt{\gamma RT}$ and divides by a_o to obtain dimensionless ratios to get what he calls the equation of the "steady-state ellipse":

$$\left(\frac{a_i}{a_o}\right)^2 + \frac{\gamma - 1}{2}\left(\frac{u_i}{a_o}\right)^2 = \left(\frac{a_r}{a_o}\right)^2 \qquad (5.12)$$

Recall that

$$\frac{a_i}{a_o} = \sqrt{\frac{T_i}{T_o}} = \left(\frac{p_i}{p_o}\right)^{\frac{k-1}{2k}} = \left(\frac{\rho_i}{\rho_o}\right)^{\frac{k-1}{2}} \qquad (5.13)$$

The desired relationship, however, would be one which permits determining the pressure distribution on the inlet flare as a function of the area ratio A/A_i where A_i is the throat or section of minimum cross-sectional area. In his section on the outflow from a reservoir through a converging nozzle, Shapiro presents an expression (pg. 964) which gives the direct isentropic relation between area ratio of the converging section and the velocities:

$$\frac{A_z}{A_y} = \frac{\rho_y}{\rho_z}\frac{u_y}{u_z} = \left(\frac{a_y}{a_z}\right)^{\frac{2}{k-1}} \frac{u_y}{u_z}$$

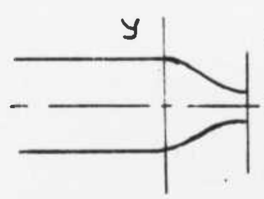

(5.14)

Then from the following isentropic wave relationship, the pressure at various area ratios could be calculated:

$$\frac{p_z}{p_y} = \left(\frac{a_z}{a_y}\right)^{\frac{2k}{k-1}} = \left[1 \pm \frac{k-1}{2}\left(\frac{u_z}{c_y} - \frac{u_y}{c_y}\right)\right]^{\frac{2k}{k-1}} \qquad (5.15)$$

where y is the starting condition when the gas is initially at rest.

But since $\left(\frac{\rho_i}{\rho_o}\right)^{\frac{k-1}{2}} = \left(\frac{p_i}{p_o}\right)^{\frac{k-1}{2k}}$,

it follows that $\frac{\rho_i}{\rho_o} = \left(\frac{p_i}{p_o}\right)^{1/k}$

so we substitute and thus modify Shapiro's expression to directly express the desired relationship between the area ratio and the pressure ratio as

$$\frac{A_z}{A_y} = \left(\frac{p_y}{p_z}\right)^{1/k} \frac{u_y}{u_z} = \left(\frac{c_y}{c_z}\right)^{\frac{2}{k-1}} \frac{u_y}{u_z} \qquad (5.16)$$

With preliminary study it appears that although this area ratio expression was derived for application to the nozzle outflow condition, it may be satisfactorily applied to the condition of inflow from static conditions in the atmosphere. Further effort will be devoted to checking these expressions to see how well they apply. It is most important to continue the "instantaneous" pressure measurements in conjunction with interface velocity measurements in order to find out how different the actual situation is from the theoretical so that the latter can be modified for a better fit.

5.4 Wave Reflection at a Contact Discontinuity

With the final fact that a compression wave is partially transmitted and partially reflected at a contact (temperature) discontinuity, such as the interface between hot and cold gases, as described in Shapiro, pp. 969-971, and Rudinger, pp. 87-94, most of the tools for analysis of the phenomenon seem to be at hand.

It now remains to check how much the jet piston acts like a solid piston in creating a compression wave ahead of it and a following rarefaction wave. The initial pressure readings in the throat (Fig. 14c) show pressures considerably lower than the "solid piston" case.

6. REFERENCES

1. Lockwood, R.M.: "Proposal for Development of an Augmented Valveless Pulsejet Lift-Propulsion System," Hiller Aircraft Corporation Report No. ARD-196, May 1958.

2. Lockwood, R.M.: "Proposal for Investigation of the Process of Energy Transfer from an Intermittent Jet to Ambient Fluid," Hiller Aircraft Corporation Report No. ARD-199, May 1958.

3. Lockwood, R.M.: "Investigation of the Process of Energy Transfer from an Intermittent Jet to Ambient Fluid - Summary Report," Hiller Aircraft Corporation Report No. ARD-238, June 1959.

4. Lockwood, R.M., Sargent, E.R. and Beckett, J.E.: "Thrust Augmented Intermittent Jet Lift-Propulsion System - 'Pulse Reactor'" - Final Report - Hiller Aircraft Corporation Report ARD-256, February 1960.

5. Rudinger, George: Wave Diagrams for Nonsteady Flow in Ducts, D. Van Nostrand Co., Inc., Princeton, N. J., 1955.

6. Kantrowitz, A.: "One-Dimensional Treatment of Nonsteady Gas Dynamics," High Speed Aerodynamics and Jet Propulsion, Vol. III, "Fundamentals of Gas Dynamics," Section C, Princeton University Press, 1958.

7. Foa, Joseph V.: "Pressure Exchange," Applied Mechanics Reviews, Vol. No. 12, December 1958, pp. 655-657.

8. Foa, Joseph V.: "A New Method of Energy Exchange Between Flows and Some of its Applications," Rensselaer Polytechnic Institute, Tech. Report TR AE5509, 1955.

9. Marlow, D. G., Nisewanger, C.R. and Cady, W.M.: "A Method for the Instantaneous Measurement of Velocity and Temperature in High Speed Air Flow," Journal of Applied Physics, Vol. 20, August 1949, pp. 771-776 incl.

10. Kuchemann, D., and Weber, J.: Aerodynamics of Propulsion, McGraw-Hill Book Company, Inc., New York, 1953, 340 pp.

11. Shapiro, Ascher H.: The Dynamics and Thermodynamics of Compressible Fluid Flow, Vol. II, Ronald Press Co., New York, 1954, 534 pp.

12. Lockwood, R.M. and Sargent, E.R.: "Direct Lift Propulsion Research," Hiller Helicopters Engineering Report No. 533.3, 1955.

13. Elias, P.: "Flame and Particle Motions in a Small Pulse Jet Engine," Project SQUID Technical Report No. 16, New York University, 1948.

14. Lockwood, R.M.: "Pulsejet Ejectors," a thesis for the Professional Degree of Mechanical Engineer, Oregon State College, Corvallis, Ore., 1953.

15. Baker, D.W.: "Seventh Partial Report on the Pulsejet Engine; Measurement of the Air-Fuel Ratio," U.S. Naval Research Laboratory, Washington, D.C., Report No. 3741, October 1950.

16. Fyfe, I.M., and Klotter, K.: "Nonlinear Problems of One-Dimensional Wave Propagation in Gases (Treated by the Ritz Method)", Stanford University, Stanford, California, 66 p. incl. illus. tables, 14 refs. (proj. 7210; Task 71706) (WADC-TR-58-293) (Contract No. AF 33(616)-3490)- Unclassified- August 1958.

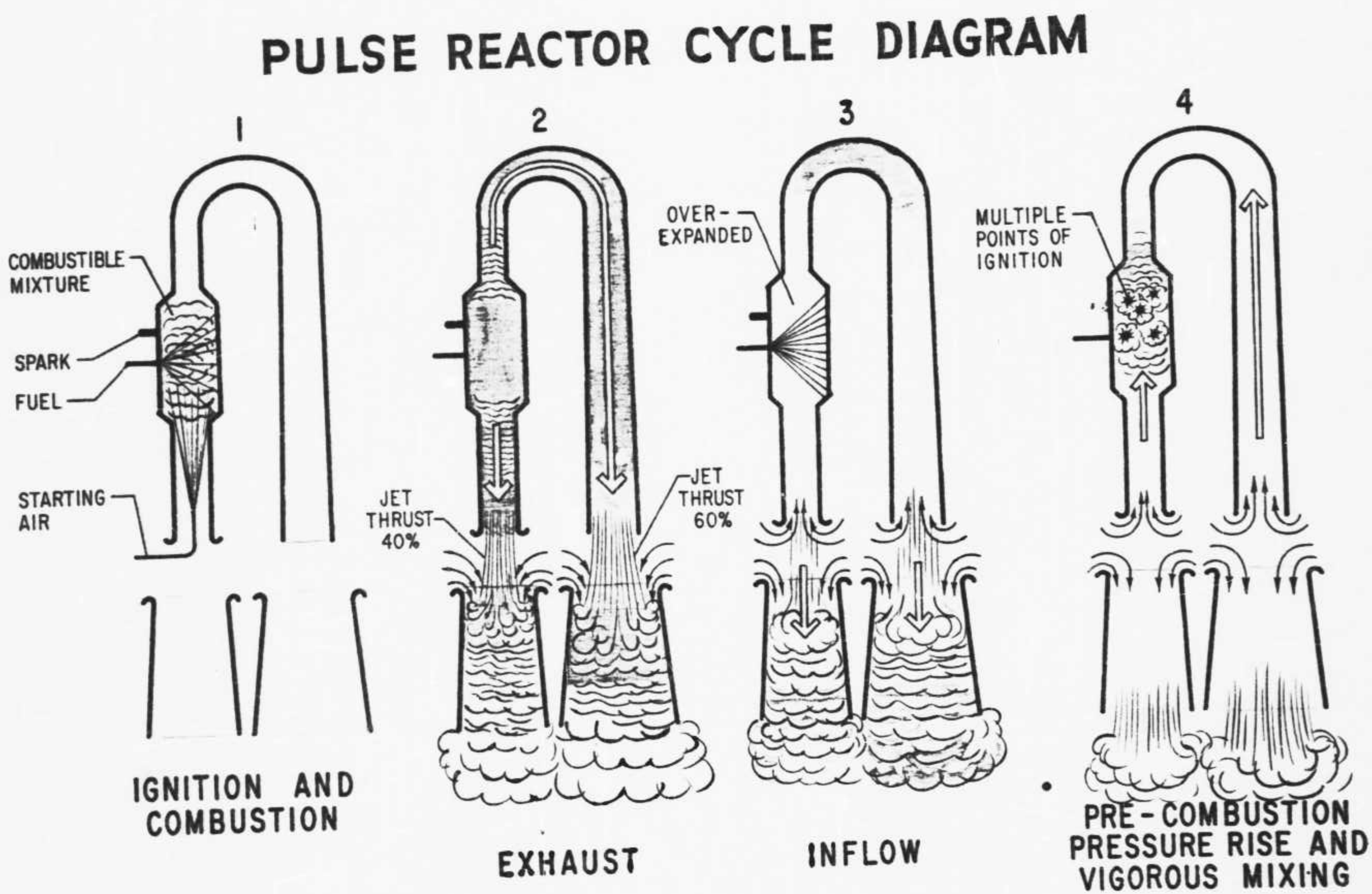
PULSE REACTOR CYCLE DIAGRAM
1
2
3
4
COMBUSTIBLE MIXTURE
SPARK
FUEL
STARTING AIR
JET THRUST 40%
JET THRUST 60%
OVER-EXPANDED
MULTIPLE POINTS OF IGNITION
IGNITION AND COMBUSTION
EXHAUST
INFLOW
PRE-COMBUSTION PRESSURE RISE AND VIGOROUS MIXING

FIGURE 1

AUGMENTER PERFORMANCE

COMPARISON OF STEADY and INTERMITTENT JET FLOW

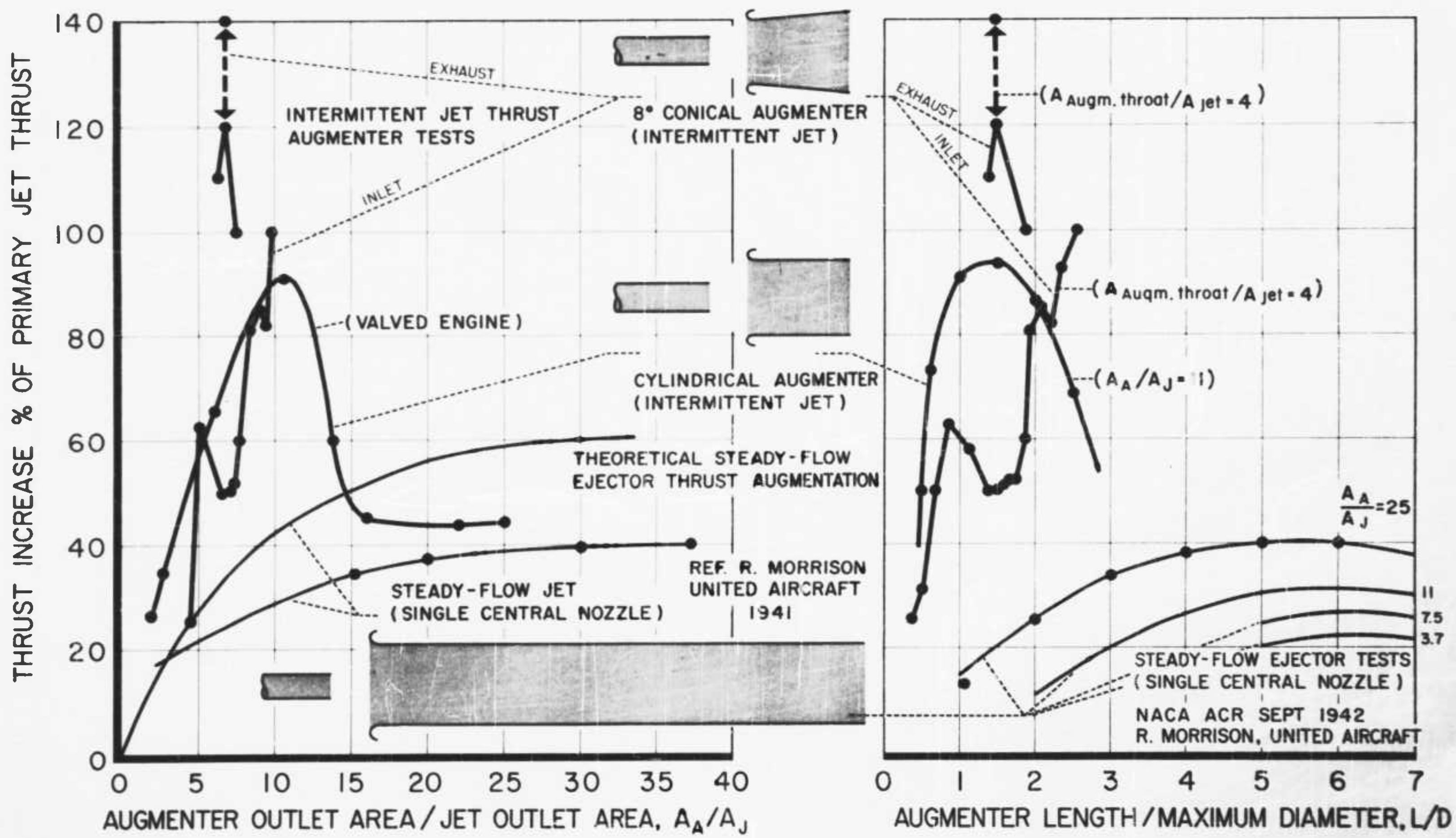

FIGURE 2

FIGURE 3. PULSE REACTOR SCALE MODEL

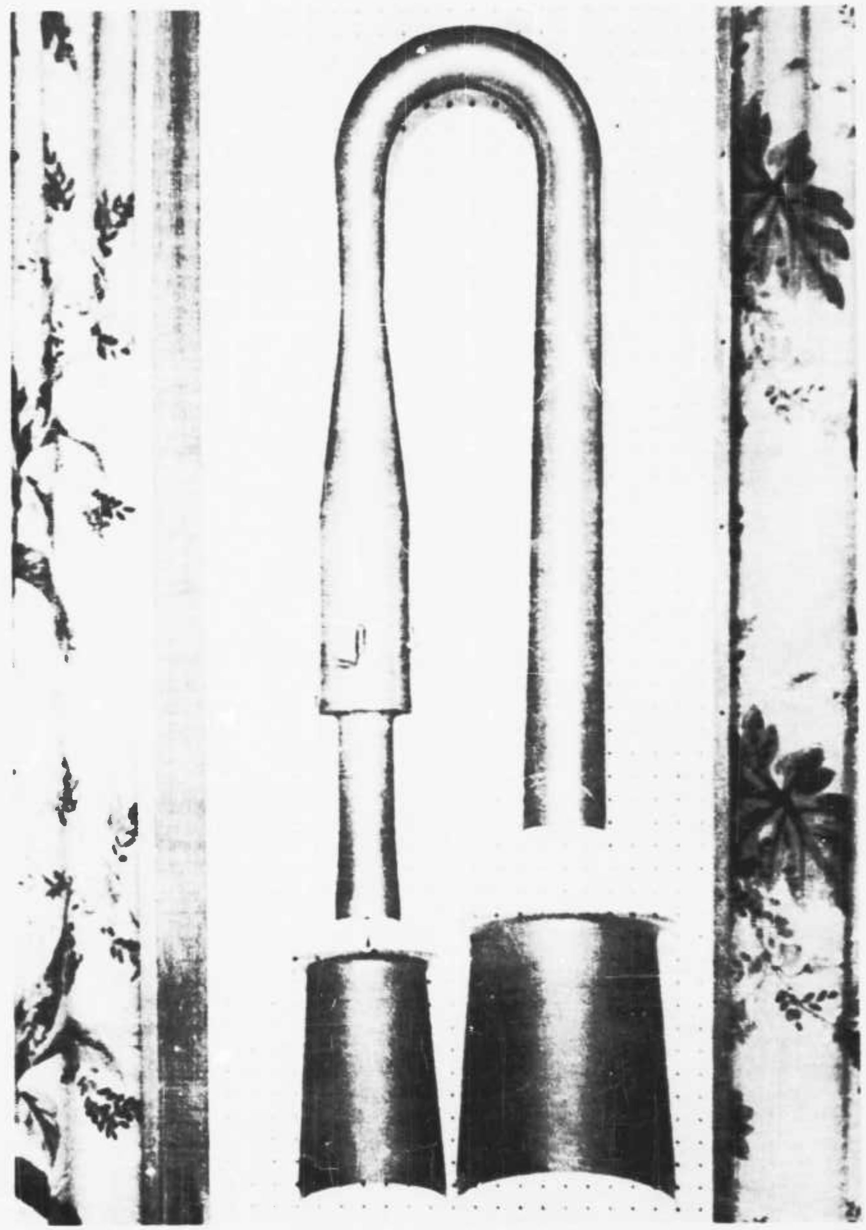

FIGURE 4. PULSE REACTOR CUTAWAY MODEL

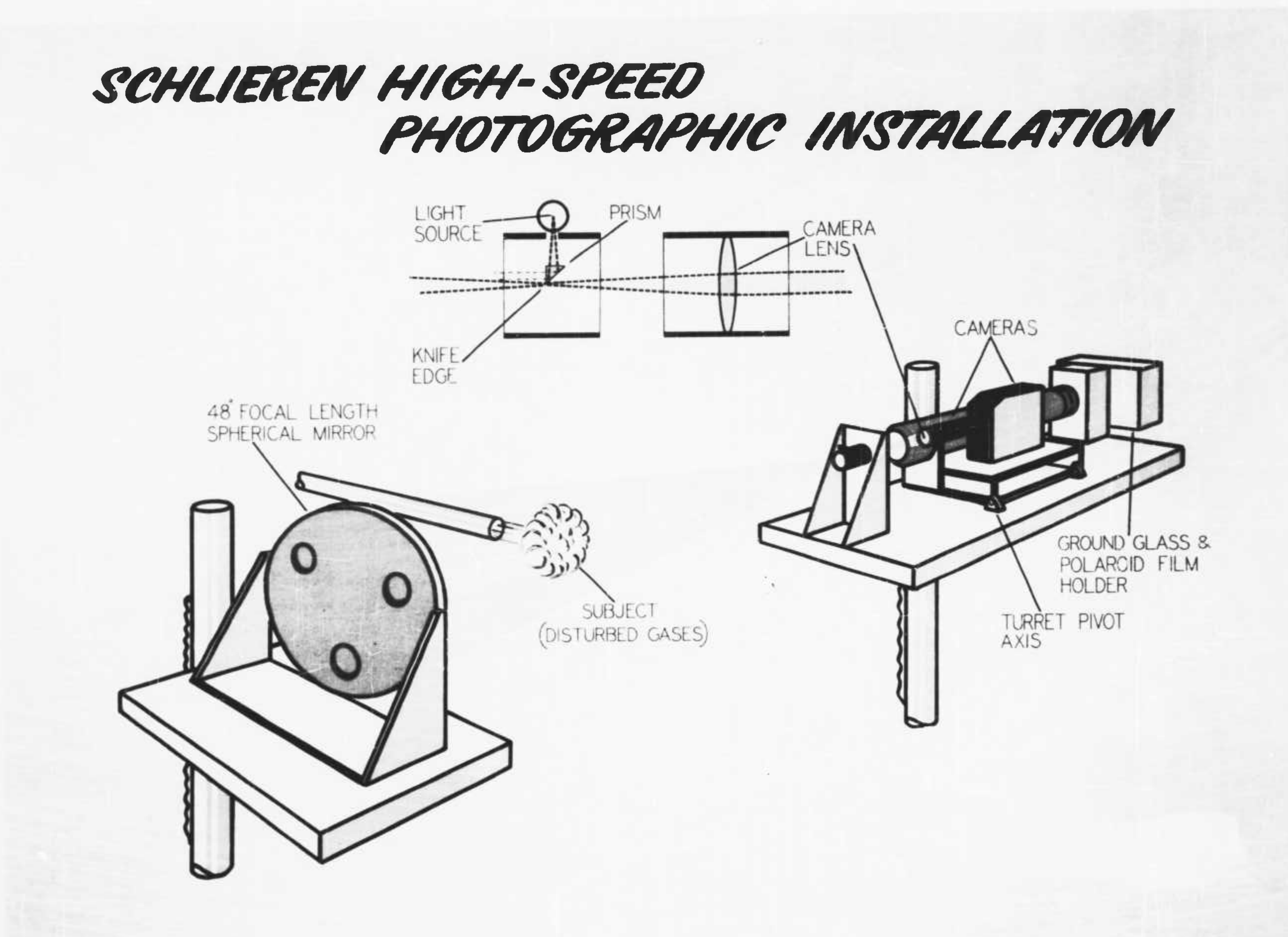
SCHLIEREN HIGH-SPEED
PHOTOGRAPHIC INSTALLATION
LIGHT SOURCE
PRISM
CAMERA LENS
KNIFE EDGE
CAMERAS
48" FOCAL LENGTH SPHERICAL MIRROR
SUBJECT (DISTURBED GASES)
GROUND GLASS & POLAROID FILM HOLDER
TURRET PIVOT AXIS

FIGURE 5a

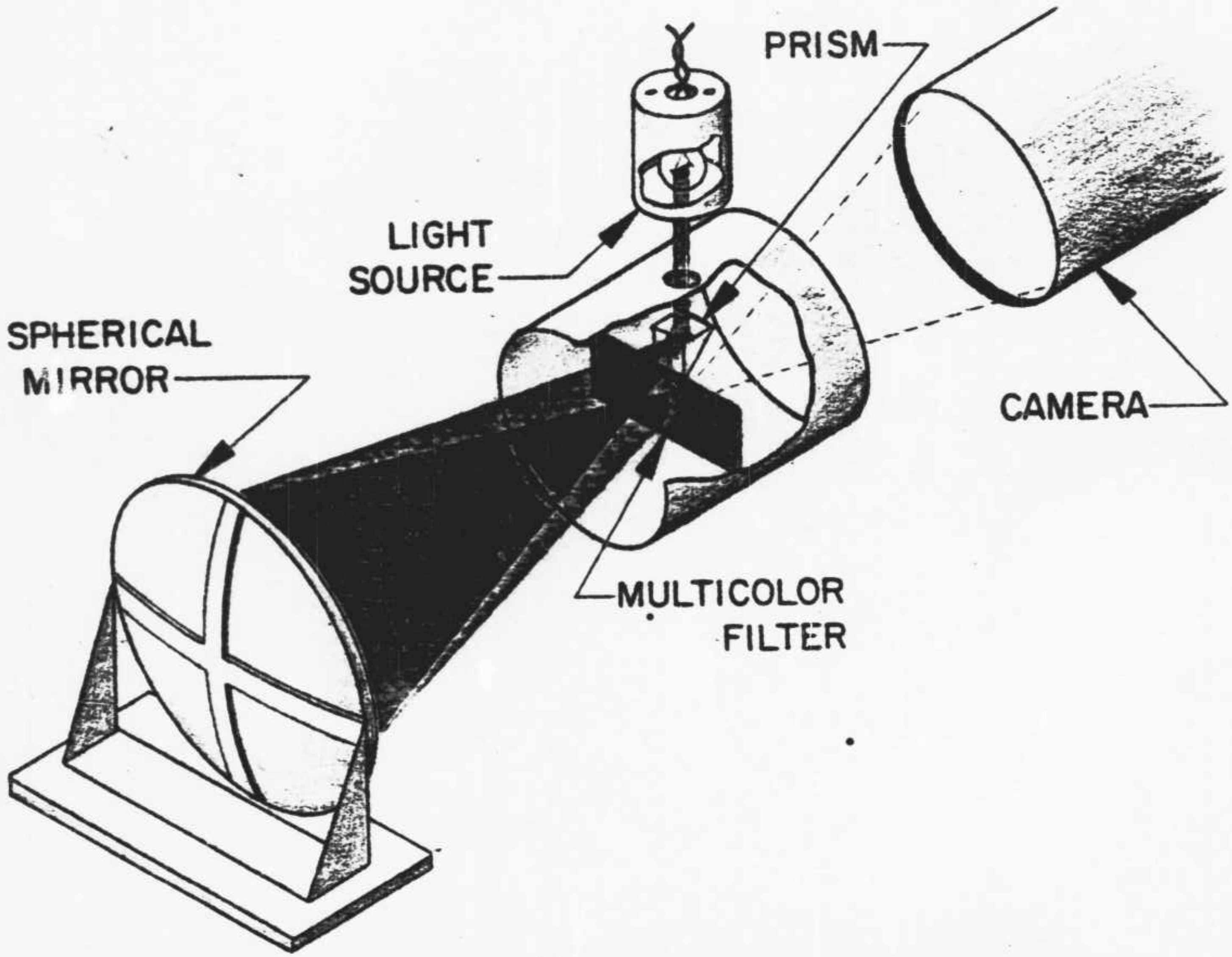

COLOR MODIFICATION TO SCHLIEREN PHOTOGRAPHIC INSTALLATION

FIGURE 5b

FIGURE 6a: INTERMITTENT JET ENERGY TRANSFER TEST SETUP SHOWING COMPONENTS FOR FLOW VISUALIZATION AND SIMULTANEOUS PRESSURE, VELOCITY, THRUST, AND FLOW-RATE MEASUREMENTS.

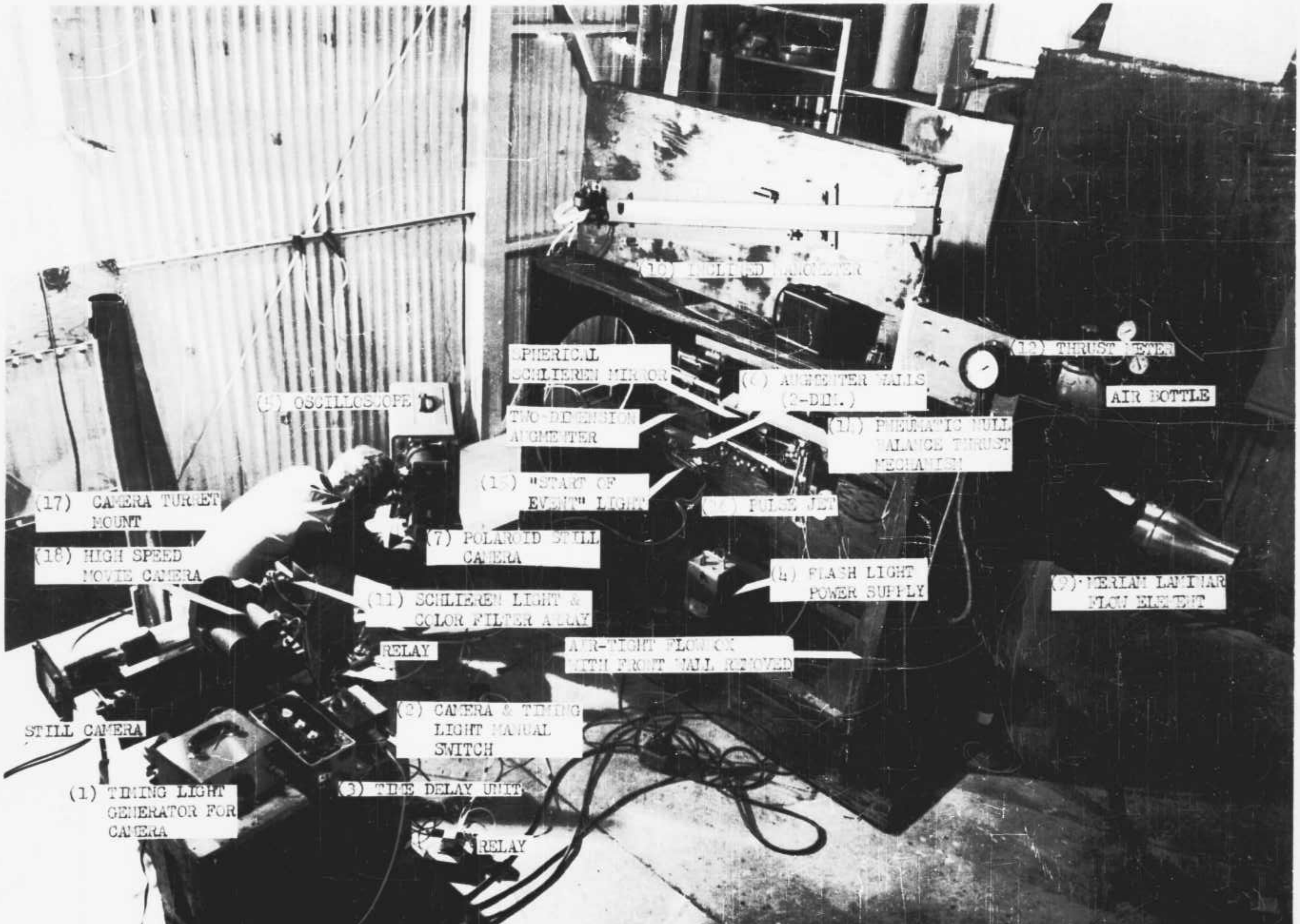

Fig. 6b INTERMITTENT JET ENERGY TRANSFER TEST SETUP SHOWING COMPONENTS FOR FLOW VISUALIZATION AND SIMULTANEOUS PRESSURE, VELOCITY, THRUST, AND FLOW-RATE MEASUREMENTS

1. Timing Light Generator, 100 to 1000 cps, Model HS 10500, Fairchild Camera and Inst. Corp., Los Angeles, Calif.
2. Camera Control Unit and Time Delay Model 10500, Fairchild Camera and Inst. Corp., Los Angeles, Calif.
3. Electronic Decade Interval Timer, Model TM-8, Lektra Labs. Inc., New York, N.Y.
4. High Speed Mercury-Arc Flash Light Power Supply. "Start of Event Light", Company Manufactured.
5. Oscilloscope, 2 ea. Model 130A, Hewlett Packard, Palo Alto, California.
6. Round Glass Plates, 12" Dia. and 1¼" thick, schlieren quality, Tinsley Laboratories, Berkeley, Calif.
7. Fairchild Polaroid, Oscilloscope Camera, Model F-284, Serial No. 259, Fairchild Camera and Instrument Corporation, Jamaica, N. Y.
8. Two thermocouples Nanmac Type G "Pencil Probe" Platinum 10% Rhodium, Namac Corp., Indian Head, Maryland.
9. Meriam Laminar Flow Element, Model 50MC2-45 (4" @ 200 CFM, 8" @ 400 CFM), G.M. Cooke Company, Berkeley, Calif.
10. Precision Inclined Water Manometer, 48" Long-Range to 10" H_2O Model 40 HALCWM, Stainless Steel Trim, G. M. Cooke Company, Berkeley, California.
11. Color Schlieren System Filter Array, Action Industrial Photo, Santa Clara, California. (13 color bands).
12. Thrust Meter, Pressure Gage, 1 lb. Sub. Div. 1 lb. Per Square Inch, Crosby, Boston, USA.
13. 6"W x 11-7/8" x 1¼" Thick Glass Plates, schlieren Quality, Tinsley Laboratories, Berkeley, California.
14. Pneumatic Null-Balance Thrust Mechanism, Company Manufactured.
15. Mercury-Arc Lamp, No. BH-6, General Electric
16. Dyna-Jet Engine, 1-1/8" Tailpipe Diameter, 1-3/8" Flare Diameter.
17. Drill Press Stand (2), Delta No. 17-205, Less Head.
18. Motion Analysis Camera (1), Model No. 2-4263, No. HS 101 Ind., Fairchild Camera and Instrument Company.

FIGURE 6c: Equipment shown in Figure 6a.

PULSE REACTOR PERFORMANCE

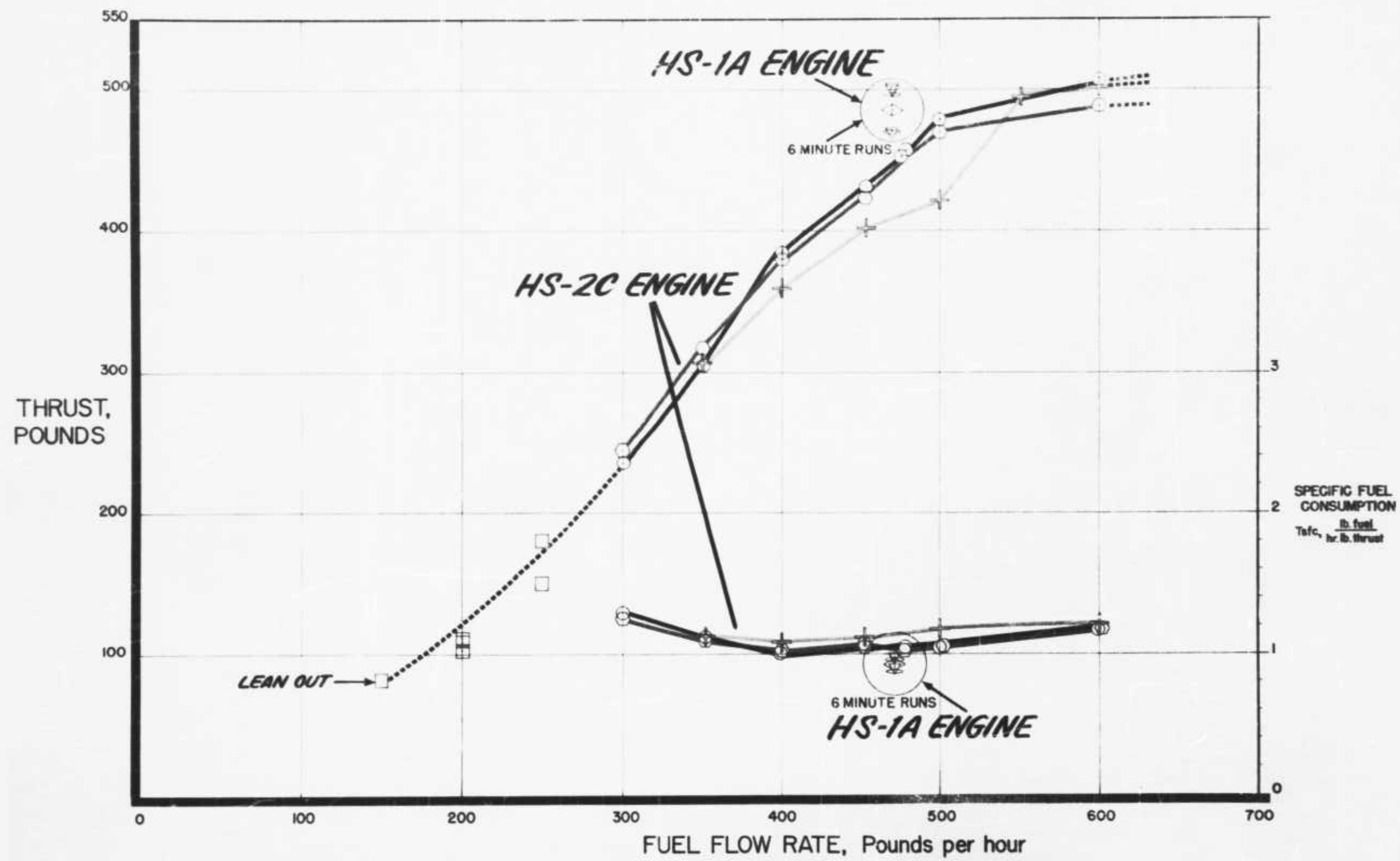

FIGURE 7

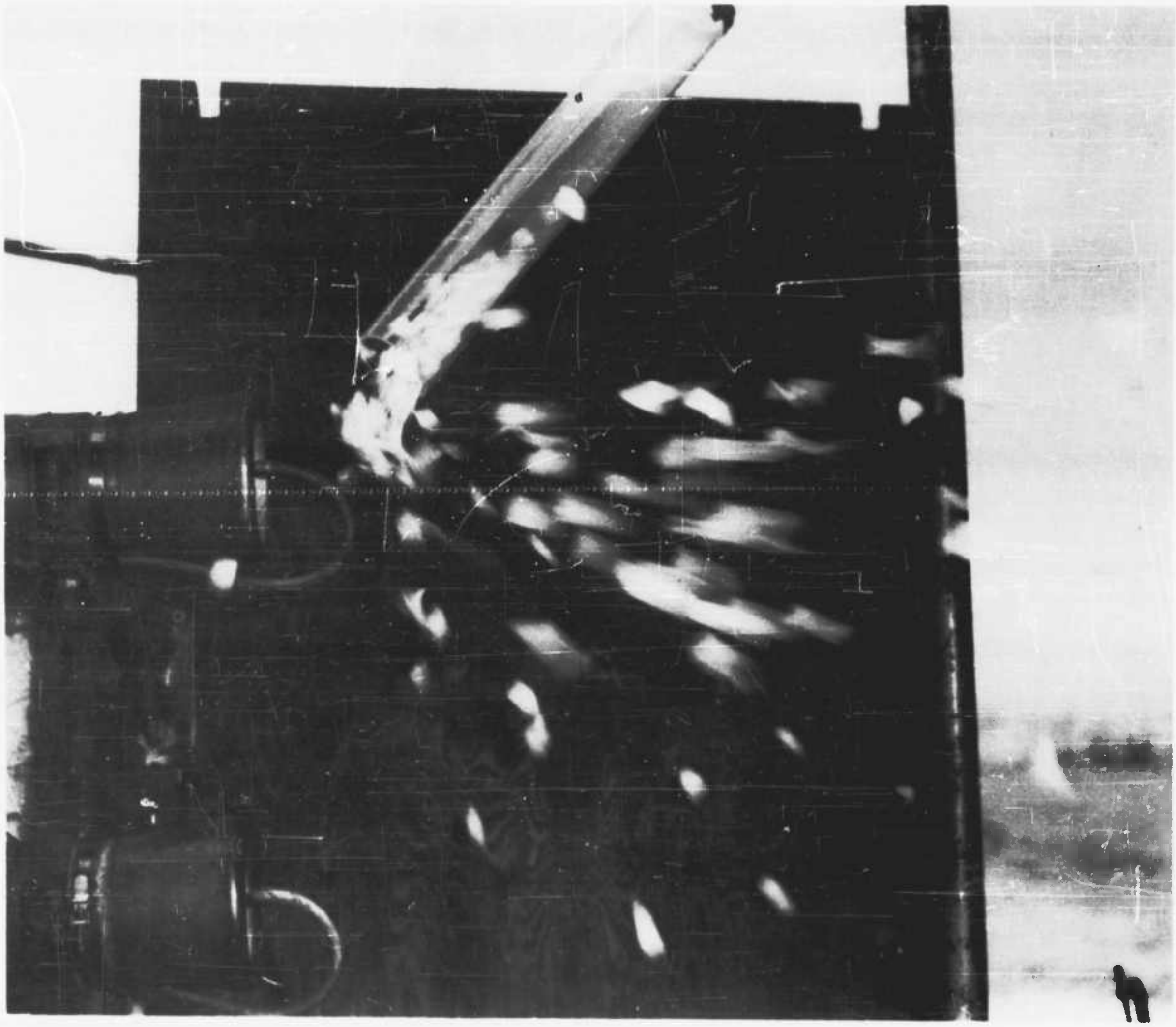

FIGURE 8: PULSE REACTOR FLOW PATTERN REJECTING ROCKS DUMPED DOWN CHUTE TOWARDS AIR INLET

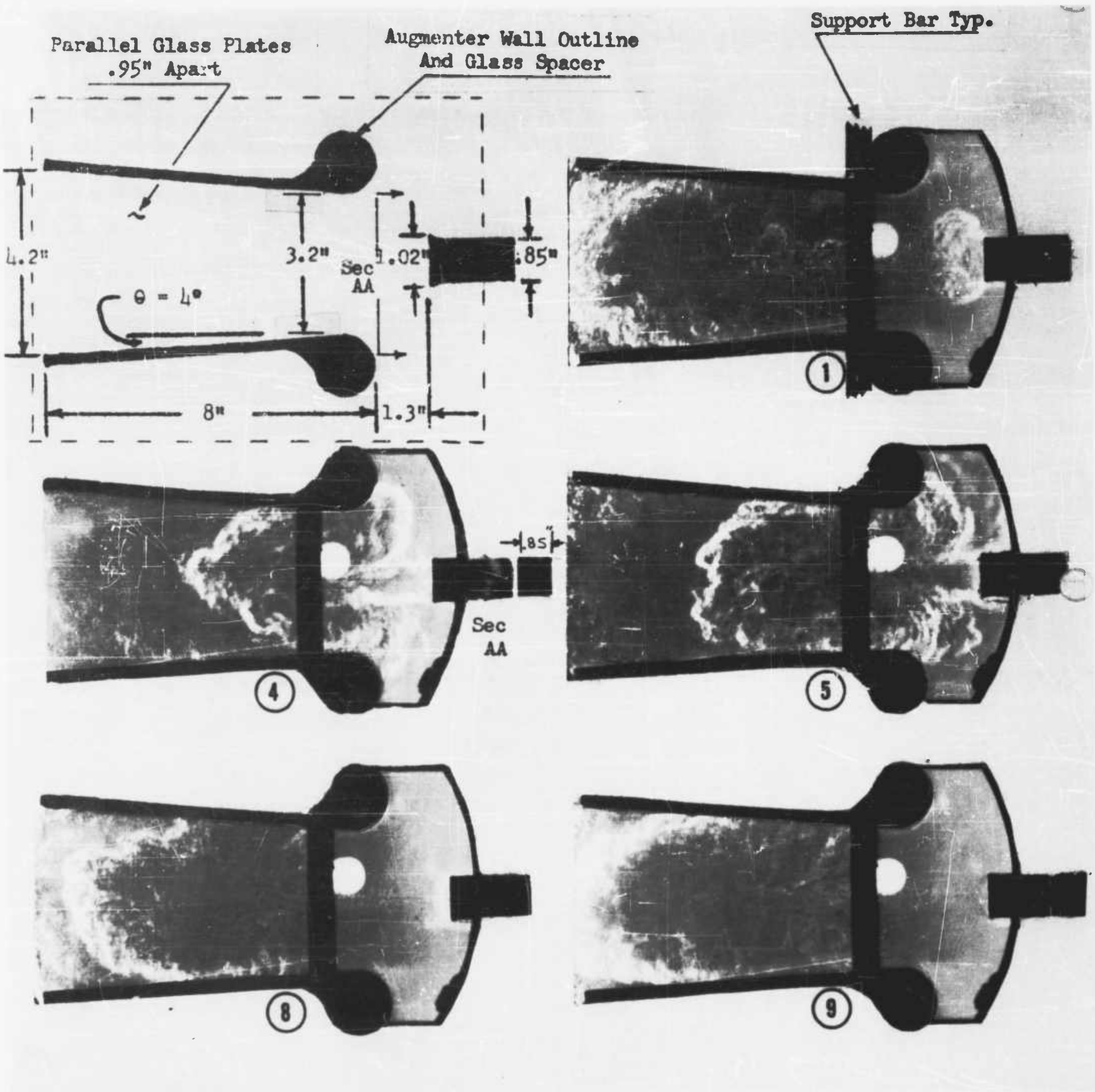

FIGURE 9: SCHLIEREN FLASH PHOTO SEQUENCES OF BASIC VALVED PULSEJET AUGMENTER CYCLE, (FROM RANDOM SHOTS OF EXHAUST,) OPERATING FREQUENCY 300+ C.P.S.

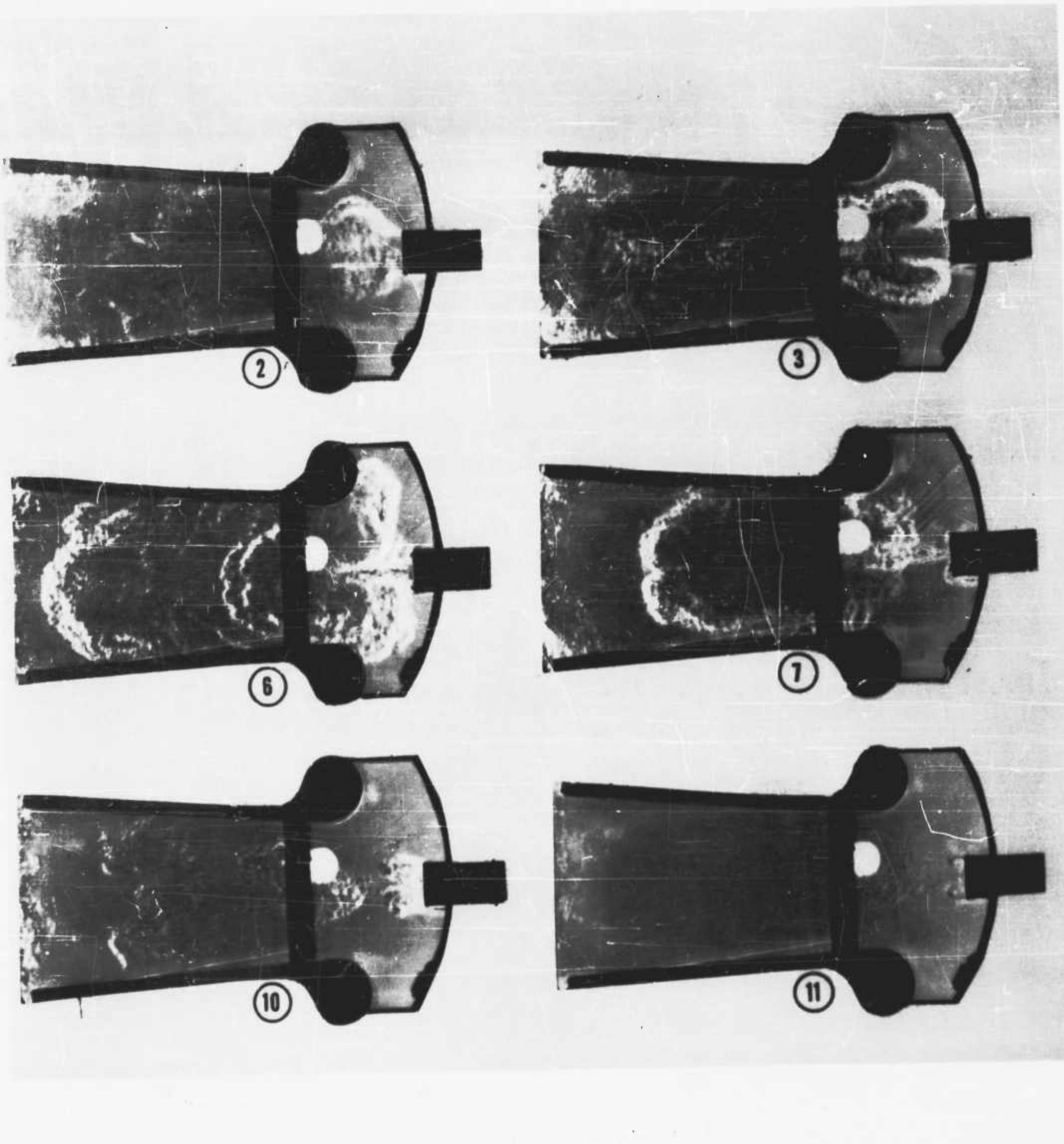
2
3
6
7
10
11

CAM SHAPES FOR 5:1 AND 1/1 RATIOS OF
PISTON EFFLUX TO INFLOW VELOCITY

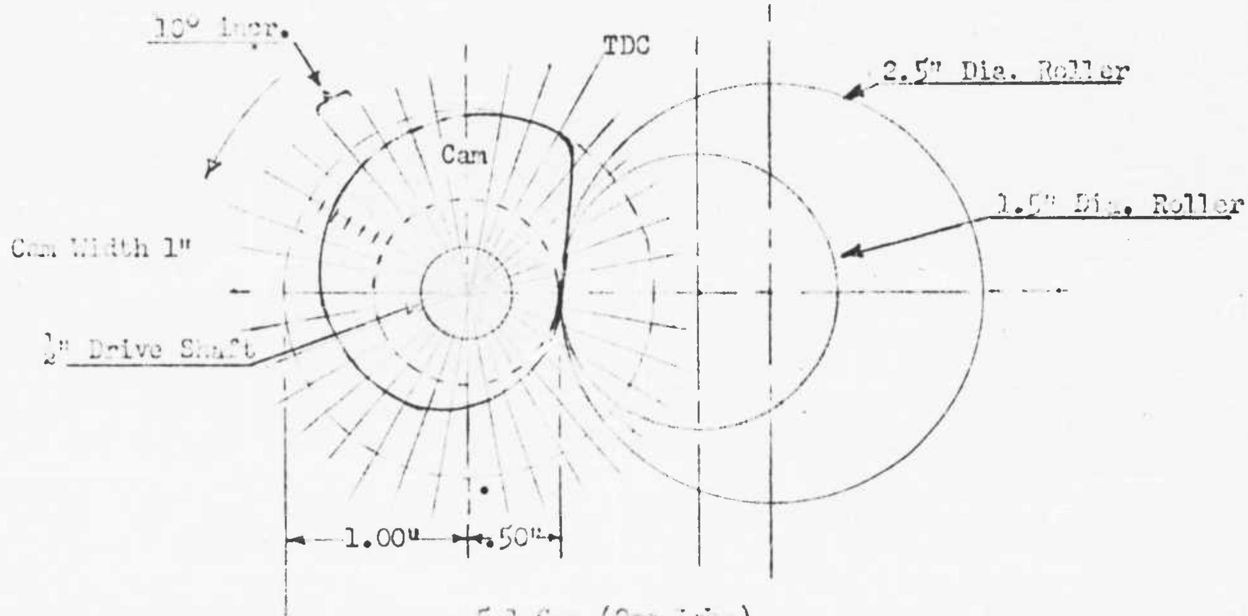

5:1 Cam (One Lobe)

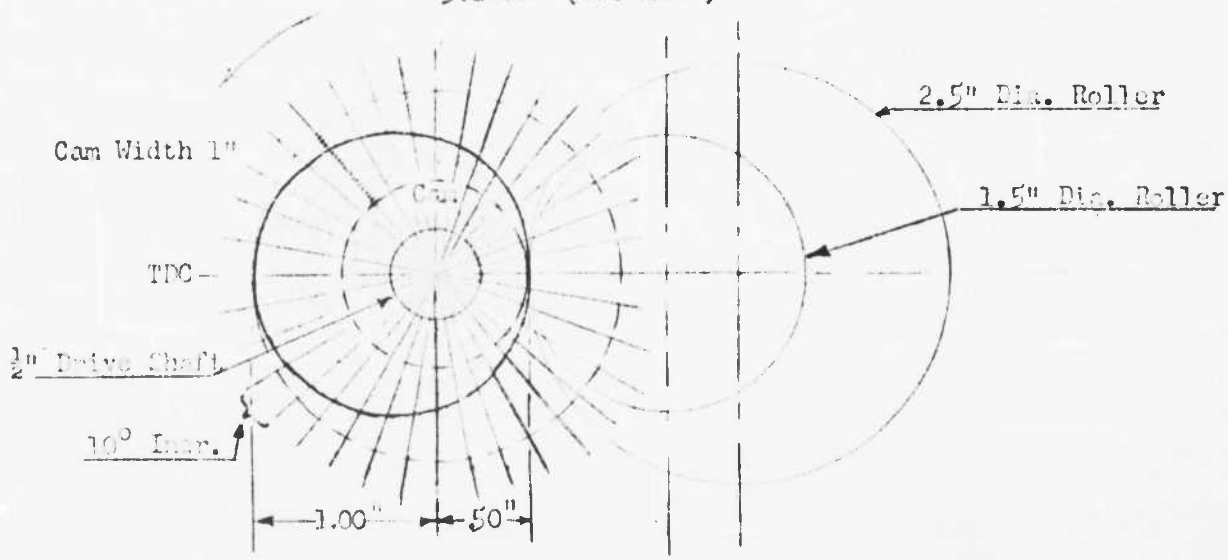

1.1 Cam (Symm - One Lobe)

FIGURE 10

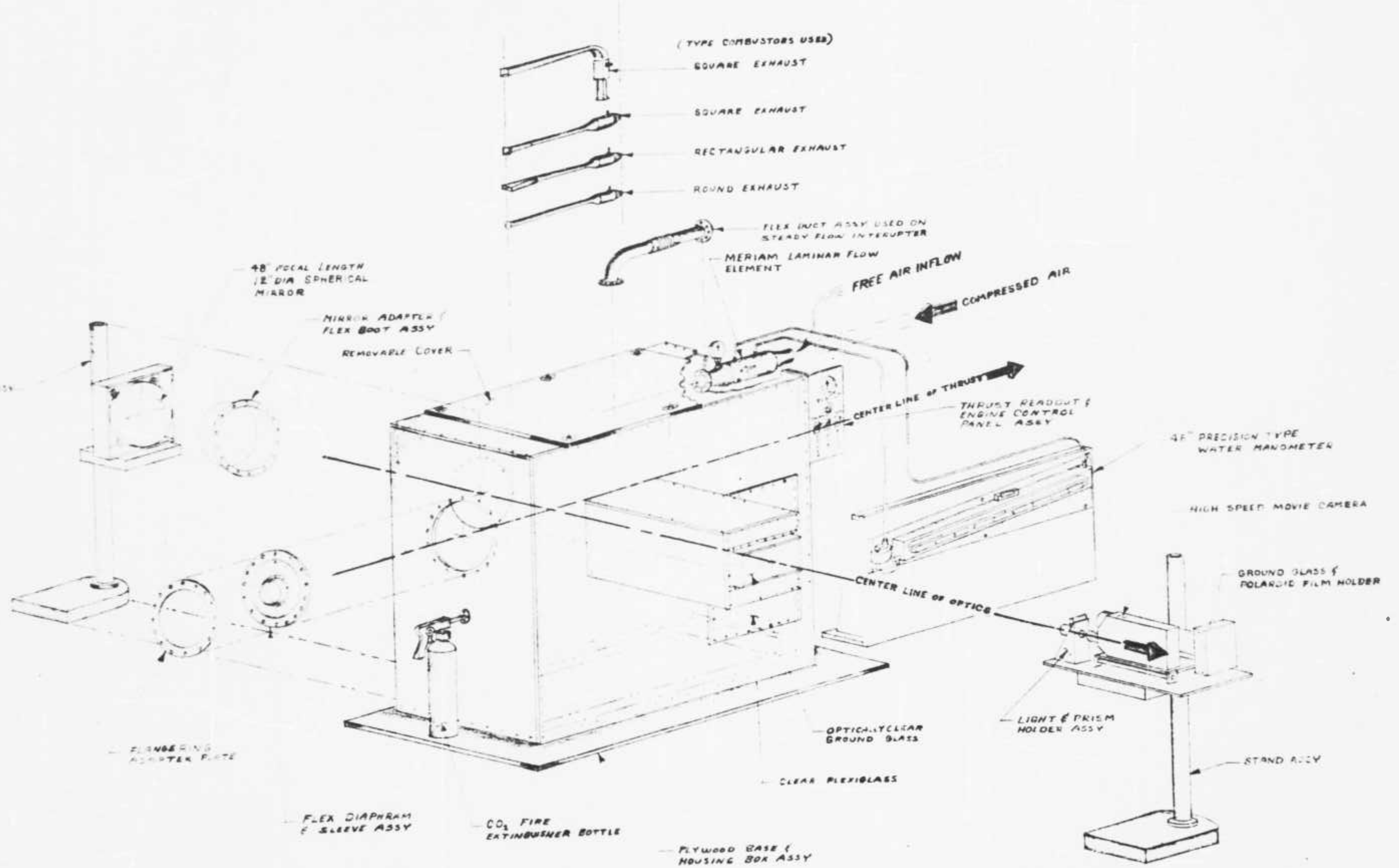

FIGURE 11a AIR-TIGHT FLOW CELL FOR MEASURING INTERMITTENT FLOW AND SCHLIEREN PHOTOGRAPHIC SETUP FOR FLOW VISUALIZATION AND FLOW VELOCITY MEASUREMENT.

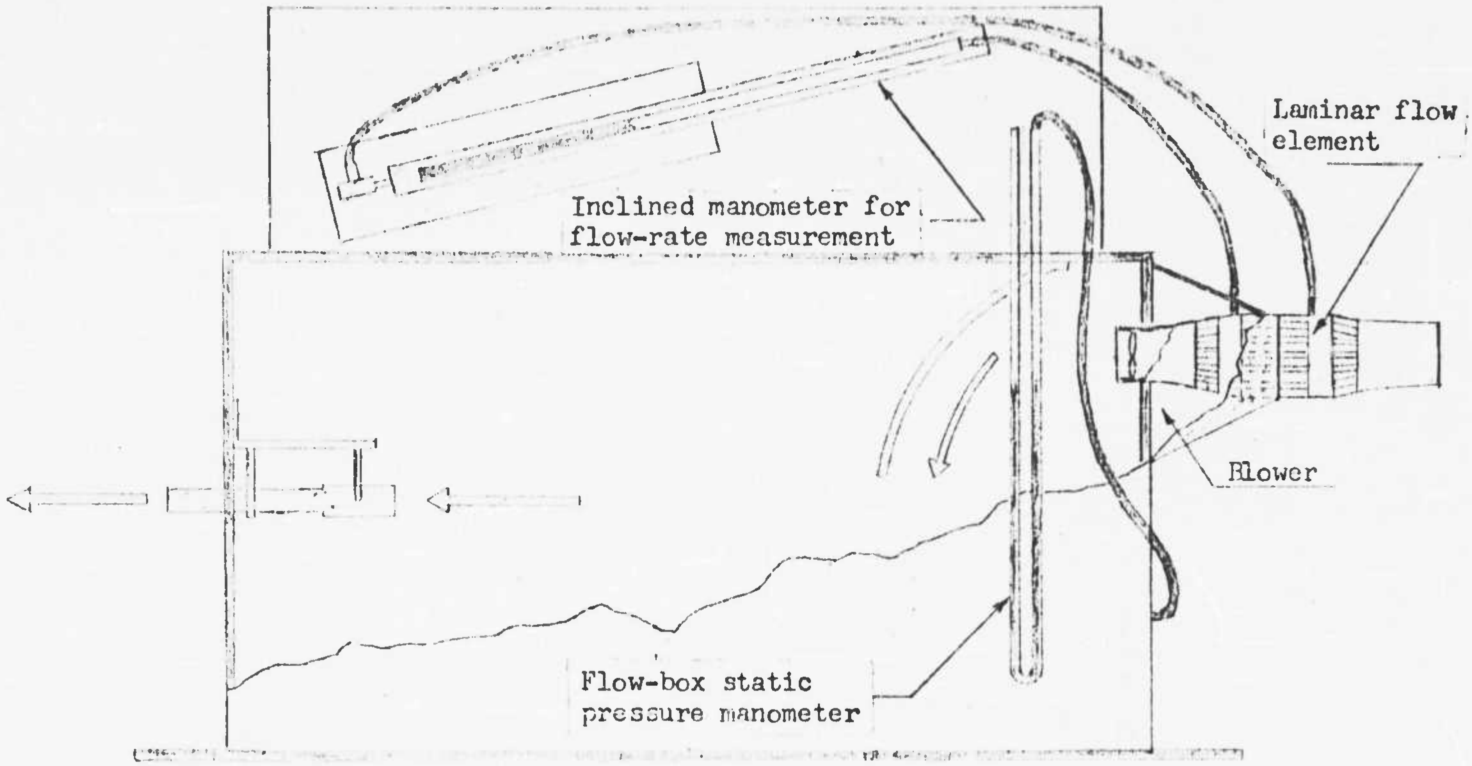

Test Setup For Air Flow Rate of Pulsejet Only

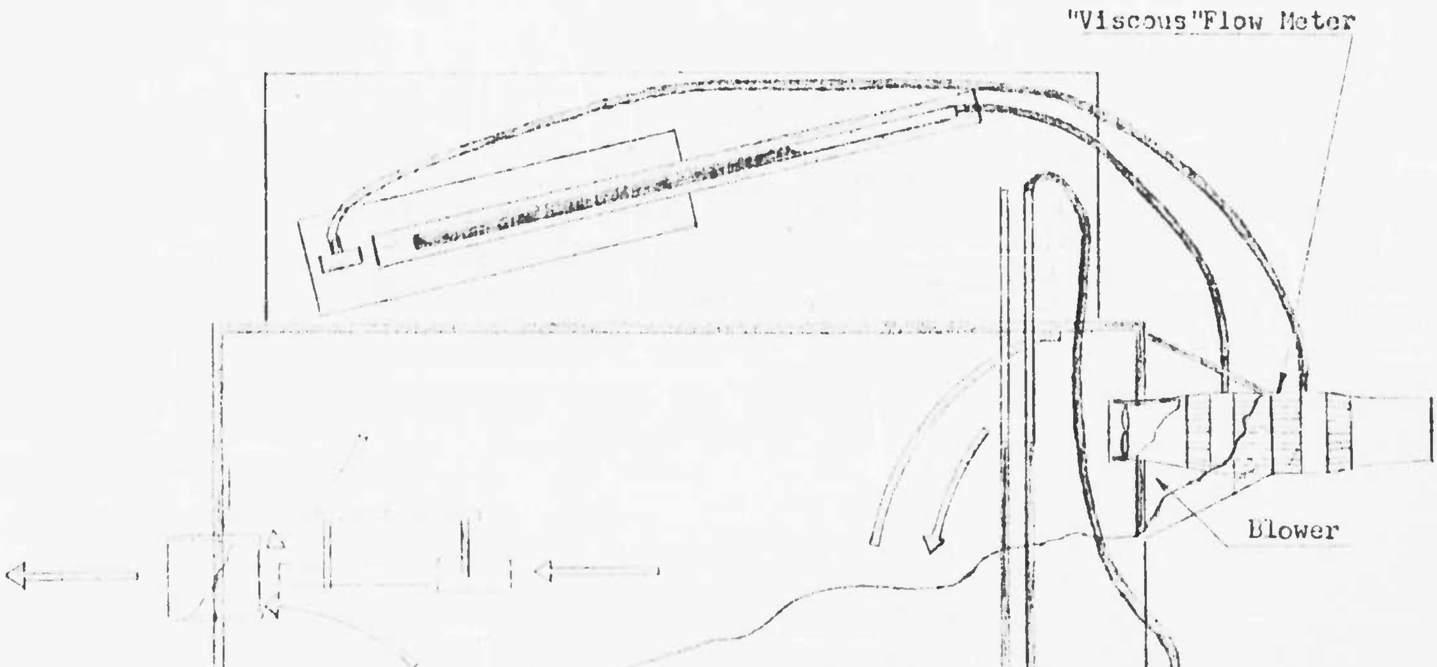

Test Setup for Combined Air Flow Rate of Pulsejet and Thrust Augmenter

FIGURE 11b AIR-TIGHT FLOW BOX FOR MEASUREMENT OF UNSTEADY FLOWS WITH "VISCOUS" FLOW METER

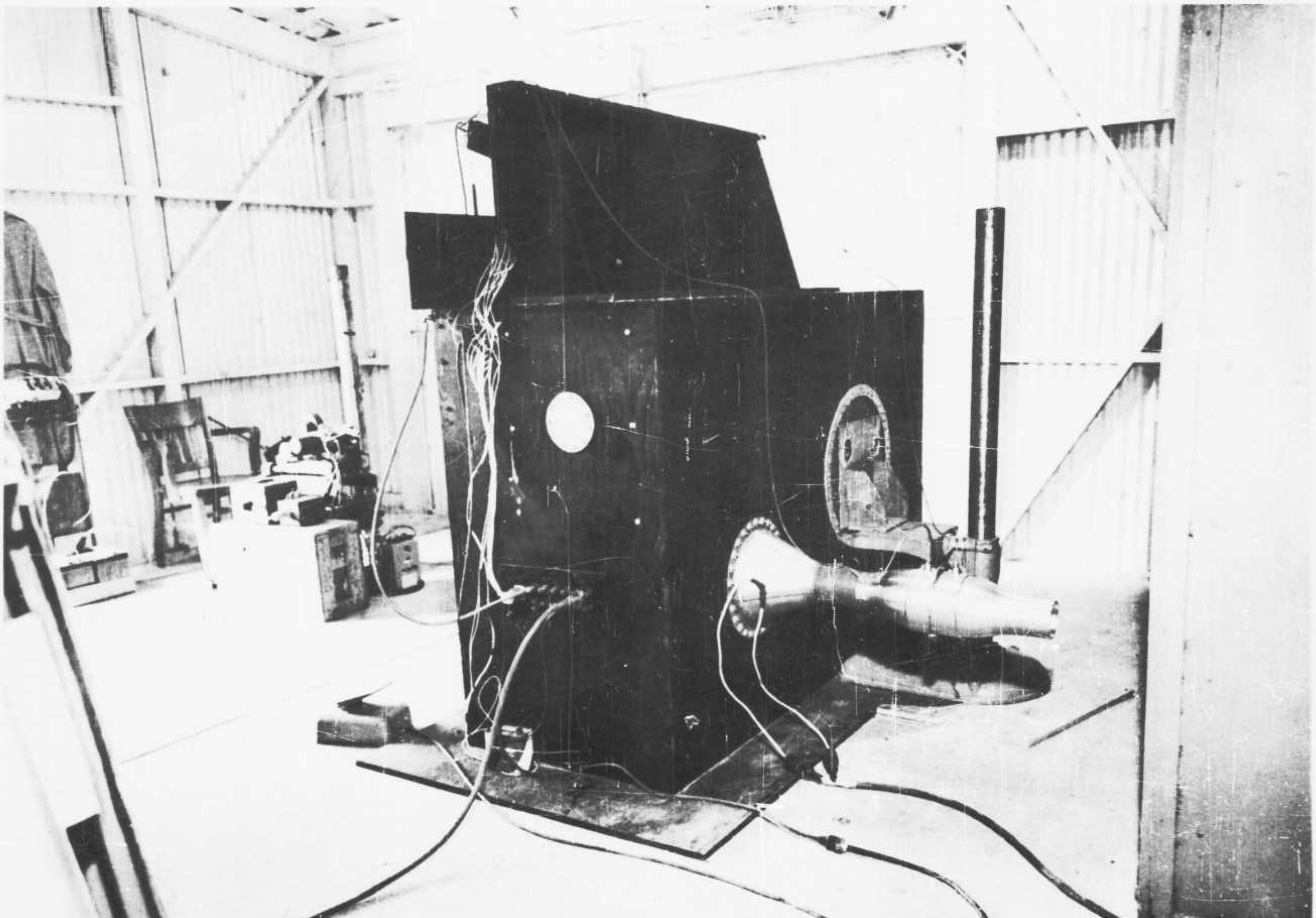

FIGURE 11c: BACK SIDE OF INTERMITTENT JET FLOW CELL AND FLOW VISUALIZATION TEST RIG. NOTE "LAMINAR" FLOW METER IN FOREGROUND AND RUBBER DIAPHRAGM BEHIND ON BACKWALL TO SEAL SPHERICAL SCHLIEREN MIRROR TO FLOW BOX.

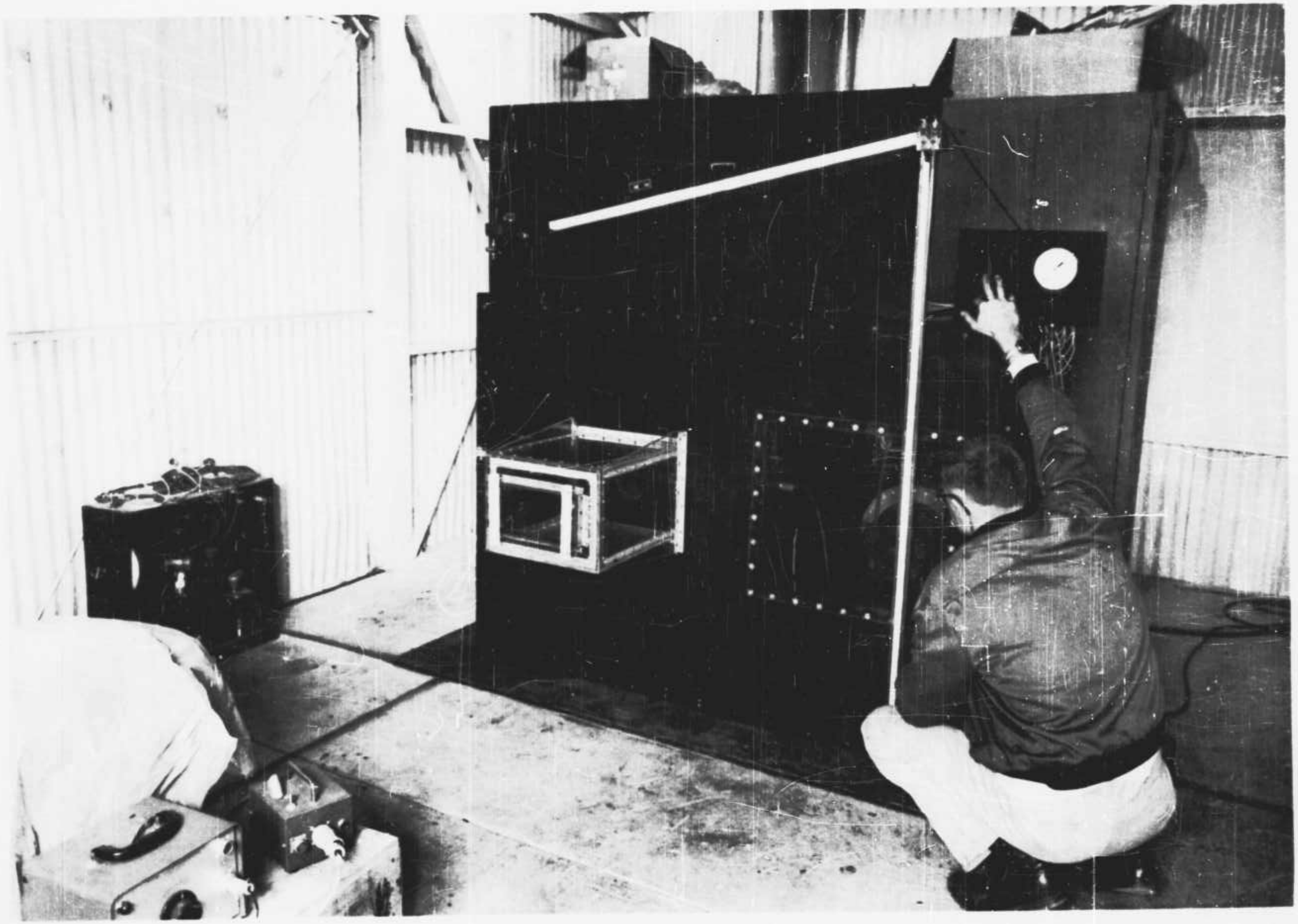

FIGURE 11d: FRONT SIDE OF INTERMITTENT JET FLOW CELL AND FLOW VISUALIZATION TEST RIG. NOTE TIMING LIGHT GENERATOR AND MOTION PICTURE CAMERA CONTROL BOX IN LOWER LEFT FOREGROUND.

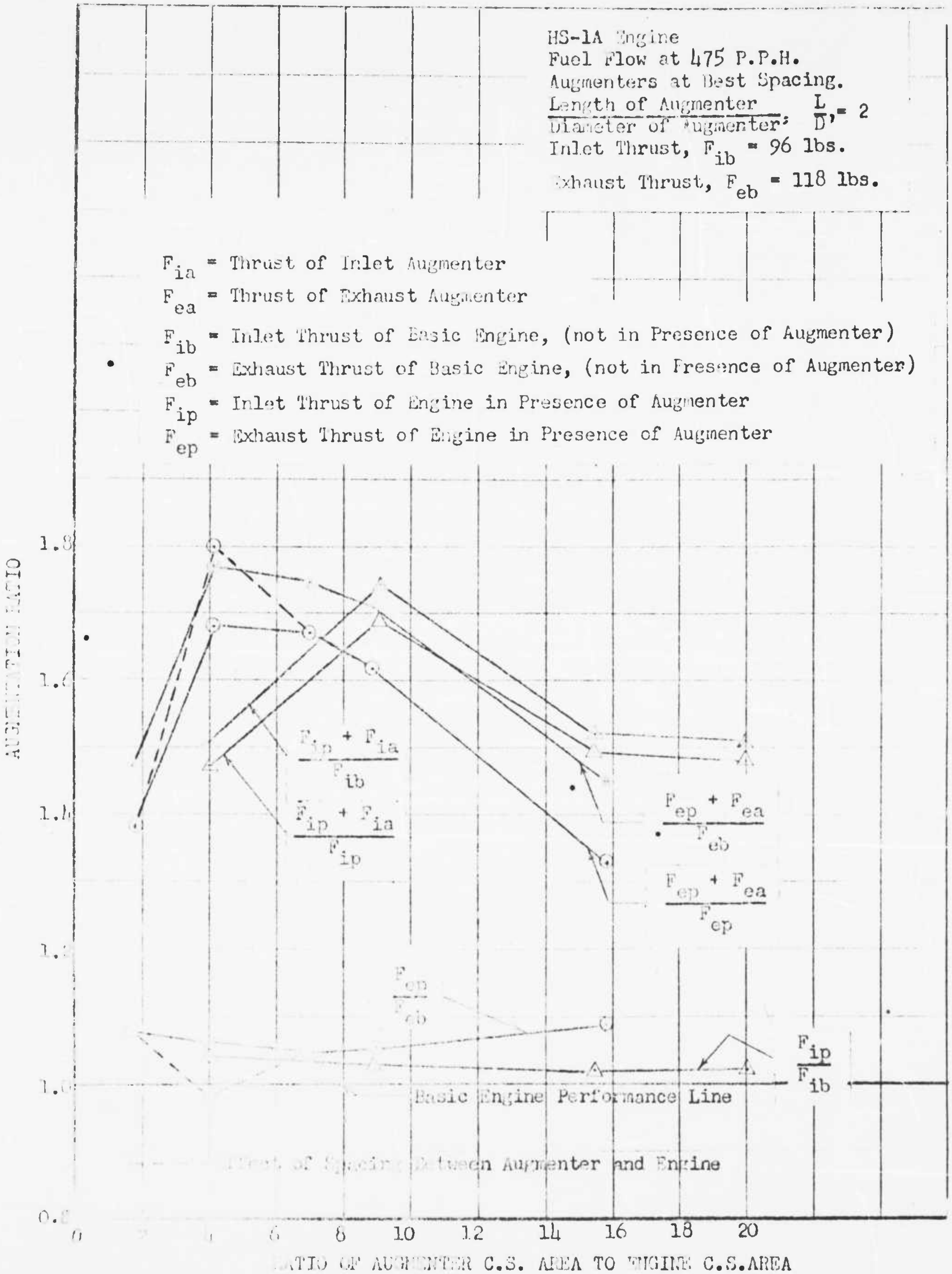

FIGURE 12 PERFORMANCE OF CYLINDRICAL AUGMENTERS
(Extracted from ARD-256, Fig. 15)

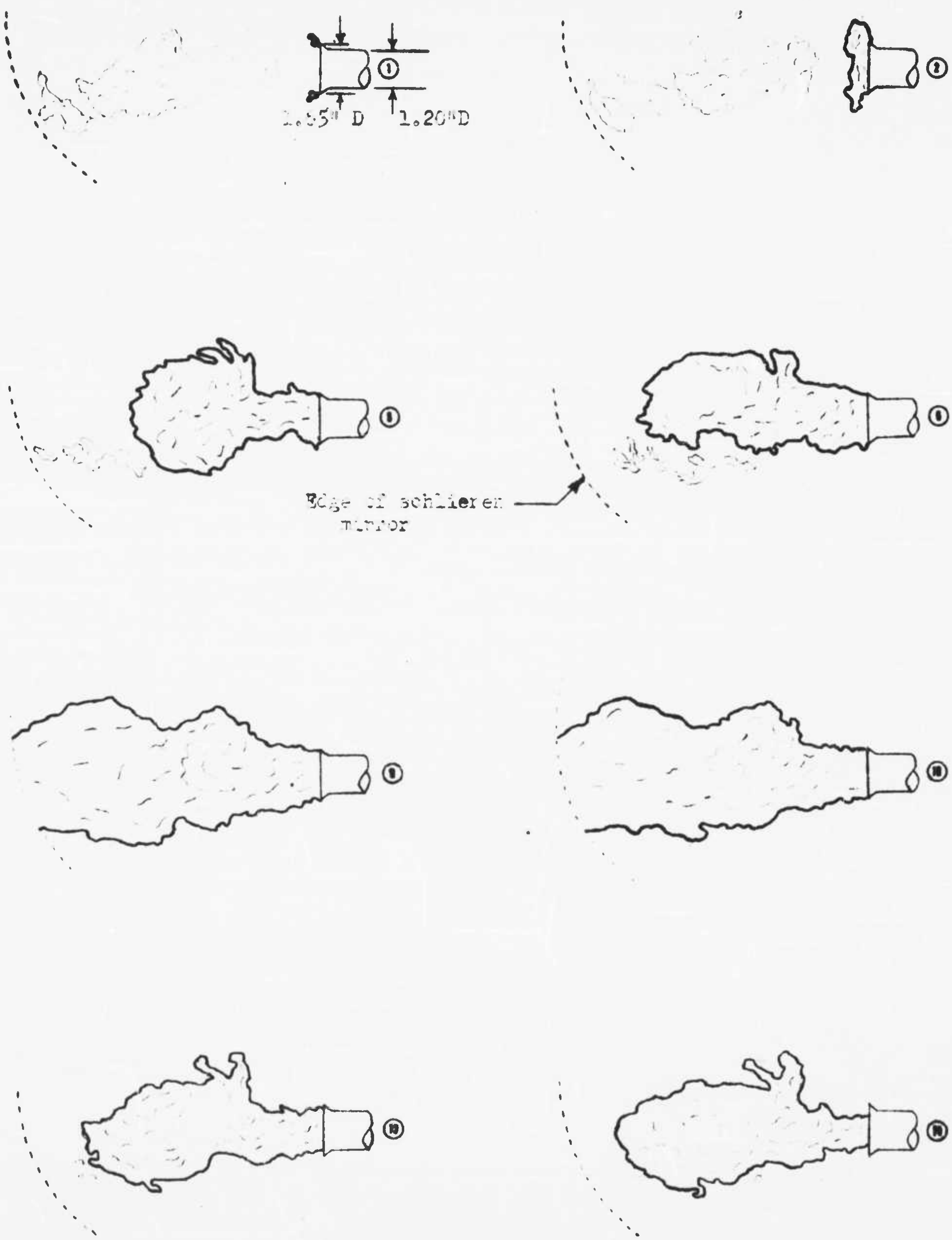

FIGURE 13: TYPICAL CYCLE OF INTERMITTENT JET IN OPEN AIR.
JET WAS ISSUING FROM "DYNAJET" VALVED PULSEJET AT 203 CPS.

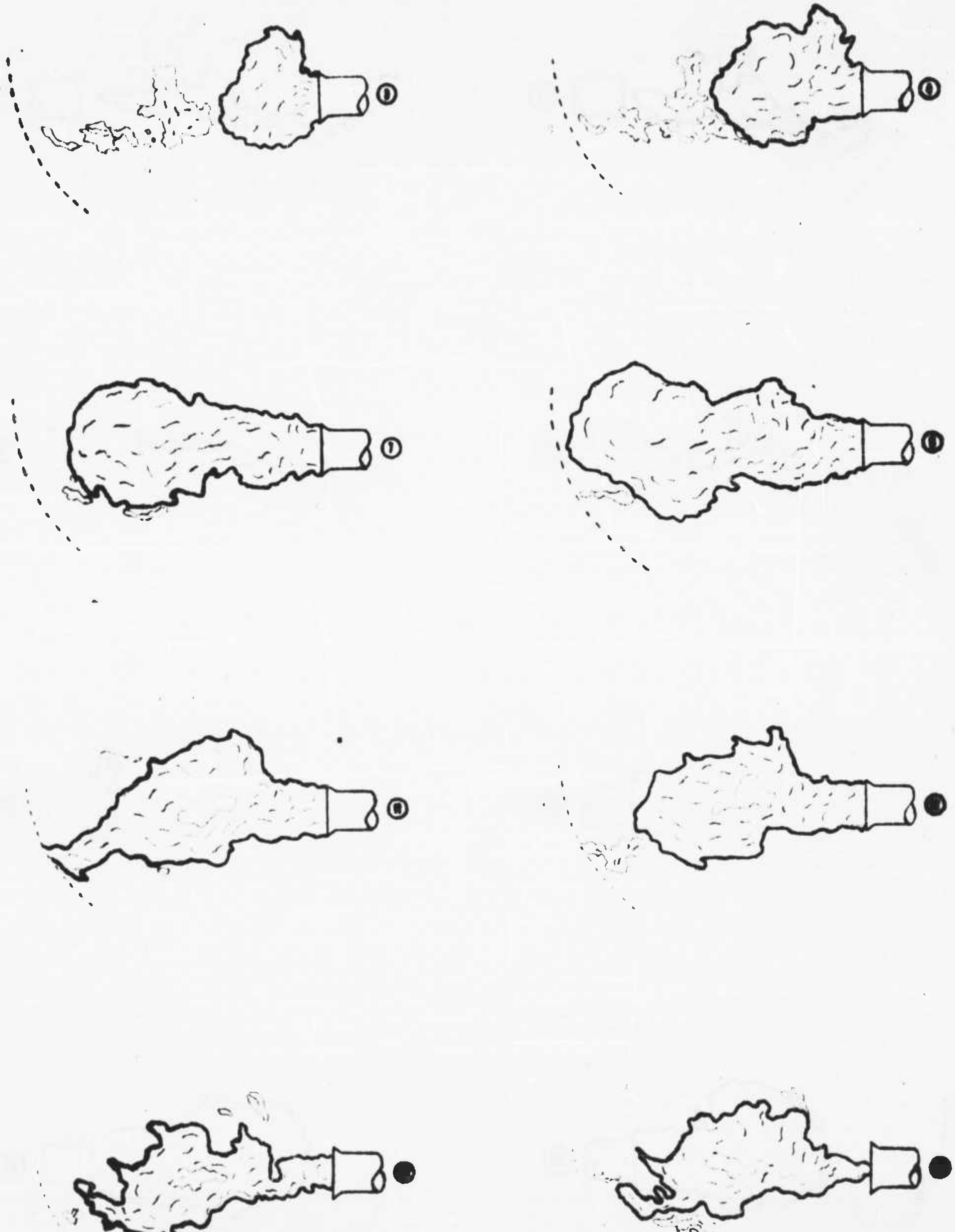

CYCLE WAS TRACED FROM ENLARGEMENTS OF 16mm MOTION PICTURES TAKEN at 4870 FRAMES PER SECOND.

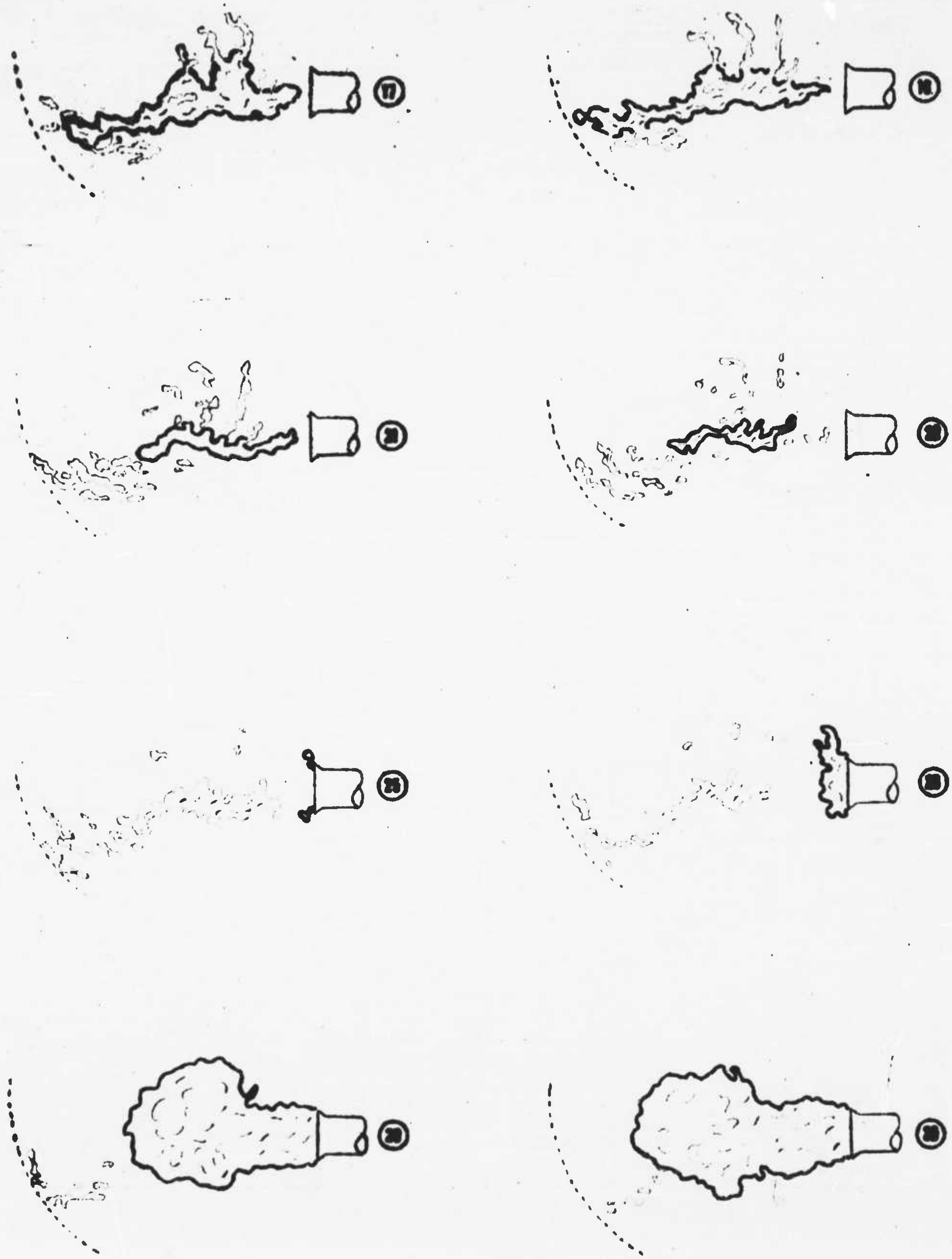

19

20

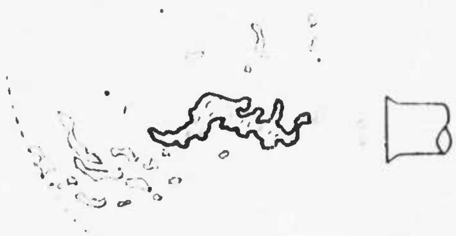

23

24

27

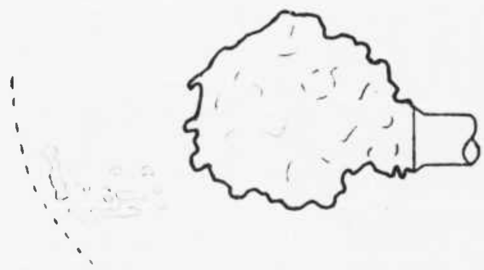

28

31

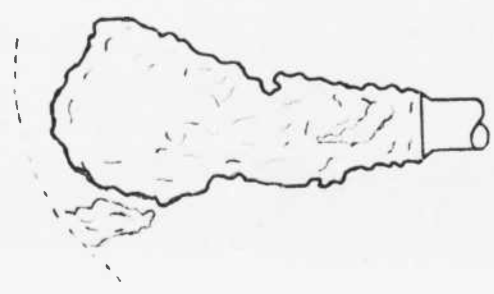

32

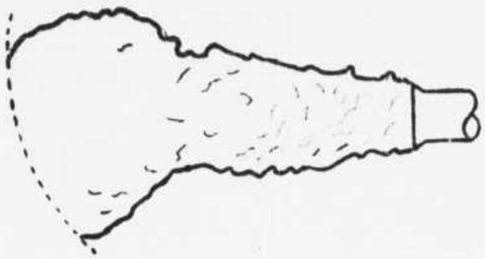
33

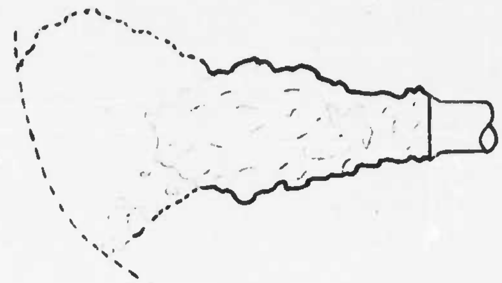
34

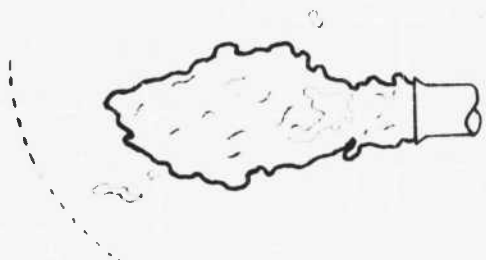
35

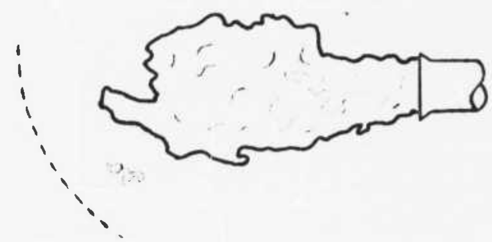
36


37

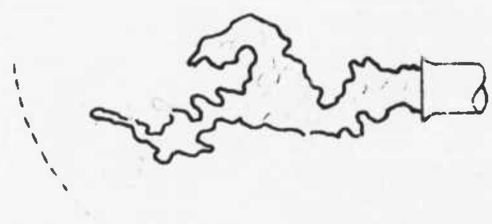
38

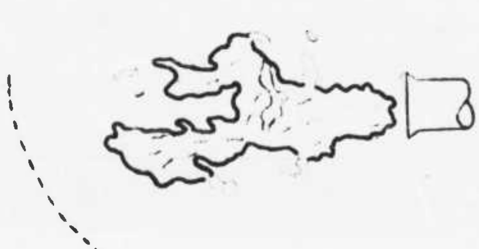
39

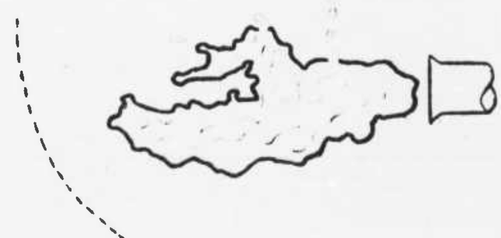
40

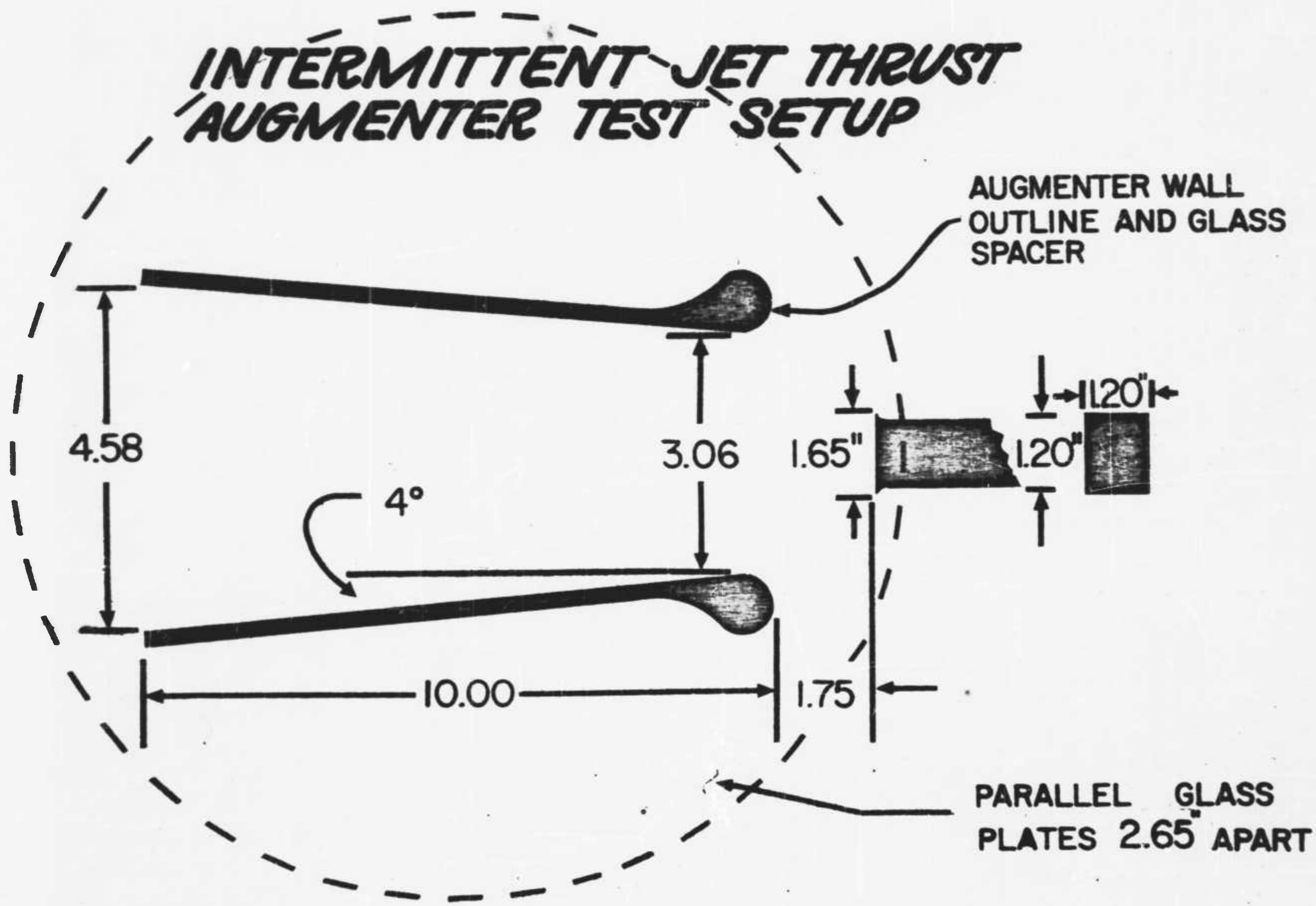
INTERMITTENT-JET THRUST
AUGMENTER TEST SETUP
AUGMENTER WALL
OUTLINE AND GLASS
SPACER
4.58
3.06
4°
1.65"
1.20"
1.20"
10.00
1.75
PARALLEL GLASS
PLATES 2.65" APART

FIGURE 14a

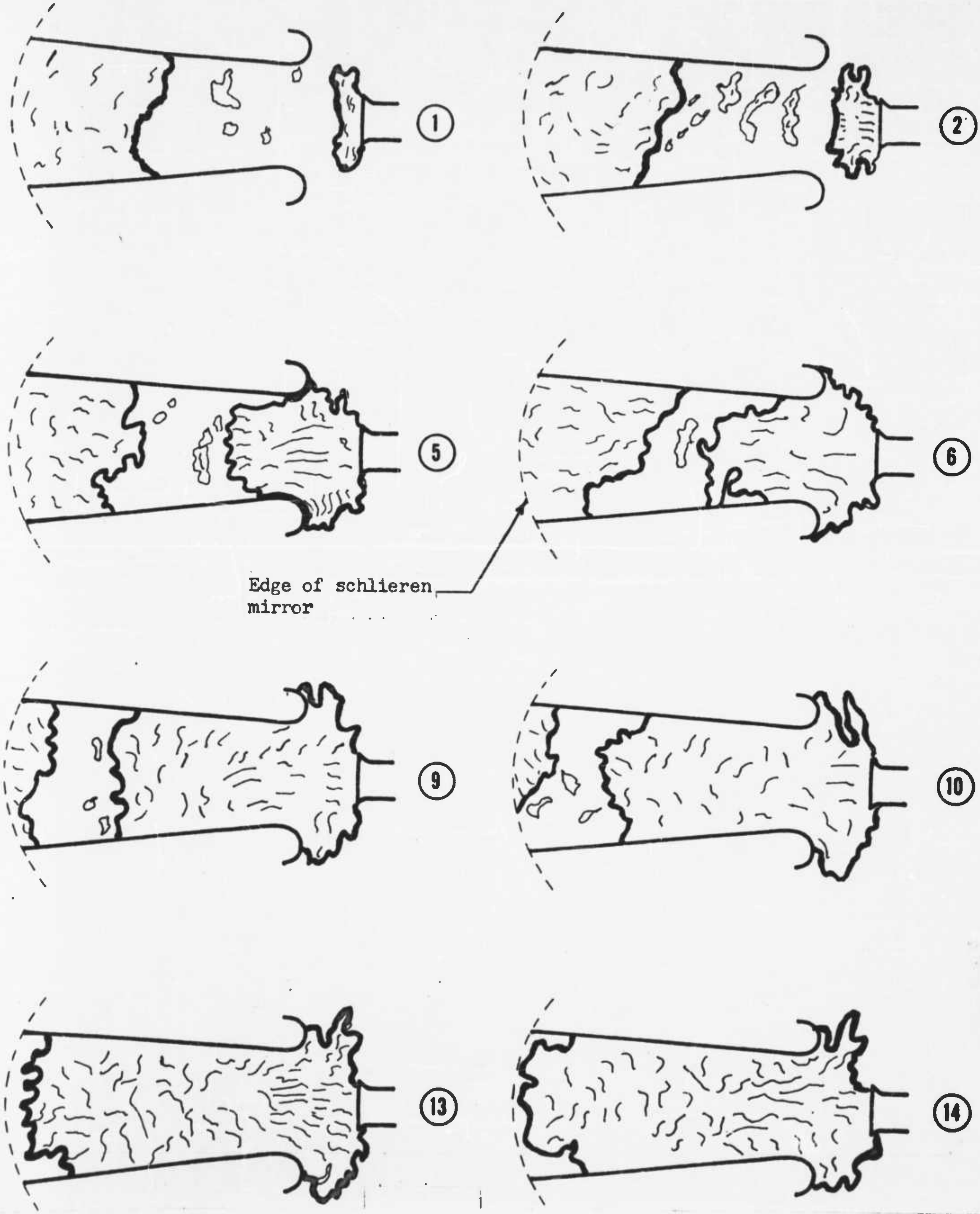

FIGURE 14b: TYPICAL CYCLE OF INTERMITTENT JET IN OPEN AIR. JET WAS ISSUING FROM "DYNAJET" VALVED PULSEJET AT 203 CPS.

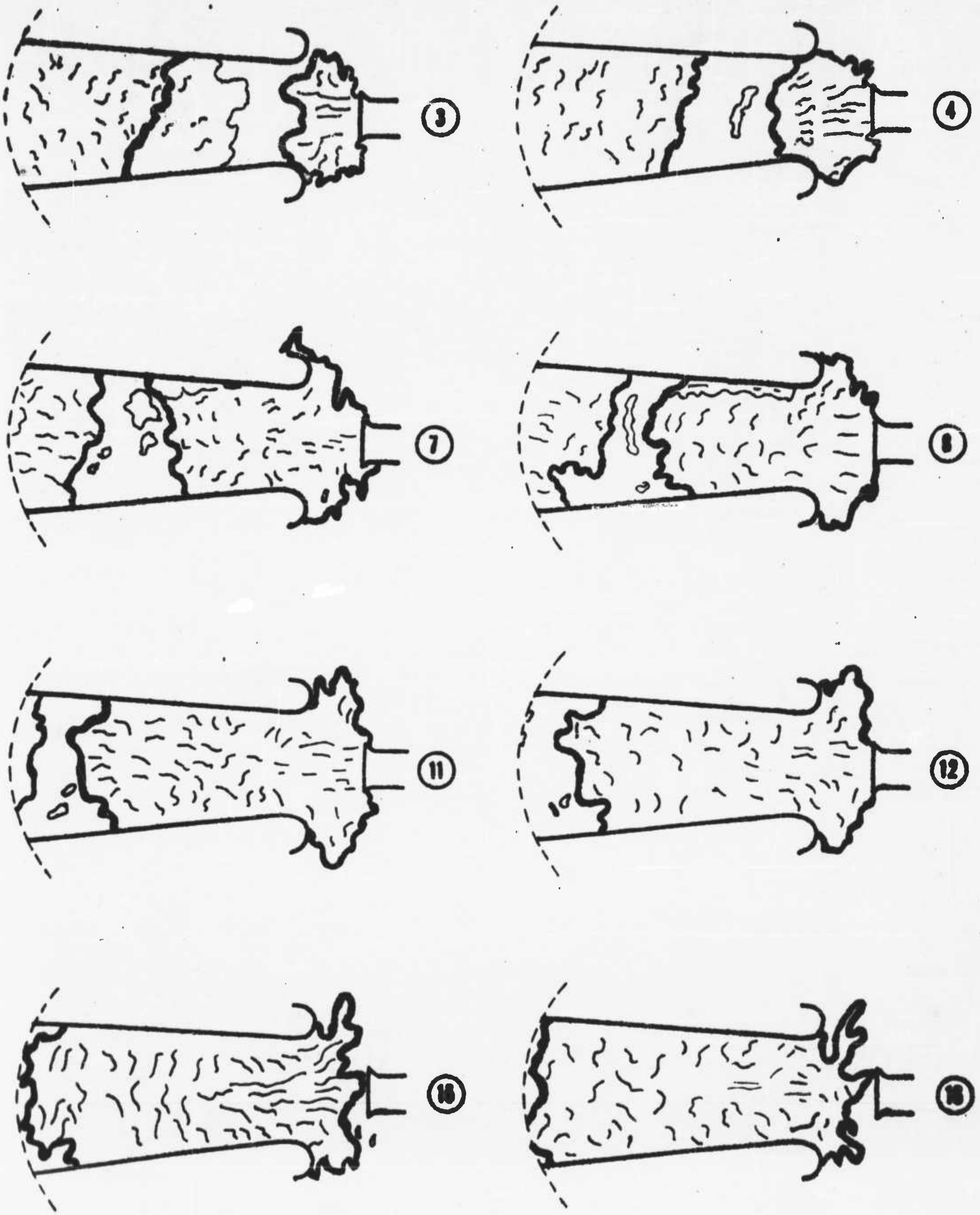

CYCLE WAS TRACED FROM ENLARGEMENTS OF 16mm MOTION PICTURES TAKEN AT 4870 FRAMES PER SECOND.

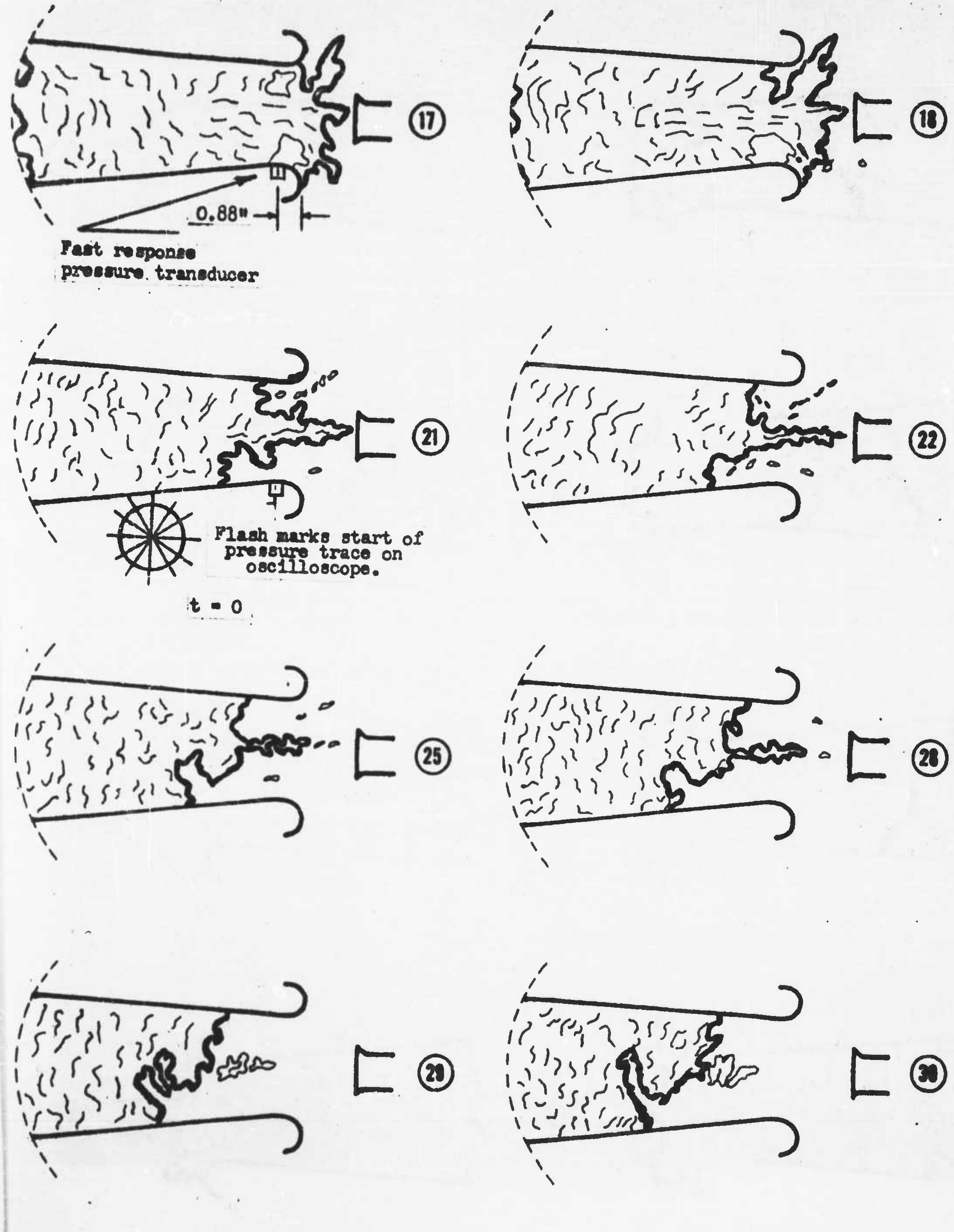

17
0.88"
Fast response pressure transducer
18
21
Flash marks start of pressure trace on oscilloscope.
t = 0
22
25
28
29
30

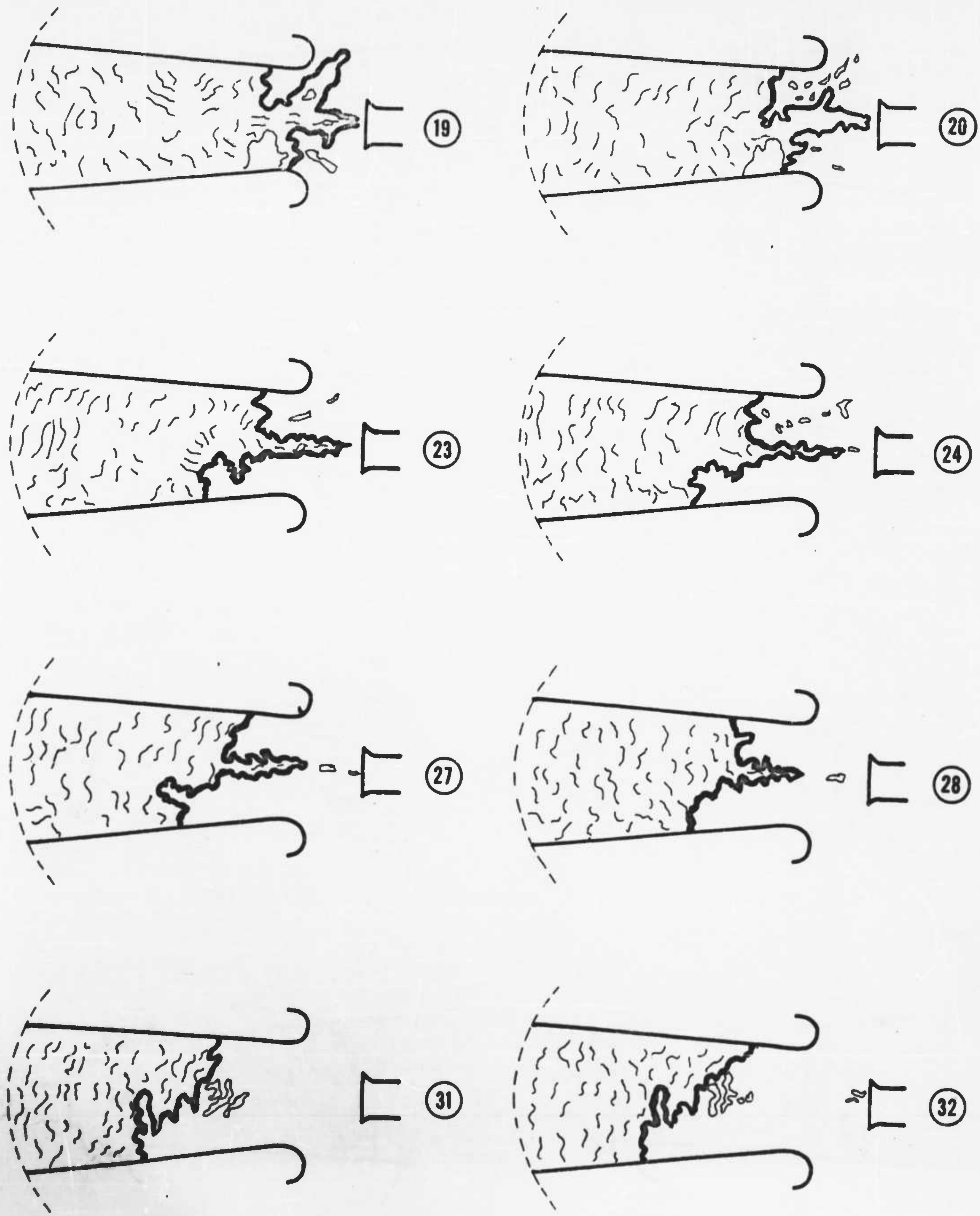
19
20
23
24
27
28
31
32

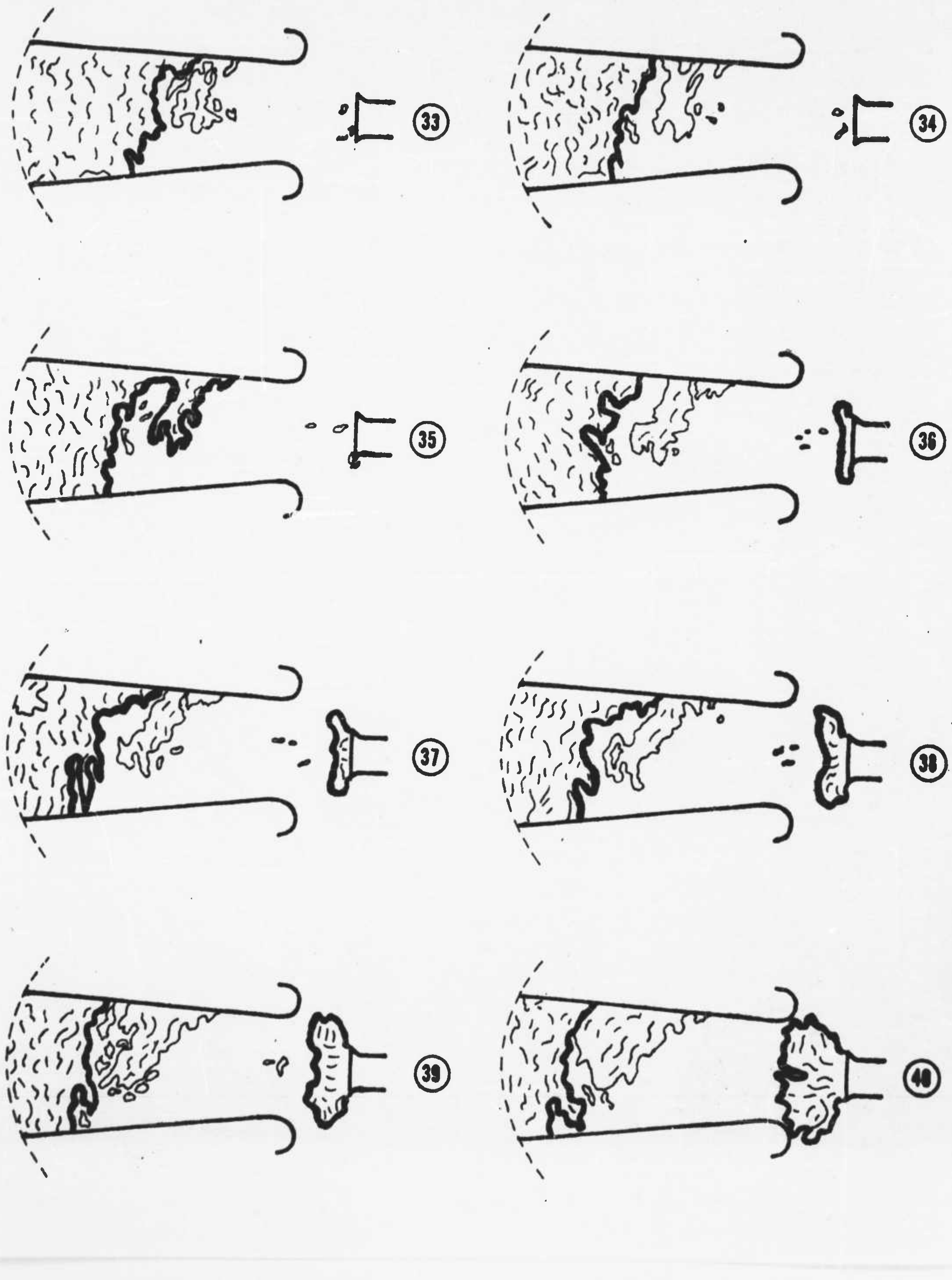

33
34
35
36
37
38
39
40

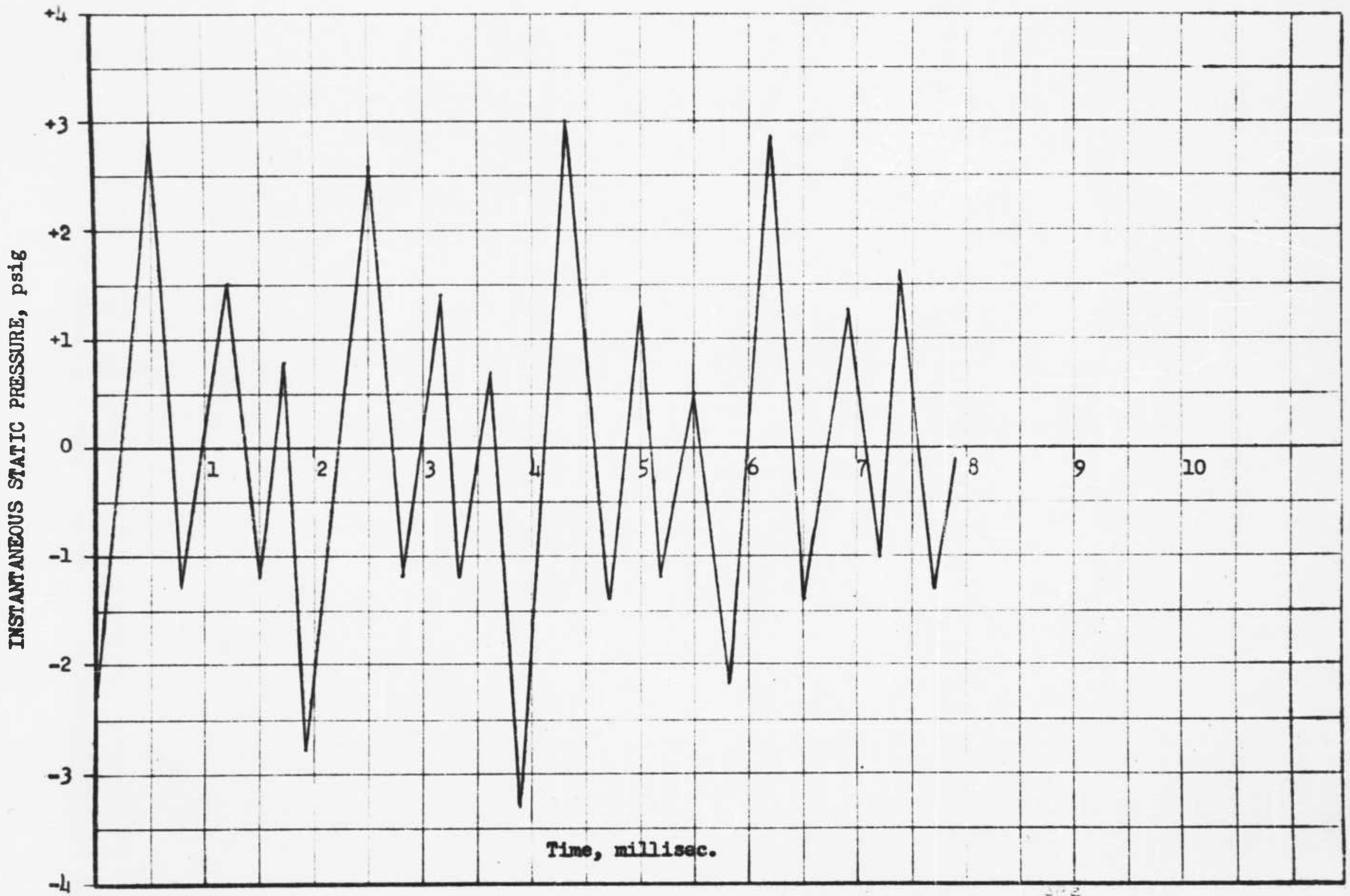

FIGURE 14c: VARIATION OF INSTANTANEOUS STATIC PRESSURE IN AUGMENTER THROAT (Fig. 14b, No. 21, Sta.1)

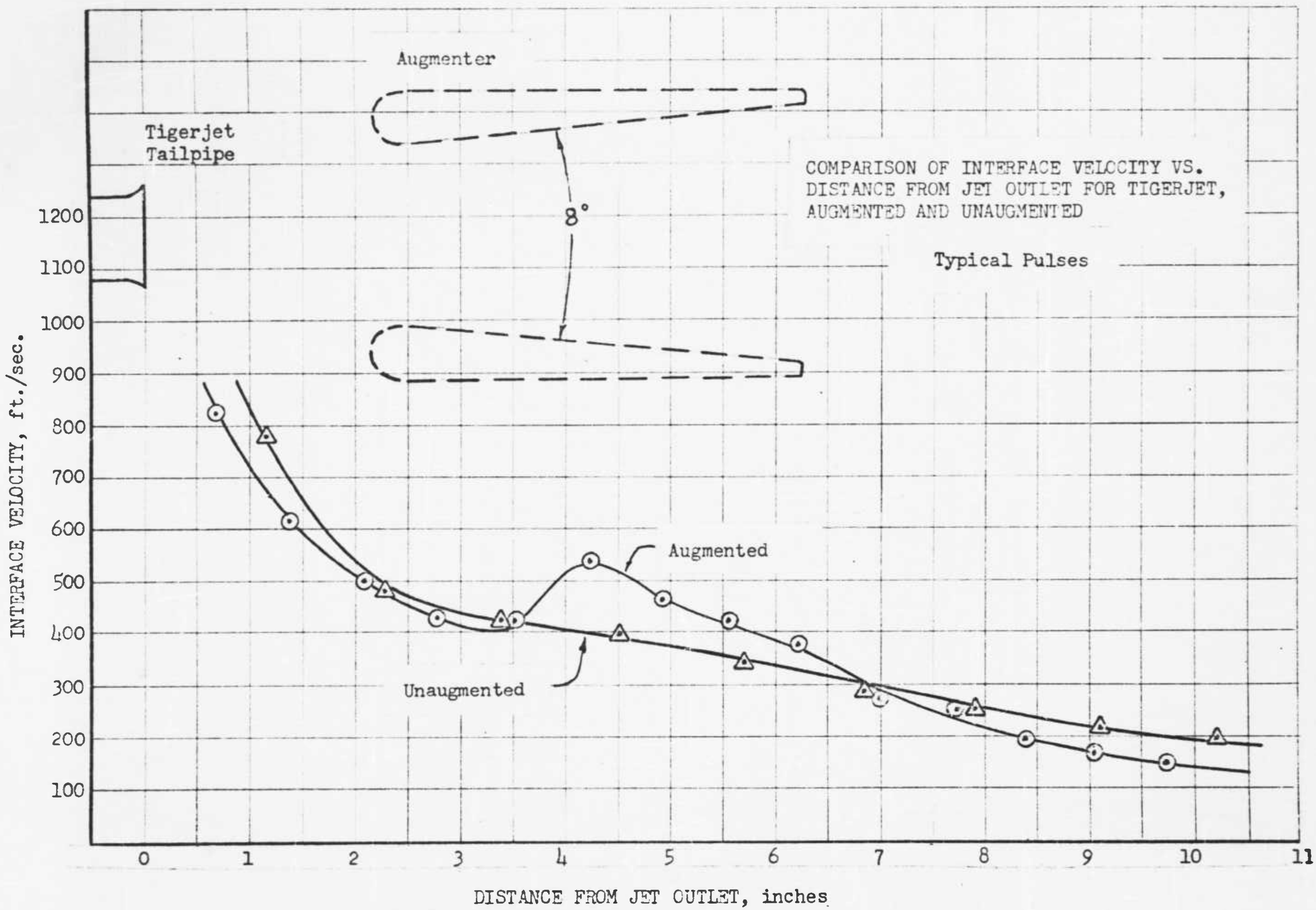
COMPARISON OF INTERFACE VELOCITY VS. DISTANCE FROM JET OUTLET FOR TIGERJET, AUGMENTED AND UNAUGMENTED
Typical Pulses
Augmenter
Tigerjet
Tailpipe
8°
Augmented
Unaugmented
INTERFACE VELOCITY, ft./sec.
1200
1100
1000
900
800
700
600
500
400
300
200
100
0
1
2
3
4
5
6
7
8
9
10
11
DISTANCE FROM JET OUTLET, inches

FIGURE 15

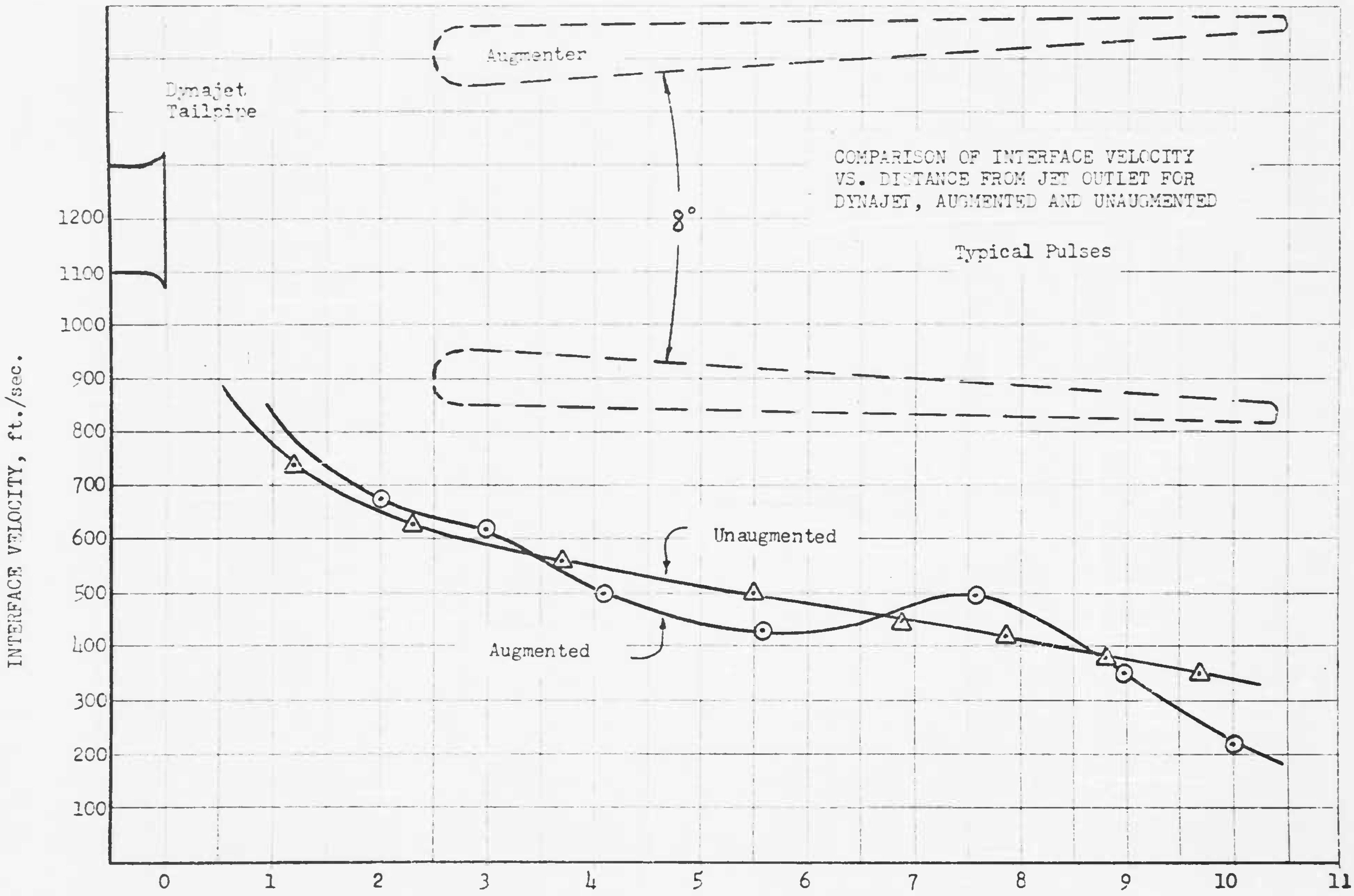
Augmenter
Dynajet
Tailpipe
8°
COMPARISON OF INTERFACE VELOCITY
VS. DISTANCE FROM JET OUTLET FOR
DYNAJET, AUGMENTED AND UNAUGMENTED
Typical Pulses
Unaugmented
Augmented
INTERFACE VELOCITY, ft./sec.
1200
1100
1000
900
800
700
600
500
400
300
200
100
0
1
2
3
4
5
6
7
8
9
10
11
DISTANCE FROM JET OUTLET, Inches
FIGURE 16a

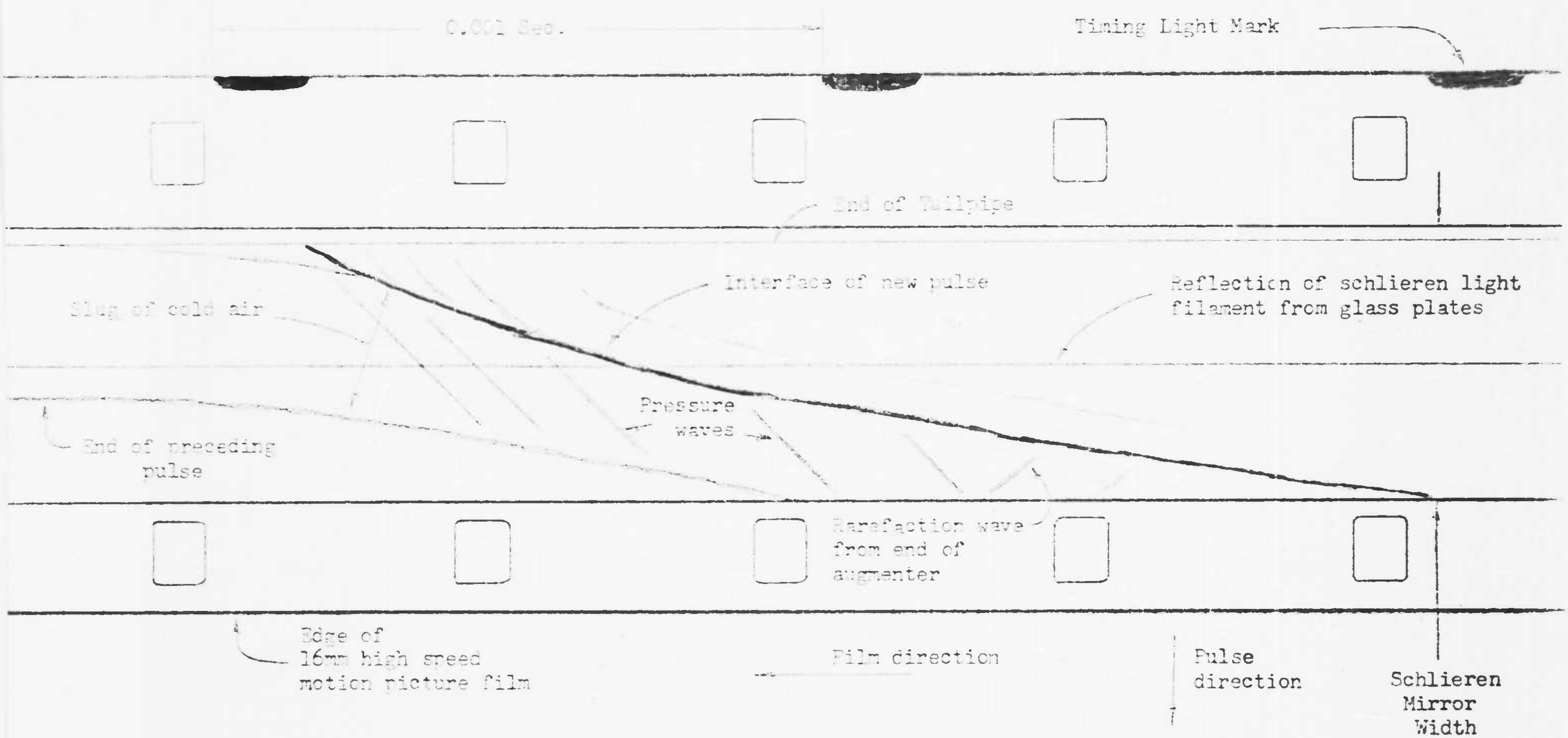

FIGURE 16b: SKETCH OF HIGH SPEED STREAK PHOTOGRAPH (AUGMENTED DYNAJET)

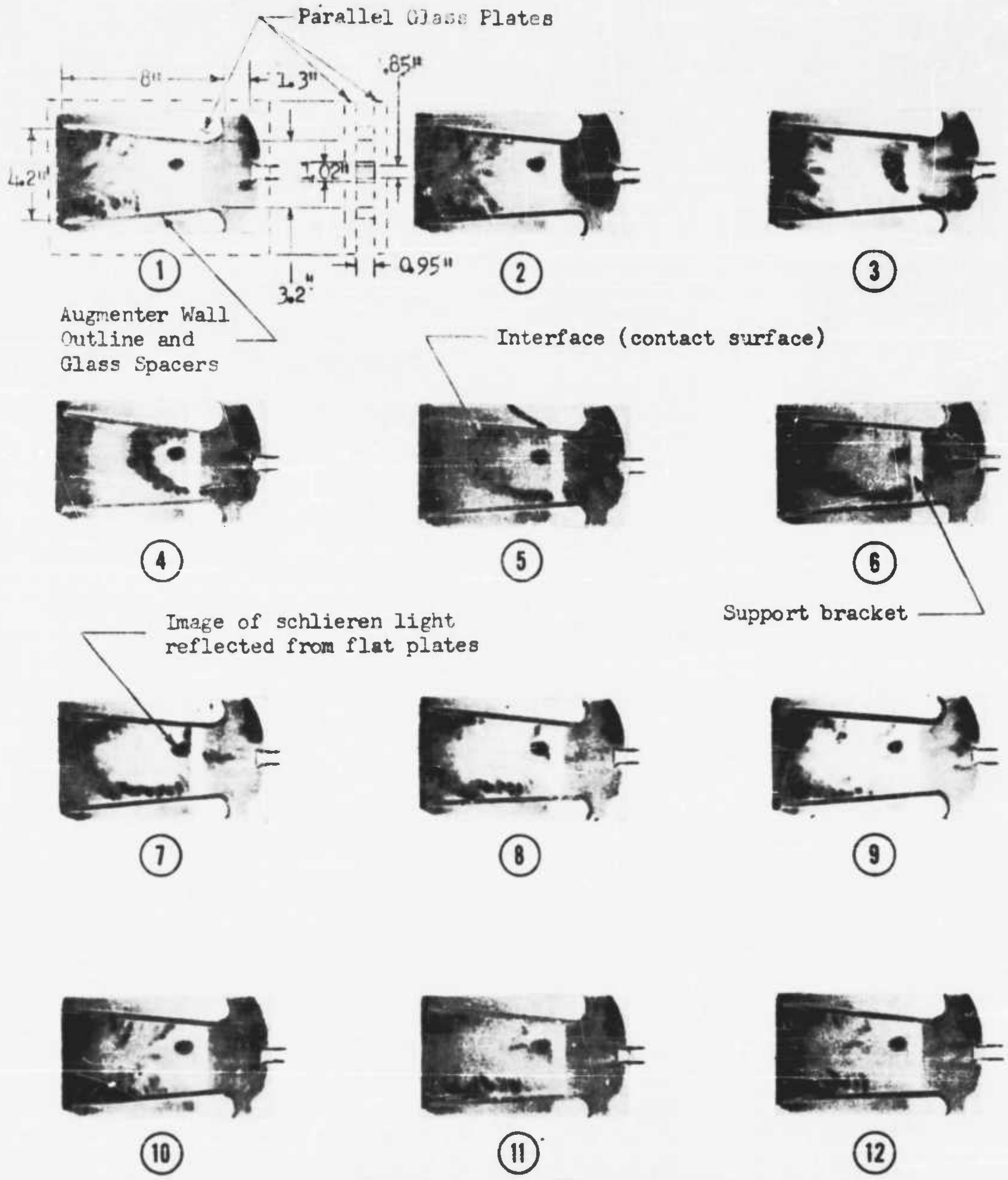

FIGURE 17: TYPICAL CYCLE OF VALVED PULSEJET ("TIGER-JET") WITH THRUST AUGMENTER. 16mm SCHLIEREN MOTION PICTURES ENLARGED. NOTE PRONOUNCED DARK OUTLINE OF INTERFACE BETWEEN DRIVING JET EFFLUX AND AMBIENT AIR IN TWO-DIMENSIONAL TESTS.

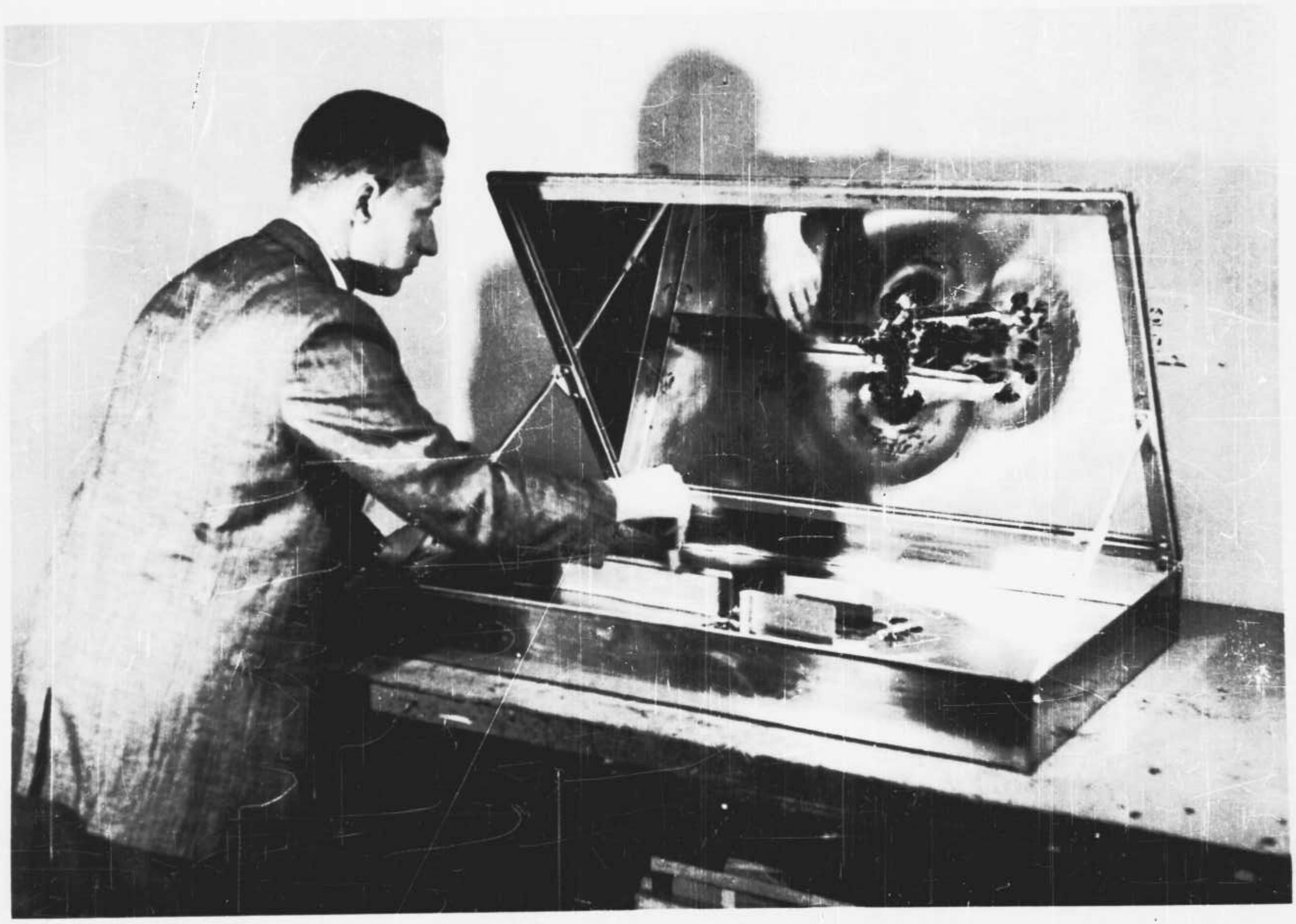

FIGURE 18: WATER TABLE TEST SET-UP DEMONSTRATING INTERMITTENT JET MOTION INTO THRUST AUGMENTER.

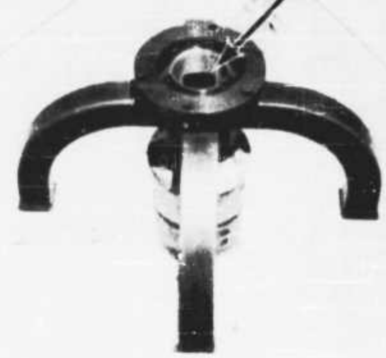

(a.) Photograph showing near and far ports full open

(b.) View showing all ports half opened

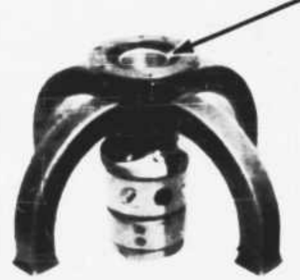

(c.) View showing porting cycle in half phase position

FIGURE 19: PORTING DEVICE FOR MAKING A STEADY FLOW UNSTEADY WITHOUT SENDING A HAMMER WAVE UP-STREAM

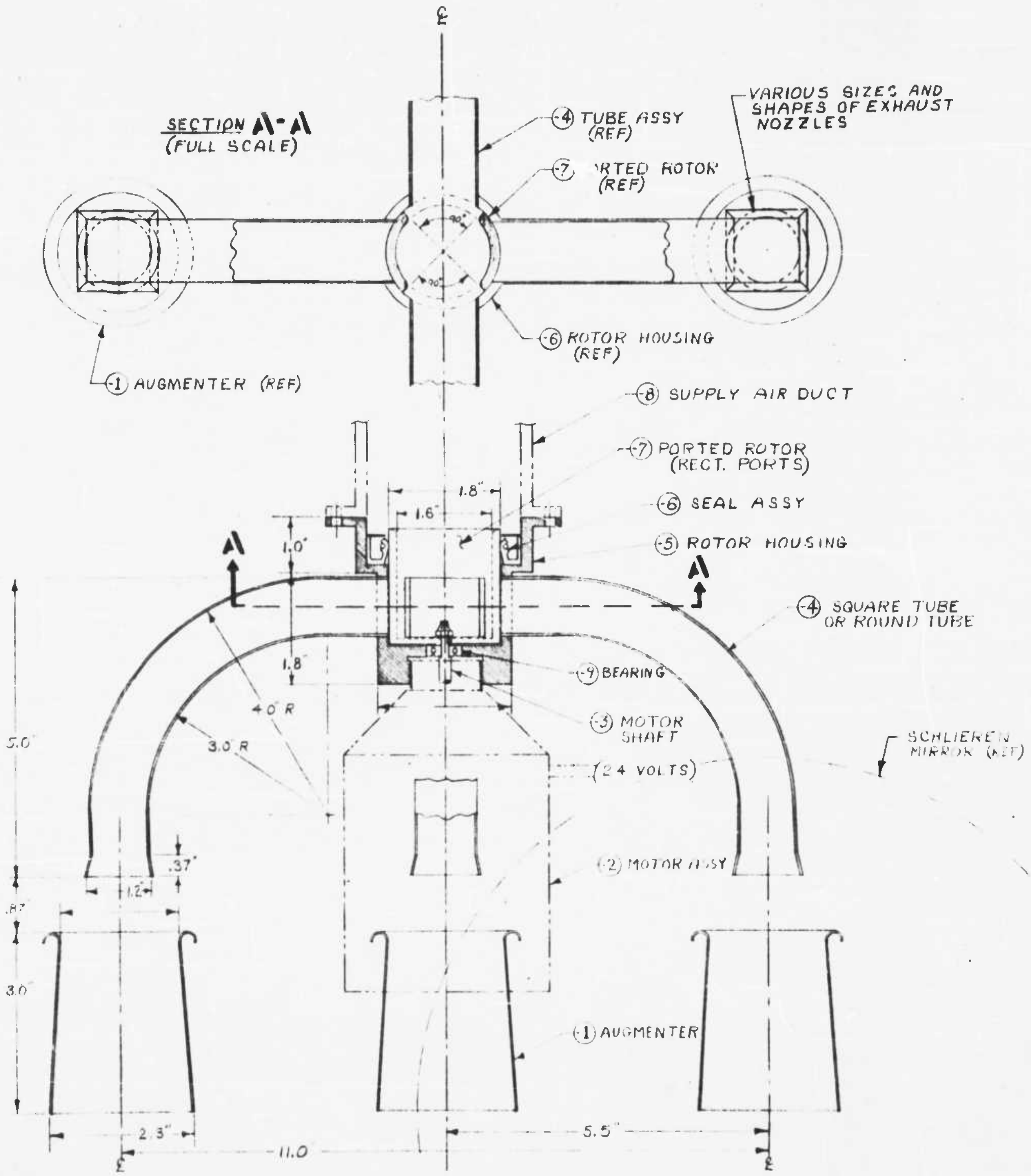

FIGURE 20: DEVICE TO MAKE A STEADY FLOW INTERMITTENT WITHOUT SENDING A "HAMMER WAVE" UP STREAM TO THE GAS GENERATOR

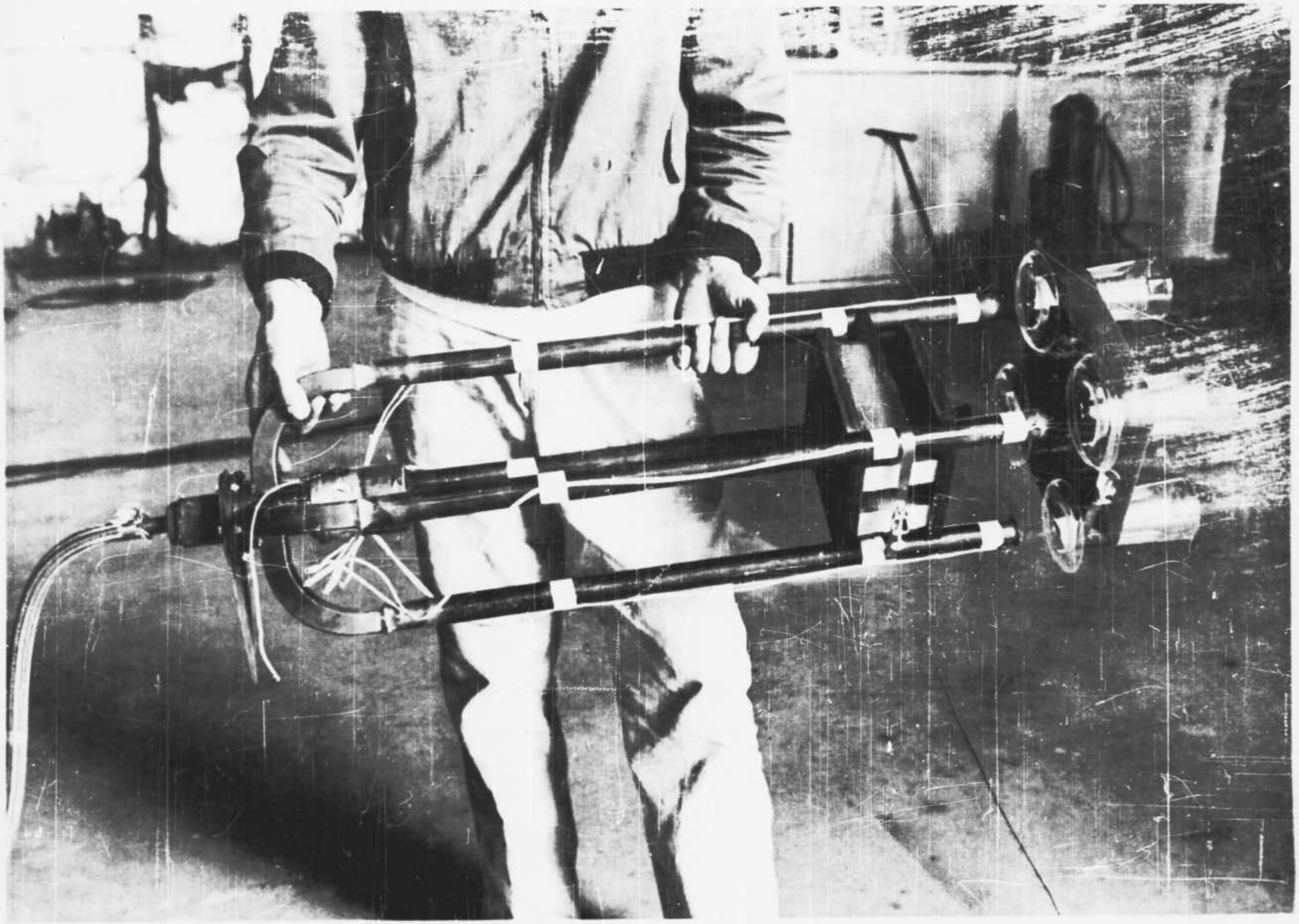

FIGURE 21: TEST DEVICE FOR CONVERTING STEADY FLOW TO INTERMITTENT FLOW, WITHOUT SENDING A HAMMER WAVE UPSTREAM, AND TAKING ADVANTAGE OF HIGH THRUST AUGMENTATION FROM INTERMITTENT JET.

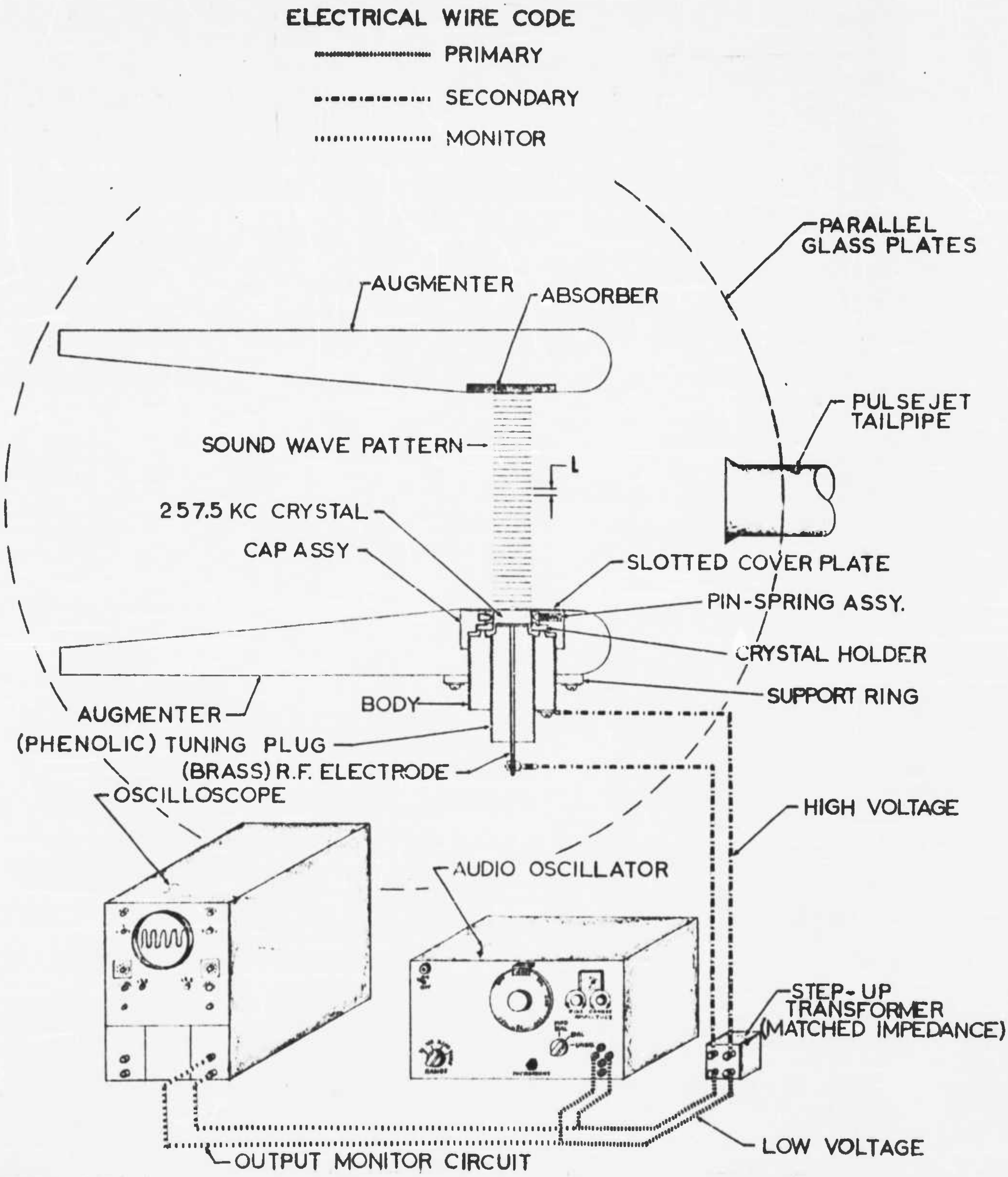

FIG. 22

AN "ULTRASONIC THERMOMETER" METHOD OF MEASURING INSTANTANEOUS TEMPERATURE IN A SCHLIEREN PHOTOGRAPHIC TEST RIG.

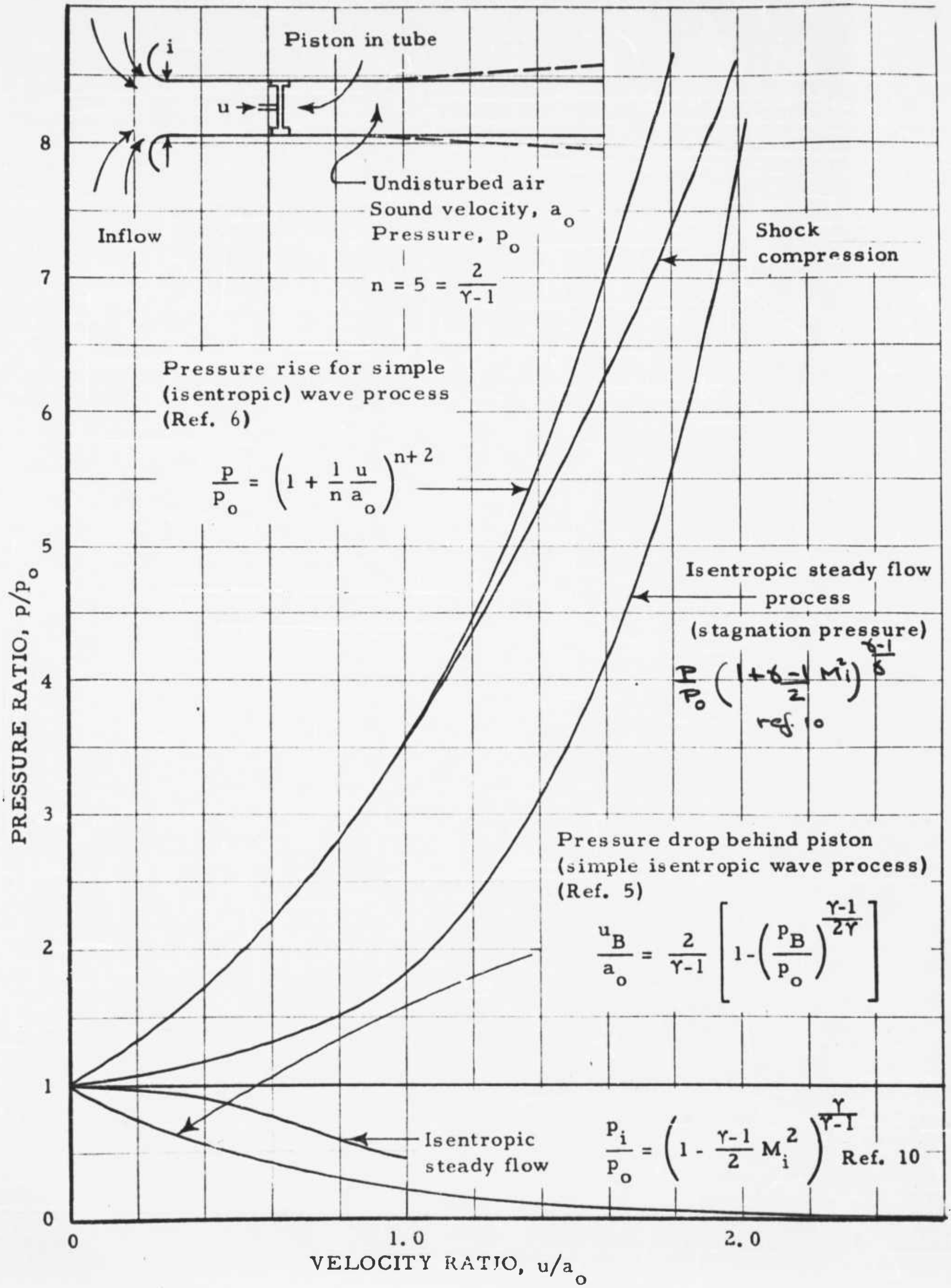

FIGURE 23. COMPARISON OF ISENTROPIC WAVE AND STEADY FLOW PROCESSES

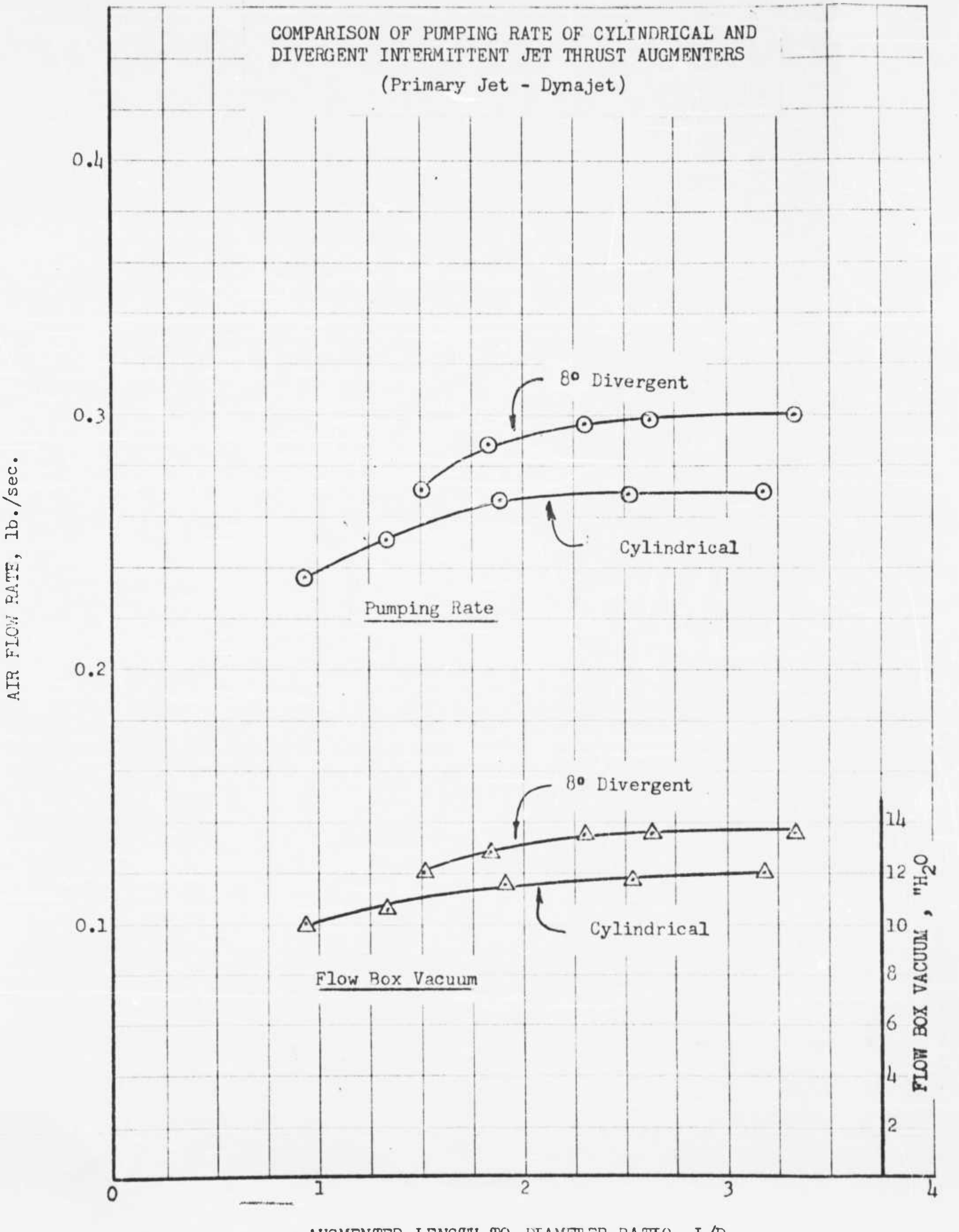

COMPARISON OF PUMPING RATE OF CYLINDRICAL AND
DIVERGENT INTERMITTENT JET THRUST AUGMENTERS
(Primary Jet - Dynajet)
8° Divergent
Cylindrical
Pumping Rate
8° Divergent
Cylindrical
Flow Box Vacuum
AIR FLOW RATE, lb./sec.
0.4
0.3
0.2
0.1
0
1
2
3
4
FLOW BOX VACUUM , "H_2O
14
12
10
8
6
4
2
AUGMENTER LENGTH TO DIAMETER RATIO, L/D

FIGURE 24a

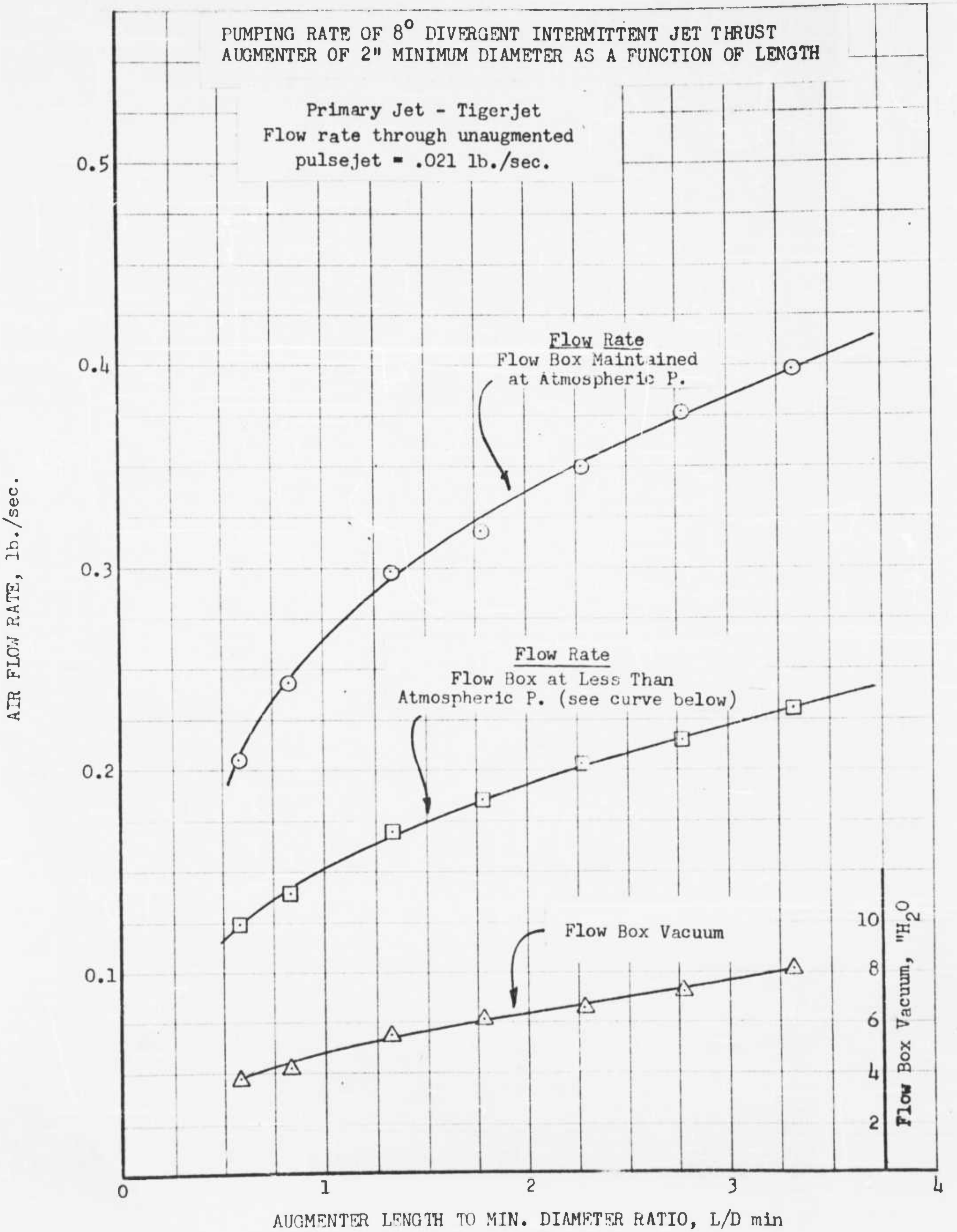

PUMPING RATE OF 8° DIVERGENT INTERMITTENT JET THRUST AUGMENTER OF 2" MINIMUM DIAMETER AS A FUNCTION OF LENGTH
Primary Jet - Tigerjet
Flow rate through unaugmented pulsejet = .021 lb./sec.
Flow Rate
Flow Box Maintained at Atmospheric P.
Flow Rate
Flow Box at Less Than Atmospheric P. (see curve below)
Flow Box Vacuum
AIR FLOW RATE, lb./sec.
0.5
0.4
0.3
0.2
0.1
Flow Box Vacuum, "H_2O
10
8
6
4
2
0
1
2
3
4
AUGMENTER LENGTH TO MIN. DIAMETER RATIO, L/D min

FIGURE 24b

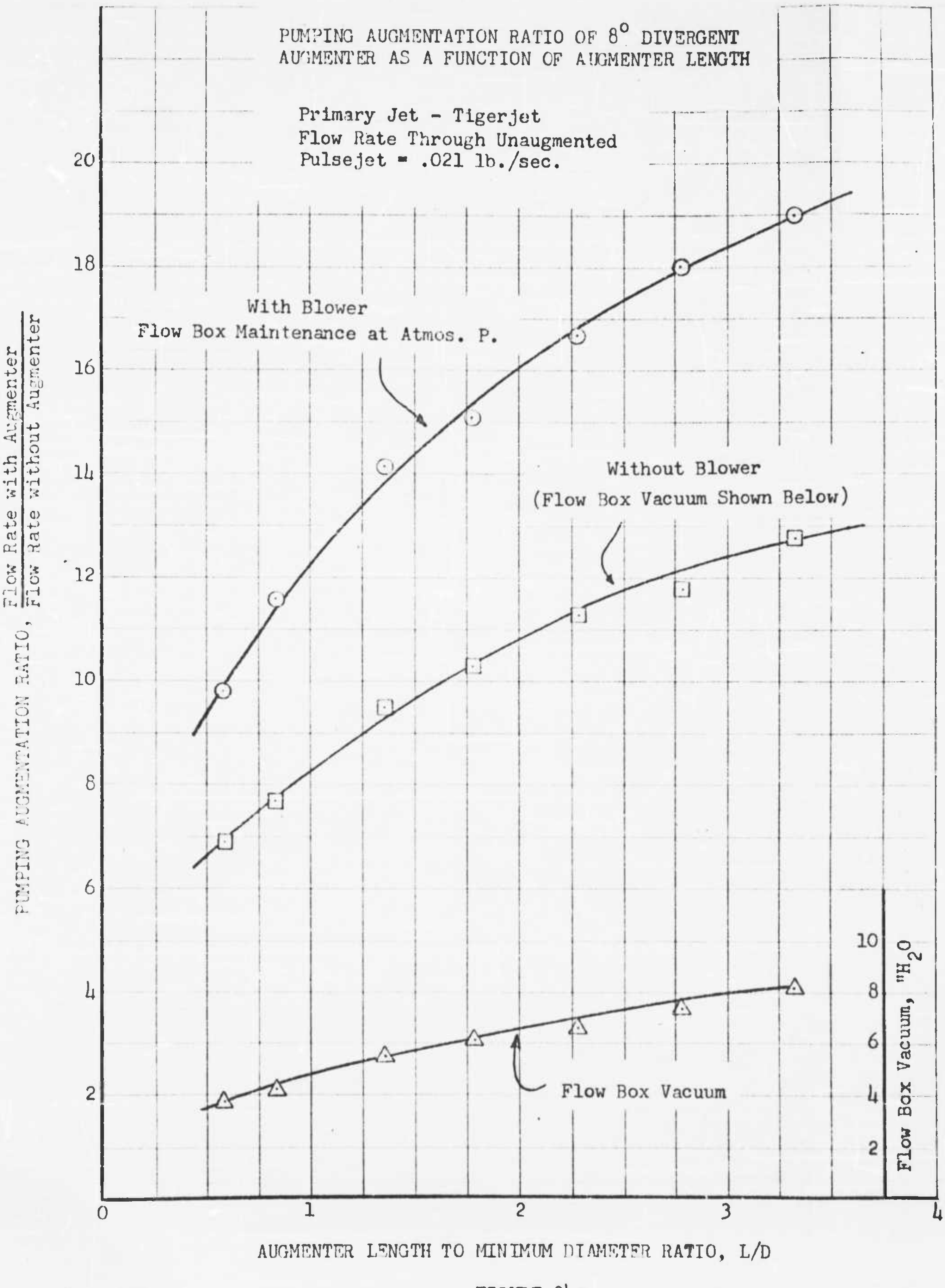
PUMPING AUGMENTATION RATIO OF 8° DIVERGENT AUGMENTER AS A FUNCTION OF AUGMENTER LENGTH
Primary Jet - Tigerjet
Flow Rate Through Unaugmented Pulsejet = .021 lb./sec.
With Blower
Flow Box Maintenance at Atmos. P.
Without Blower
(Flow Box Vacuum Shown Below)
Flow Box Vacuum
PUMPING AUGMENTATION RATIO, Flow Rate with Augmenter / Flow Rate without Augmenter
Flow Box Vacuum, "H2O
AUGMENTER LENGTH TO MINIMUM DIAMETER RATIO, L/D
0
1
2
3
4
2
4
6
8
10
12
14
16
18
20
2
4
6
8
10

FIGURE 24c

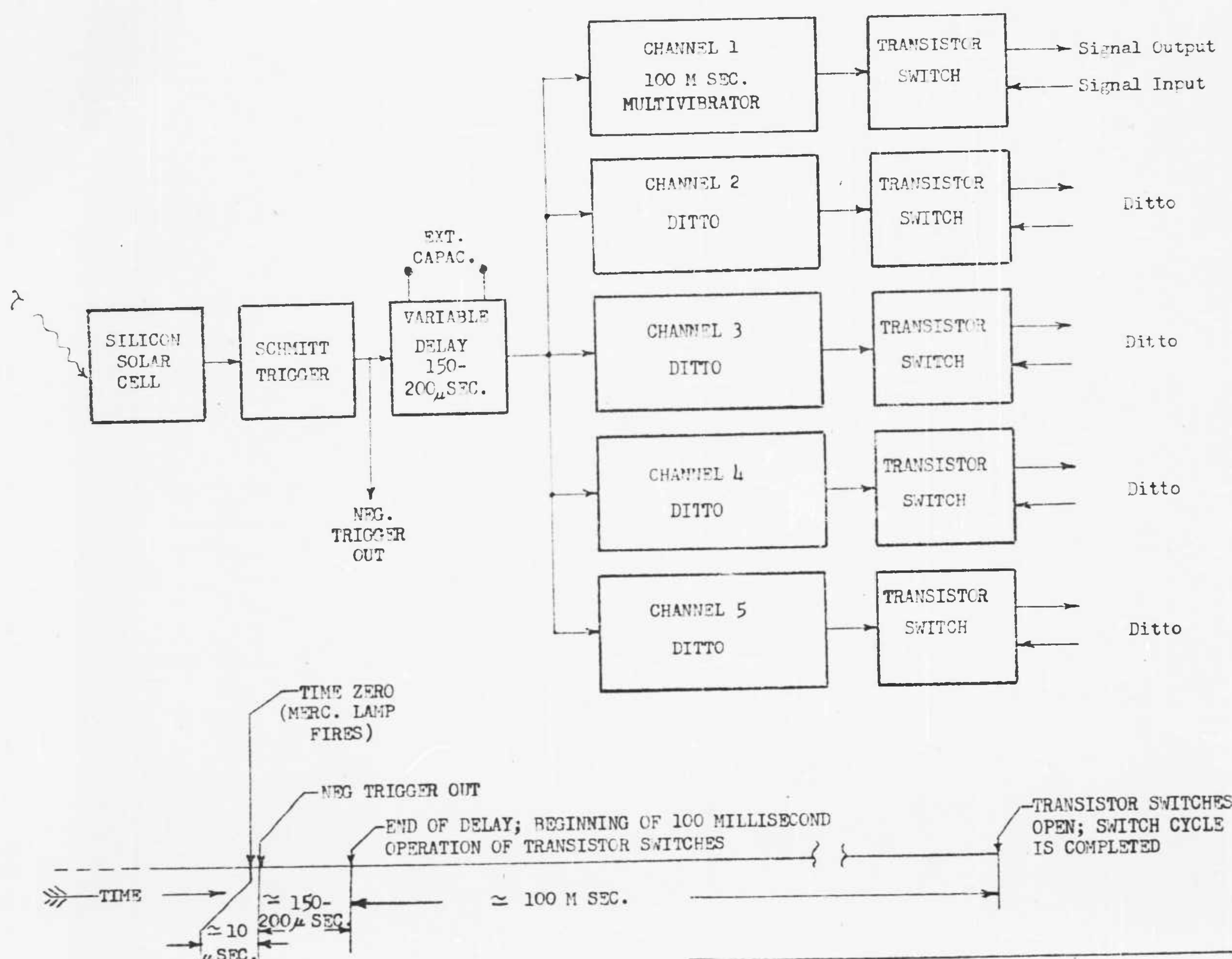

FIGURE 25

ELECTRONIC MULTIPLE CHANNEL SIMULTANEOUS SWITCH

FUNCTIONAL BLOCK DIAGRAM

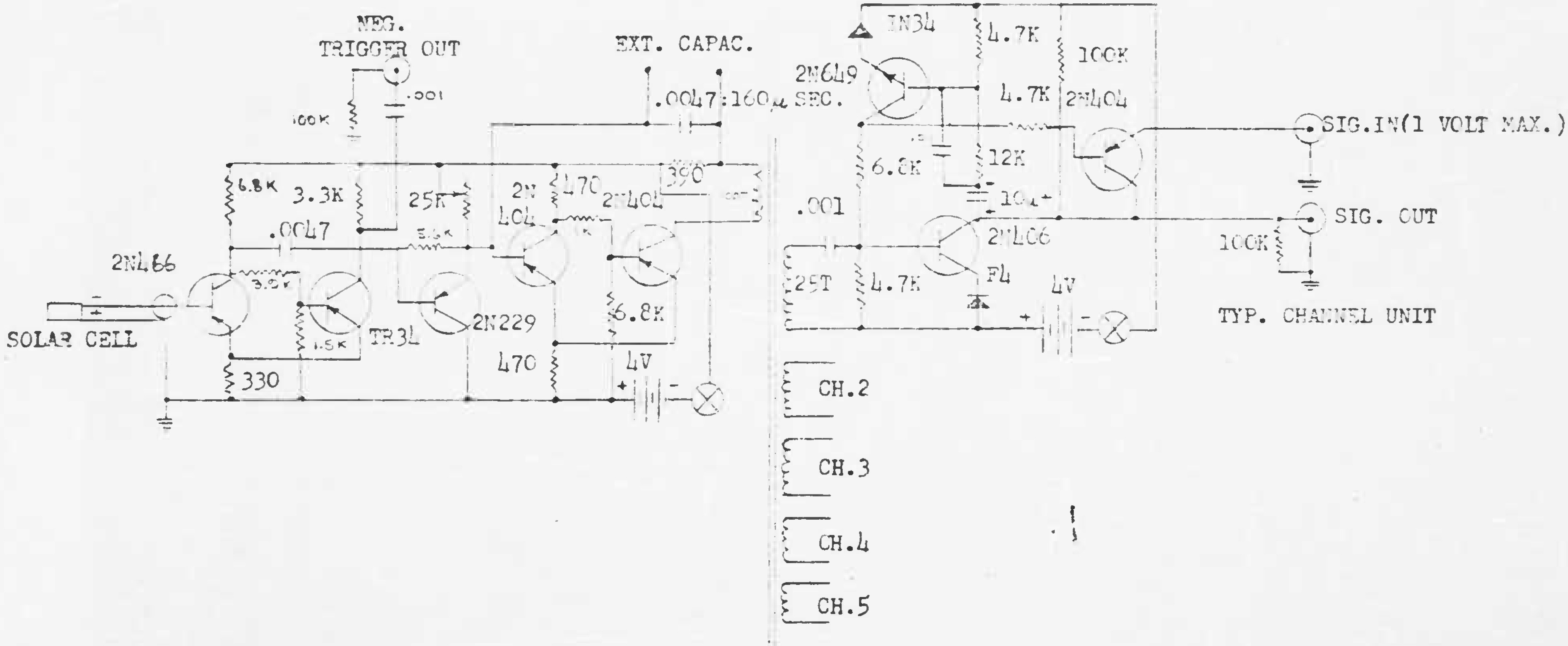

FIGURE 26: CIRCUIT DIAGRAM

ELECTRONIC MULTIPLE CHANNEL
SIMULTANEOUS SWITCH

HIGH SPEED COLOR SCHLIEREN SLIDES OF PULSEJET, AUGMENTED AND UNAUGMENTED WITH ASSOCIATED STREAK PICTURE

1. DYNAJET: Unaugmented. Interface velocities, determined from film velocity and angle between interface streak and film edge, are in the range of 800 ft/sec where angle is greatest to 350 ft/sec where angle is smallest. The actual distance the pulse travels in moving across the film is approximately 10". Tailpipe diameter is 1.2"

   Note: fairly uniform fall-off velocity

2. DYNAJET: Augmented, 8^{o} divergent. Interface velocities in range of 800 ft/sec to 250 ft/sec

   Note: Slug of cold ambient air trapped between the two pulses. Note pressure waves - velocity 1500 ft/sec with respect to augmenter. Light line across center of streak film is reflection of schlieren light filament from glass plates used to form augmenter set-up.

3. TIGERJET: Augmented, 0^{o}. Provides photograph of augmenter outlet. Tailpipe diameter = 0.85"

   Note: pulse spillage and flow reversal over lip of augmenter; also vortex at exit of augmenter. Interface velocities similar to Dynajet (800 ft/sec to 200 ft/sec). Note inflection of interface streak (non-uniform rate of velocity change).

4. TIGERJET: Augmented, 24^{o}. Note: strong pressure wave streaks and lack of vortex at augmenter outlet.

1. Dynajet - Unaugmented

2. Dynajet - Augmented, 8°

3. Tigerjet - Augmented, 0°

4. Tigerjet - Augmented, 24°

FIGURE 27: 35mm SLIDES OF COLOR SCHLIEREN PHOTOGRAPHY

DISTRIBUTION LIST

Chief, Bureau of Naval Weapons (RAAD-3)
Dept. of the Navy
Washington 25, D. C.
Attn: Mr. Desmond (1)

Chief of Naval Research (Code 429)
Dept. of the Navy
Washington 25, D. C.
Attn: Power Branch (1)

Chief, Bureau of Naval Weapons (RAPP-331)
Dept. of the Navy
Washington 25, D. C.
Attention: Mr. Nagelhout (2)

Chief, Bureau of Naval Weapons (RR-25)
Dept of the Navy
Washington 25, D. C.
Attn: Mr. Hollenberg (1)

Chief of Naval Research (Code 461)
Dept. of the Navy
Washington 25, D. C. (4)

Commanding Officer and Director
David Taylor Model Basin
Aerodynamics Laboratory Library
Washington 7, D. C. (1)

Commanding Officer
ONR Branch Office
1000 Geary Street
San Francisco 9, California (1)

Commanding Officer
Office of Naval Research Branch Office
The John Crerar Library Building
86 E. Randolph Street
Chicago 1, Illinois (1)

Commanding Officer
Office of Naval Research Branch Office
346 Broadway
New York 13, New York (1)

Commanding Officer
Office of Naval Research Branch Office
1030 E. Green Street
Pasadena, California (1)

Director
Naval Research Laboratory
Technical Information Office
Washington 25, D. C. (6)

Commanding Officer - Office of Naval Research Branch Office
Navy #100 Fleet Post Office, Box #39
New York, New York
Attn: Head Documents Section (1)

U. S. Air Force
Office of Scientific Research
Washington 25, D. C.
Attn: SRGL (1)

Wright Aeronautical Systems Division
Division Advanced Systems Technology (WWRPS)
Wright-Patterson Air Force Base, Ohio (1)

Office of Chief of Transportation (TAFO-R)
Dept. of the Army
Washington 25, D. C. (1)

Commanding Officer
U. S. Army Transportation Research Command (TCREC-AD)
Fort Eustis, Virginia (3)

Office of Chief of Research and Development
Department of the Army
Washington 25, D. C.
Attn: Air Mobility Division (1)

DISTRIBUTION LIST (Continued)

Armed Services Technical Information Agency
Document Service Center
Arlington Hall Station
Arlington 12, Virginia (10)

National Aeronautics and Space Administration
1512 H Street, N. W.
Washington 25, D. C.
Attn: Jack Brewer, Code RAA (1)

National Aeronautics and Space Administration
Lewis Research Center
2100 Brook Park Road
Cleveland 11, Ohio (1)

National Aeronautics and Space Administration
Ames Research Center
Moffett Field, California
Attn: Mr. C. W. Harper (1)

National Aeronautics and Space Administration
Langley Research Center
Langley Air Force Base, Virginia
Attn: Mr. Donnelly (1)

National Bureau of Standards
Department of Commerce
Washington 25, D. C.
Attn: Dr. G. B. Schubauer (1)

Office of Technical Services
Department of Commerce
Washington 25, D. C. (1)

California Institute of Technology
Aeronautics Department
Pasadena, California
Attn: Dr. Clark Millikan (1)

Cornell University
Graduate School of Aeronautics
Ithaca, New York
Attn: Dr. W. R. Sears (1)

Georgia Institute of Technology
Guggenheim School of Aeronautics
Atlanta 13, Georgia
Attn: D. W. Dutton (1)
Robin B. Gray

Jet Propulsion Laboratory
Pasadena, California (1)

University of Minnesota
Rosemount Aeronautical Laboratories
Rosemount, Minnesota
Attn: Mr. Rose (1)

Mississippi State University
Engineering and Industrial Research Station
State College, Mississippi
Attn: Dr. J. Cornish (1)

Naval Postgraduate School
Aeronautical Engineering Dept.
Monterey, California
Attn: Dr. R. Head (1)
M. H. Vavra

Stanford University
Guggenheim School of Aeronautics
Stanford, California
Attn: Profs. E. G. Reid (1)
S. J. Klein

Syracuse University
Mechanical Engineering Dept.
Syracuse, New York
Attn: Dr. S. Eskinasi (1)

Princeton University
Aeronautical Engineering Department
The James Forrestal Research Center
Princeton, New Jersey
Attn: Prof. D. C. Hazen (1)

DISTRIBUTION LIST (Continued)

Convair Division
General Dynamics Corporation
San Diego 12, California
Attn: Mr. John W. Shue (1)

Cornell Aeronautical Lab., Inc.
4455 Genesee Street
Buffalo 21, New York
Attn: Dr. George Rudinger (1)

Therm Advanced Research, Therm, Inc.
Ithaca, New York
Attn: Dr. A. Ritter (1)

Library
Institute of the Aerospace Sciences
2 East 64 Street
New York 21, New York (1)

Vidya, Inc.
2626 Hanover Street
Stanford Industrial Park
Palo Alto, California
Attn: Dr. Al Sacks (1)

Dr. Harvey D. Christianson
Head, Mechanical Engineering Dept.
University of Arizona
Tucson, Arizona (1)

University of California,
Detonation Laboratory,
Richmond Field Station
Richmond, California
Attn: Dr. Laderman (1)

University of Virginia
Aeronautical Engineering Dept.
Charlottesville, Va.
Attn: Dr. George Matthews and
Dr. John Scott (1)

Rensselaer Polytechnic Institute
Department of Aero. Engr.
Troy, New York
Attn: Dr. J. V. Foa (1)

AD ______________________ ACCESSION NO. ______________

Hiller Aircraft Corp., Advanced Research Division, Palo Alto, California

INTERIM SUMMARY REPORT ON INVESTIGATION OF THE PROCESS OF ENERGY TRANSFER FROM AN INTERMITTENT JET TO SECONDARY FLUID IN AN EJECTOR-TYPE THRUST AUGMENTER, Raymond M. Lockwood, Principal Investigator

Report No. ARD-286, 31 March 1961, 70 pp incl. illus.
(Contract Nonr 3082(00)) UNCLASSIFIED REPORT

Experiments with ejector-type thrust eugmenters using an intermittent jet have shown eugmentation ratios as high as 2.4 with eugmenter length-to-diameter ratio of less than 2 and jet outlet to eugmenter x-section area ratio of 7. This high performance as compared with a steady flow device of similar proportions, is tentatively explained by the higher pressure ratios obtained with an isentropic wave process, as idealized by a piston traveling in a tube, over those of the isentropic steady flow process. Results from this program have contributed to the practical development of a propulsion engine, the "Pulse Reactor", which uses a high performance valveless pulsejet to produce the intermittent jet. A converter to produce intermittent flow from a steady flow, such as provided by a turbojet, was built and shows potential for further development.

The majority of effort during this phase of the investigation was directed towards instrumentation and techniques for gathering data to support the energy transfer analyses. A color-modified schlieren system with a high-speed motion picture camera provides visualization of the jet interface movement and the pressure waves generated in the augmenter. Jet velocity ranges from 1000 ft/sec at the jet outlet to approximately 250 ft/sec at 10 diameters downstream. "Instantaneous" pressure measurements indicate wave amplitudes in the augmenter of +3 to -3 psig. Air flow rate measurements with a Meriam laminar flow meter show a pumping augmentation ratio of 16 to 1.

UNCLASSIFIED

I R. M. Lockwood

II Contract Nonr 3082(00)

III Uniterms:

jet

intermittent

augmentation

thrust

energy

transfer

pressure

wave

ejector

schlieren

AD ______________________ ACCESSION NO. ______________

Hiller Aircraft Corp., Advanced Research Division, Palo Alto, California

INTERIM SUMMARY REPORT ON INVESTIGATION OF THE PROCESS OF ENERGY TRANSFER FROM AN INTERMITTENT JET TO SECONDARY FLUID IN AN EJECTOR-TYPE THRUST AUGMENTER, Raymond M. Lockwood, Principal Investigator

Report No. ARD-286, 31 March 1961, 70 pp incl. illus.
(Contract Nonr 3082(00)) UNCALSSIFIED REPORT

Experiments with ejector-type thrust augmenters using an intermittent jet have shown augmentation ratios as high as 2.4 with augmenter length-to-diameter ratio of less than 2 and jet outlet to augmenter x-section area ratio of 7. This high performance as compared with a steady flow device of similar proportions, is tentatively explained by the higher pressure ratios obtained with an isentropic wave process, as idealized by a piston traveling in a tube, over those of the isentropic steady flow process. Results from this program have contributed to the practical development of a propulsion engine, the "Pulst Reactor", which uses a high performance valveless pulsejet to produce the intermittent jet. A converter to produce intermittent flow from a steady flow, such as provided by a turbojet, was built and shows potential for further development.

The majority of effort during this phase of the investigation was directed towards instrumentation and techniques for gathering data to support the energy transfer analyses. A color-modified schlieren system with a high-speed motion picture camera provides visualization of the jet interface movement and the pressure waves generated in the augmenter. Jet velocity ranges from 1000 ft/sec at the jet outlet to approximately 250 ft/sec at 10 diameters downstream. "Instantaneous" pressure measurements indicate wave amplitudes in the augmenter of +3 to -3 psig. Air flow rate measurements with a Meriam laminar flow meter show a pumping augmentation ratio of 16 to 1.

UNCLASSIFIED

I R. M. Lockwood

II Contract Nonr 3082(00)

III Uniterms:

jet

intermittent

augmentation

thrust

energy

transfer

pressure

wave

ejector

schlieren

AD ______________________ ACCESSION NO. ______________

Hiller Aircraft Corp., Advanced Research Division, Palo Alto, California

INTERIM SUMMARY REPORT ON INVESTIGATION OF THE PROCESS OF ENERGY TRANSFER FROM AN INTERMITTENT JET TO SECONDARY FLUID IN AN EJECTOR-TYPE THRUST AUGMENTER, Raymond M. Lockwood, Principal Investigator

Report No. ARD-286, 31 March 1961, 70 pp incl. illus.
(Contract Nonr 3082(00)) UNCLASSIFIED REPORT

Experiments with ejector-type thrust augmenters using an intermittent jet have shown augmentation ratios as high as 2.4 with augmenter length-to-diameter ratio of less than 2 and jet outlet to augmenter x-section area ratio of 7. This high performance as compared with a steady flow device of similar proportions, is tentatively explained by the higher pressure ratios obtained with an isentropic wave process, as idealized by a piston traveling in a tube, over those of the isentropic steady flow process. Results from this program have contributed to the practical development of a propulsion engine, the "Pulse Reactor", which uses a high performance valveless pulsejet to produce the intermittent jet. A converter to produce intermittent flow from a steady flow, such as provided by a turbojet, was built and shows potential for further development.

The majority of effort during this phase of the investigation was directed towards instrumentation and techniques for gathering data to support the energy transfer analyses. A color-modified schlieren system with a high-speed motion picture camera provides visualization of the jet interface movement and the pressure waves generated in the augmenter. Jet velocity ranges from 1000 ft/sec at the jet outlet to approximately 250 ft/sec at 10 diameters downstream. "Instantaneous" pressure measurements indicate wave amplitudes in the augmenter of +3 to -3 psig. Air flow rate measurements with a Meriam laminar flow meter show a pumping augmentation ratio of 16 to 1.

UNCLASSIFIED

I R. M. Lockwood

II Contract Nonr 3082(00)

III Uniterms:

jet

intermittent

augmentation

thrust

energy

transfer

pressure

wave

ejector

schlieren

AD ______________________ ACCESSION NO. ______________

Hiller Aircraft Corp., Advanced Research Division, Palo Alto, California

INTERIM SUMMARY REPORT ON INVESTIGATION OF THE PROCESS OF ENERGY TRANSFER FROM AN INTERMITTENT JET TO SECONDARY FLUID IN AN EJECTOR-TYPE THRUST AUGMENTER, Raymond M. Lockwood, Principal Investigator

Report No. ARD-286, 31 March 1961, 70 pp incl. illus.
(Contract Nonr 3082(00)) UNCLASSIFIED REPORT

Experiments with ejector-type thrust augmenters using an intermittent jet have shown augmentation ratios as high as 2.4 with augmenter length-to-diameter ratio of less than 2 and jet outlet to augmenter x-section area ratio of 7. This high performance as compared with a steady flow device of similar proportions, is tentatively explained by the higher pressure ratios obtained with an isentropic wave process, as idealized by a piston traveling in a tube, over those of the isentropic steady flow process. Results from this program have contributed to the practical development of a propulsion engine, the "Pulse Reactor", which uses a high performance valveless pulsejet to produce the intermittent jet. A converter to produce intermittent flow from a steady flow, such as provided by a turbojet, was built and shows potential for further development.

The majority of effort during this phase of the investigation was directed towards instrumentation and techniques for gathering data to support the energy transfer analyses. A color-modified schlieren system with a high-speed motion picture camera provides visualization of the jet interface movement and the pressure waves generated in the augmenter. Jet velocity ranges from 1000 ft/sec at the jet outlet to approximately 250 ft/sec at 10 diameters downstream. "Instantaneous" pressure measurements indicate wave amplitudes in the augmenter of +3 to -3 psig. Air flow rate measurements with a Meriam laminar flow meter show a pumping augmentation ratio of 16 to 1.

UNCLASSIFIED

I R. M. Lockwood

II Contract Nonr 3082(00)

III Uniterms:

jet

intermittent

augmentation

thrust

energy

transfer

pressure

wave

ejector

schlieren